

# **Real Time Energy Management Control Strategies for Hybrid Powertrains**

By

Mohamed Hegazi Mohamed Zaher  
B.Sc., Cairo University, 2005  
M.Sc., Cairo University, 2009

THESIS

Submitted as partial fulfillment of the requirements  
for the degree of Doctor of Philosophy in Mechanical Engineering  
in the Graduate College of the  
University of Illinois at Chicago, 2013  
Chicago, Illinois

Defense Committee:

Professor Sabri Cetinkunt, Chair and Advisor, Mechanical Engineering

Professor W.J. Minkowycz, Mechanical Engineering

Professor Lin Li, Mechanical Engineering

Professor Jeremiah Abiade, Mechanical Engineering

Professor Craig Foster, Civil and Materials Engineering

This thesis is dedicated to my family whom without their support I would not have been where I am today.

## ACKNOWLEDGMENTS

I would like to express my gratitude to my academic advisor Professor Sabri Cetinkunt for giving me the opportunity to study under him and be a part of his research team.

I would like to acknowledge and thank my thesis committee members for their support and assistance. I would like to express my gratitude to Professors W.J. Minkowycz, Lin Li, Jeremiah Abiade, and Craig Foster for their support and being my thesis committee members. This work was partially sponsored by Caterpillar Inc.

I would like to express my gratitude to Fabio Croce, Michael Mitchell, Milton Hubbard, and Rich Ingram for their continuous support during my work.

I would like to thank my colleagues Alope Mascarenhas, Ahmed Elezaby, Mohamed Abdelgayed, Sameh Alkam, Burak Karakas, Ahmed El-Ghandour, and Ashraf Hamed for their continuous help and support during my work.

Last I would like to thank my family and friends for their continuous encouragement and support without which I would not have been able to be where I am today.

## TABLE OF CONTENTS

<u>CHAPTER</u>	<u>PAGE</u>
1. INTRODUCTION .....	1
1.1. Problem Statement .....	1
1.2. Literature Review .....	7
1.3. Thesis Outline .....	20
2. MEDIUM WHEEL LOADERS AND HYBRID TECHNOLOGY .....	21
2.1. Medium Wheel Loader.....	21
2.1.1. Engine .....	24
2.1.2. Powertrain .....	27
2.1.2.1. Torque Converter and Transmission.....	28
2.1.2.2. Continuously Variable Transmission.....	31
2.1.3. Implement Hydraulics .....	35
2.1.4. Chassis.....	40
2.2. Hybrid Technology .....	40
2.2.1. Electric Hybrid .....	41
2.2.2. Hydraulic Hybrid .....	46
2.2.3. Flywheel Hybrid.....	53
3. CONTROL STRATEGIES .....	60
3.1. Rule-based Control.....	60
3.1.1. Cycle Model .....	60
3.1.2. Rule-based Logic .....	63
3.1.3. Gain Scheduling .....	70
4. RESULTS .....	74
4.1. Model Validation .....	74
4.2. Results with the 7 Liters Engine .....	80
4.2.1. Aggressive Truck Loading Cycle.....	80
4.2.2. Moderate Truck Loading Cycle .....	82
4.2.3. Short Load and Carry Cycle.....	85
4.2.4. Long Load and Carry Cycle.....	92

4.2.5. Usage of Single Set of Optimized Parameters in Any Cycle .....	95
4.3. Results with the 9 Liters Engine .....	102
4.3.1. Aggressive Truck Loading Cycle.....	102
4.3.2. Moderate Truck Loading Cycle .....	104
4.4. The Baseline, the Hybrid with 7 and 9 Liters Engines Comparison .....	106
5. CONCLUSIONS AND FUTURE WORK .....	109
5.1. Conclusions .....	109
5.2. Future Work .....	109
CITED LITERATURE .....	110
VITA.....	124

## LIST OF TABLES

<u>TABLE</u>	<u>PAGE</u>
I. MEDIUM WHEEL LOADERS WORK CYCLES DEFINITIONS .....	22
II. ENGINE RATING .....	26
III. TRANSMISSION GEAR RATIOS .....	31
IV. OPERATOR MODEL SIGNALS .....	63
V. RULE-BASED LOGIC SIGNALS .....	63
VI. AGGRESSIVE TRUCK LOADING BASELINE AND HYBRID COMPARISON .....	82
VII. AGGRESSIVE TRUCK LOADING OPTIMIZED GAINS .....	82
VIII. MODERATE TRUCK LOADING BASELINE AND HYBRID COMPARISON .....	85
IX. MODERATE TRUCK LOADING OPTIMIZED GAINS .....	85
X. SHORT LOAD AND CARRY BASELINE AND HYBRID COMPARISON .....	88
XI. SHORT LOAD AND CARRY OPTIMIZED GAINS .....	88
XII. LONG LOAD AND CARRY BASELINE AND HYBRID COMPARISON .....	95
XIII. LONG LOAD AND CARRY OPTIMIZED GAINS .....	95
XIV. OPTIMIZED GAINS .....	97
XV. AGGRESSIVE TRUCK LOADING BASELINE AND HYBRID COMPARISON .....	102
XVI. AGGRESSIVE TRUCK LOADING OPTIMIZED GAINS .....	102
XVII. MODERATE TRUCK LOADING BASELINE AND HYBRID COMPARISON .....	104
XVIII. MODERATE TRUCK LOADING OPTIMIZED GAINS .....	104
XIX. AGGRESSIVE TRUCK LOADING BASELINE AND HYBRID COMPARISON .....	106
XX. MODERATE TRUCK LOADING BASELINE AND HYBRID COMPARISON .....	106

## LIST OF FIGURES

<u>FIGURE</u>	<u>PAGE</u>
1. Torque versus speed motoring and generating quadrants (from [2]). .....	2
2. Regeneration opportunities. ....	3
3. Hybrid vehicle configurations: (a) Series, (b) Parallel, and (c) Power-split (from [3]). ....	5
4. Medium Wheel Loader.....	22
5. Wheel loader block diagram. ....	23
6. Wheel loader systems. ....	24
7. Wheel loader engine.....	25
8. Rated 9 Liters engine lug curve and power rating (from [106]).....	25
9. Rated 7 Liters engine lug curve and power rating (from [106]).....	26
10. Brake specific fuel consumption map. ....	28
11. Torque converter.....	29
12. Torque converter characteristics. ....	30
13. Planetary gearbox.....	32
14. Hydraulic parallel path variable. ....	33
15. Hydraulic parallel path variable System. ....	34
16. Hydrostatic continuously variable transmission.....	35
17. Load sensing axial piston pump with swash plate. ....	37
18. Traditional load sensing hydraulic circuit. ....	38
19. Post compensator configuration in multifunction hydraulic circuit [2]. ....	39
20. Test bed hybrid concepts implementation.....	42
21. Electric hybrid concept.....	43
22. Electric hybrid powertrain for wheel loader.....	44
23. Electric hybrid powertrain for wheel loader prototype. ....	45
24. Hydraulic hybrid concept. ....	47
25. Hydraulic hybrid powertrain for wheel loader block diagram. ....	48
26. Hydraulic hybrid circuit. ....	49
27. Hydraulic hybrid circuit charging. ....	50
28. Hydraulic hybrid circuit discharging.....	51
29. Hydraulic hybrid concept. ....	52
30. Flywheel hybrid block concept. ....	54
31. Flywheel hybrid block diagram.....	55
32. Toroidal CVT Concept.....	56
33. Toroidal CVT Principle.....	57
34. Flywheel hybrid.....	59
35. Rule –based control block diagram. ....	61
36. Rule –based control upper level Simulink diagram. ....	62

37. Cycle model Simulink diagram.....	64
38. Time Based commands Simulink diagram.....	65
39. Distance Based commands Simulink diagram. ....	66
40. Rule-based control logic Simulink diagram.....	67
41. GPS gain scheduling algorithm.....	71
42. Validation lift command.....	75
43. Validation tilt command.....	75
44. Validation brake command. ....	76
45. Validation gear command. ....	76
46. Validation machine velocity.....	77
47. Validation engine speed. ....	77
48. Validation torque converter output speed. ....	78
49. Validation consumed fuel.....	79
50. Simulation Error Percentage. ....	79
51. Aggressive truck loading cycle. ....	81
52. ATL hybrid versus baseline. ....	83
53. Hybrid machine ATL torque values.....	84
54. Engine and hybrid system ATL torque contribution.....	84
55. MTL hybrid versus baseline.....	86
56. Moderate truck loading cycle.....	87
57. Hybrid machine MTL torque values. ....	89
58. Engine and hybrid system MTL torque contribution. ....	89
59. SLC hybrid versus baseline.....	90
60. Short load and carry cycle.....	91
61. Hybrid machine SLC torque values. ....	92
62. Engine and hybrid system SLC torque contribution. ....	93
63. LLC hybrid versus baseline.....	94
64. Long load and carry cycle. ....	96
65. Effect of different gain groups on the ATL cycle. ....	98
66. Effect of different gain groups on the MTL cycle.....	99
67. Effect of different gain groups on the SLC cycle.....	100
68. Effect of different gain groups on cycles' productivity.....	101
69. Effect of different gain groups on cycles' fuel reduction.....	101
70. ATL 9 liters hybrid versus baseline. ....	103
71. MTL 9 liters Hybrid versus Baseline. ....	105
72. ATL Hybrid versus Baseline.....	107
73. MTL Hybrid versus Baseline. ....	108



## LIST OF ABBREVIATIONS

ANOVA	Analysis of the Variance
ATL	Aggressive Truck-loading
BSFC	Brake Specific Fuel Consumption
CARIMA	Controller Auto-Regressive Moving-Average
CVT	Continuously Variable Transmission
ECLT	Electric Convertless automatic Transmission
ECMS	Equivalent Consumptions Minimization Strategies
GPC	Generalized Predictive Control
GPS	Global Positioning System
HJB	Hamilton-Jacobi-Bellman
HPPV	Hydraulic Parallel Path Variable
ISG	Integrated Starter Generator
KERS	Kinetic Energy Recovery System
LLC	Long Load-and-Carry
MPC	Model Predictive Control
MTL	Moderate Truck-Loading
MWL	Medium Wheel Loader
NARX	Nonlinear Auto-Regressive Exogenous
PHEV	Plug-in Hybrid Electric Vehicle
PI	Proportional–Integral

PID	Proportional–Integral- Derivative
PSHEV	Power-Split Hybrid Electric Vehicle
PWM	Pulse Width Modulation
SDP	Stochastic Dynamic Programming
SLC	Short Load-and-carry
SOC	State of Charge
THS	Toyota Hybrid System
TC	Torque Converter
VPD	Virtual Product Development

## SUMMARY

In order to **improve fuel efficiency and reduce emissions** of mobile vehicles, various hybrid power-train concepts have been developed over the years. This thesis focuses on embedded control of hybrid powertrain concepts for mobile vehicle applications. Optimal robust control approach is used to develop a real time energy management strategy for continuous operations. The main idea is to store the normally wasted mechanical **regenerative energy** in energy storage devices for later usage. The regenerative energy recovery opportunity exists in any condition where the speed of motion is in opposite direction to the applied force or torque. This is the case when the vehicle is braking, decelerating, or the motion is driven by gravitational force, or load driven. There are three main concepts for regenerative energy storing devices in hybrid vehicles: electric, hydraulic, and flywheel.

The real time control challenge is to balance the system power demand from the engine and the hybrid storage device, without depleting the energy storage device or stalling the engine in any work cycle, while making optimal use of the energy saving opportunities in a given operational, often repetitive cycle. In the worst case scenario, only engine is used and hybrid system completely disabled. A rule based control is developed and tuned for different work cycles and linked to a gain scheduling algorithm. A gain scheduling algorithm identifies the cycle being performed by the machine and its position via GPS, and maps them to the gains.

## 1. INTRODUCTION

This chapter presents the problem statement of this thesis, explaining the problem being solved, and the reasons for interest in solving that problem, and the proposed methodologies to solve that problem.

### 1.1. Problem Statement

Fuel efficiency is one of the most important performance measures in all combustion based power generation, including diesel engines. Diesel engines have almost double the fuel efficiency compared with gasoline engines. The increase in engine output power in the past years has been mainly due to supercharging and turbocharging. This enabled downsizing the engines, increased specific brake power, provided better fuel economy and reduced CO<sub>2</sub> emissions. Recently there has been a growing demand in reducing the highly toxic nitrogen oxides (NO<sub>x</sub>) and particulate matter (PM) emissions in diesel engines, which called for complicated control strategies and after-treatment systems due to the presence of a tradeoff between NO<sub>x</sub> and PM. Among these systems are the exhaust gas recirculation (EGR), selective catalytic reduction (SCR), diesel particulate filter (DPM), and variable geometry turbochargers. However, the demand for reducing exhaust emissions is still increasing [1].

Due to that fact, governments and environmental agencies demand vehicle manufacturers to come up with methods to **improve fuel efficiency and reduce emissions** of the manufactured vehicles. In order to meet these demands, alternative powertrain concepts including electric, hybrid and fuel cell are being developed. The concept behind the hybrid devices is to store the regenerative mechanical energy that would otherwise wasted, in energy storage devices and

reuse that energy in future operations. The regenerative mechanical energy recovery opportunity exists in any condition where the speed of motion is in opposite direction to the applied force or torque (Fig. 1 [2]). This condition is satisfied in various conditions such as (Fig. 2):

1. vehicle braking,
2. vehicle is moving down a hill and braking must be applied to maintain a desired speed ,
3. load is moved by gravitational (load) force.

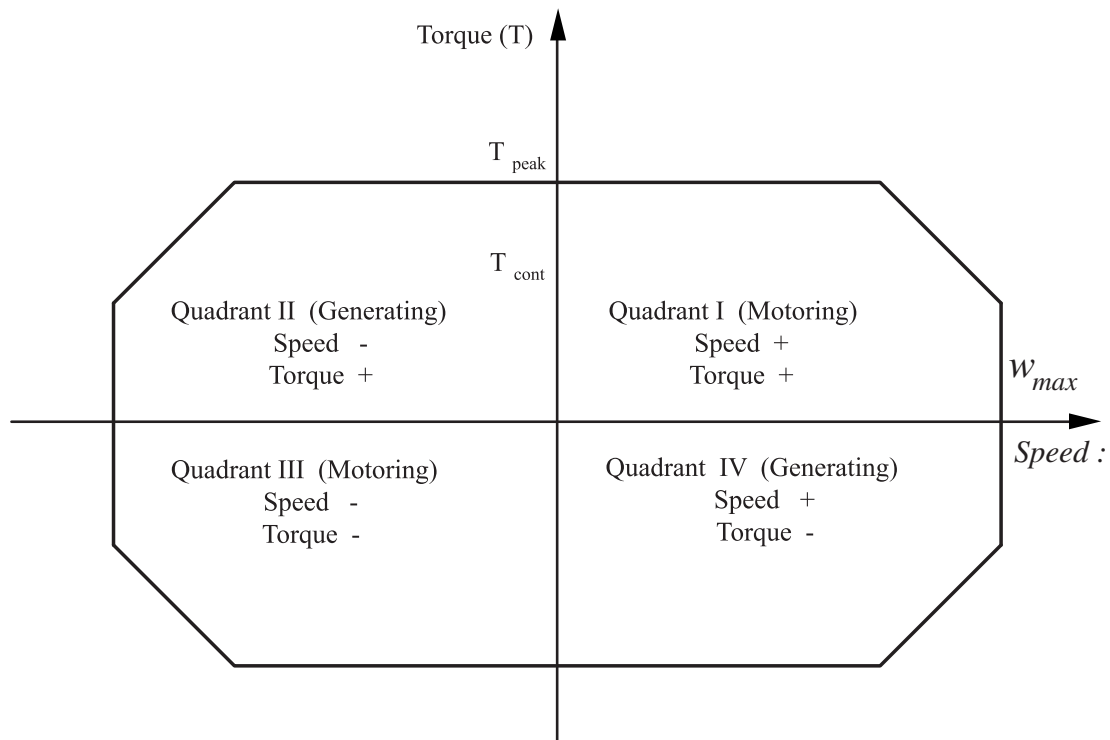


Figure 1: Torque versus speed motoring and generating quadrants (from [2]).

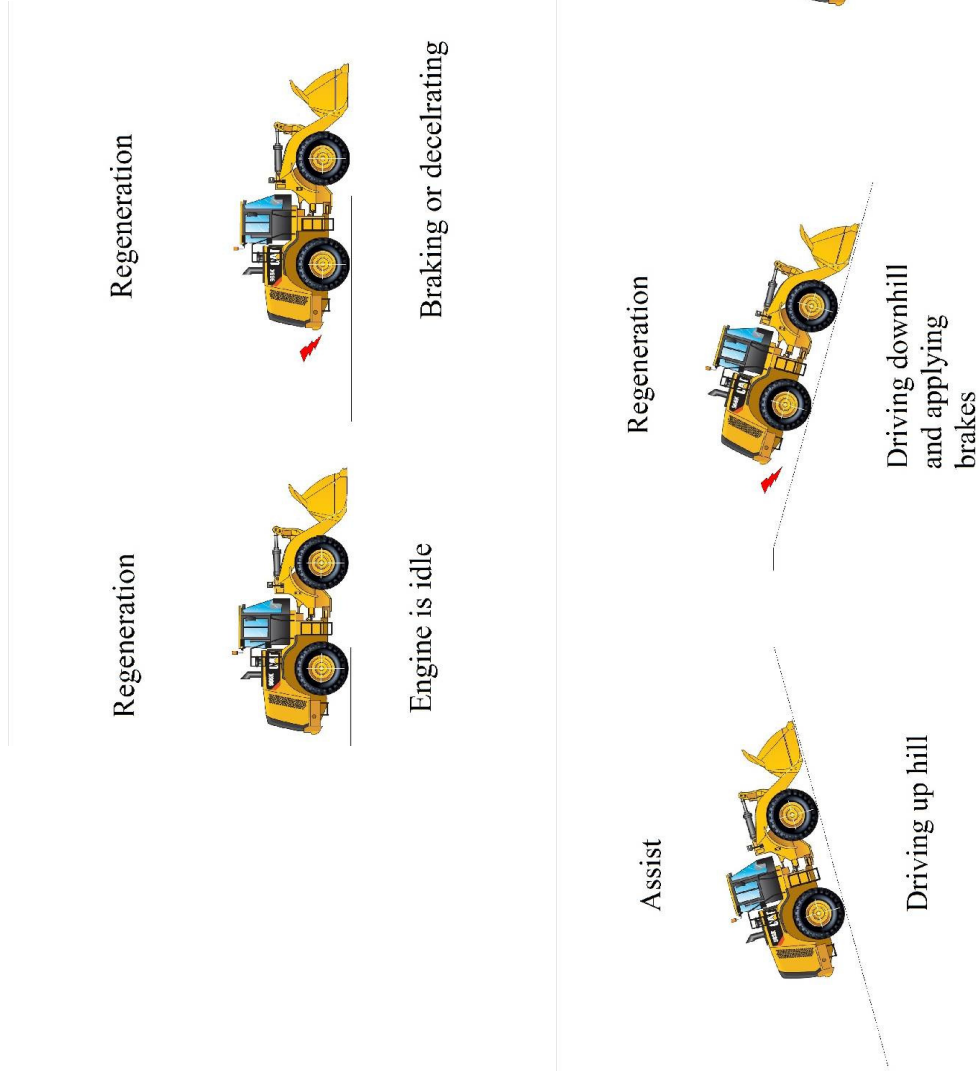


Figure 2: Regeneration opportunities.

There are three full/power-assist hybrid powertrain configurations (Fig.3 [3]) in existence: series, parallel and power-split configurations. The series hybrid configuration uses the engine to charge the energy storage device which supplies all the power demand of the vehicle. This configuration increases the size of the vehicle as higher energy storage capacity needed would be large but it is very efficient in its energy usage. The parallel configuration utilizes power from both the engine and the motor to drive the vehicle. This configuration limits the use of regenerative energy to the times when the battery is not being recharged. The power-split configuration combines both concepts and through the separation of the motor and the generator, a continuous supply of energy from the motor is available even during recharge phase.

There are three main concepts for energy storing devices in hybrid vehicles:

1. electric hybrid,
2. hydraulic hybrid,
3. flywheel (mechanical) hybrids.

Both the electric and hydraulic concepts employ energy conversion concepts between mechanical, electrical and hydraulic energies. The mechanical hybrid system keeps the energy in mechanical form at all times in the form of kinetic energy. The real time control challenge is to balance the machine power demands from both the engine and the hybrid storage device.

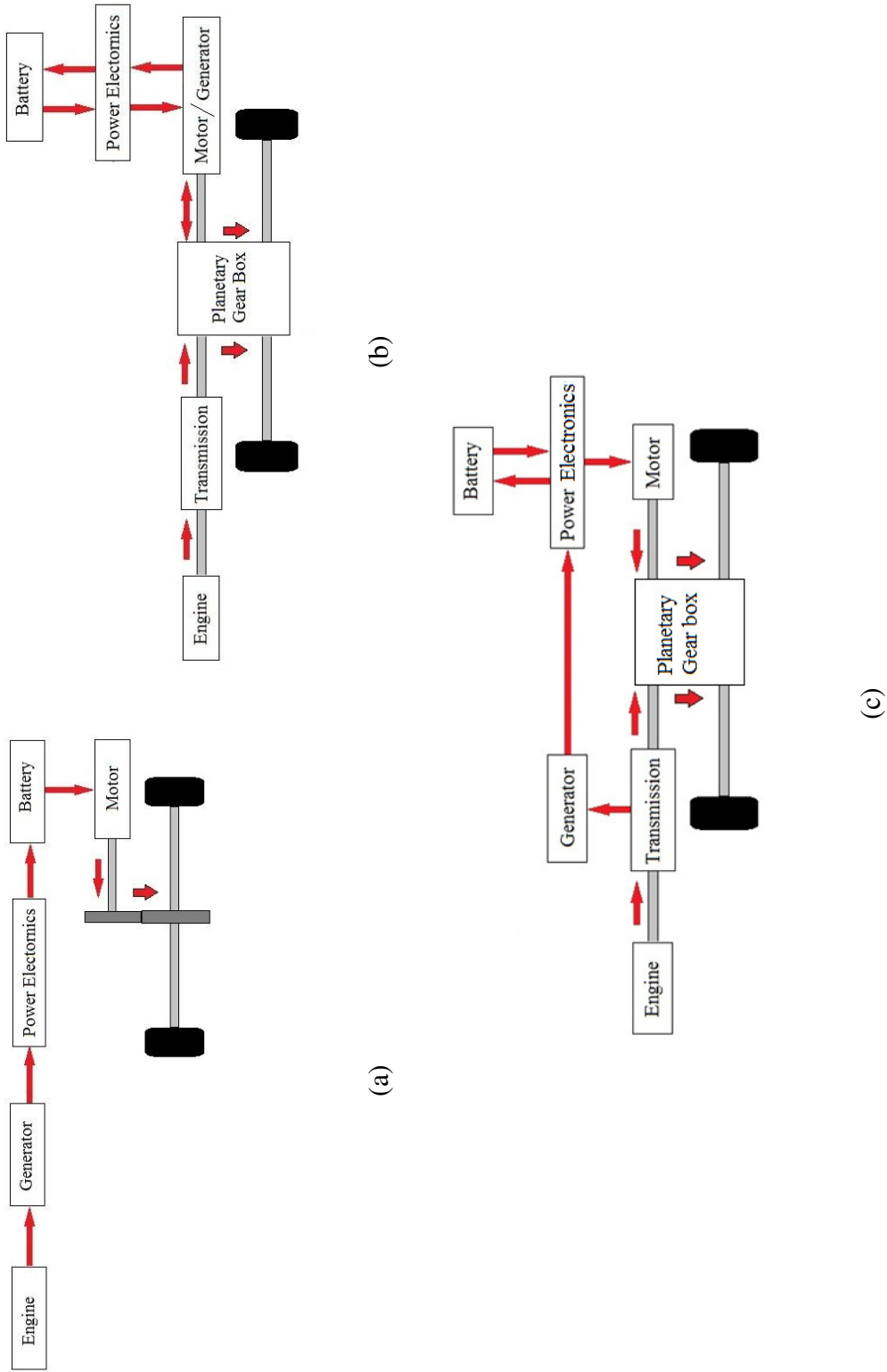


Figure 3: Hybrid vehicle configurations: (a) Series, (b) Parallel, and (c) Power-split (from [3]).



The constraints faced in developing the control strategy are:

1. maintain or improve the vehicle productivity,
2. improve fuel efficiency,
3. prevent the depletion of the energy storage device, and maintain an acceptable state of charge (SOC).

In other words, the objective is to make optimal use of the energy saving opportunities in a given operational, often repetitive, cycle. In the worst case scenario, the hybrid system is not utilized properly, causing the system to be unbalance and draining the energy stored. A rule based control with multiple tunable gains tuned for different work cycles is developed. To select the appropriate gains for a given operational cycle, a gain scheduling algorithm is developed. The gain scheduling algorithm identifies the cycle being performed by the machine and its position via GPS, and then uses that information to look up the gains from a table. If the vehicle is on a known path, the algorithm seeks historic data to check the last performed cycle on that path and set the gains of the controller to that of the work cycle. If the machine breaks from that path, the controller checks to see if it is still a known path and reset the gains if that was the case. If the machine is not on a known path then cycle identification takes over and once the cycle is identified, the path and the gains are mapped to each other. In control strategies, the gains and the control algorithm should be robust and have low sensitivity to gain changes to accommodate real working conditions. This thesis focuses on controlling a hybrid powertrain application for construction machines in real time via an optimal robust control that will enable continuous operation through repetitive and between different cycles.

## **1.2. Literature Review**

Gonder and Simpson [4] differentiated between plug-in hybrid electric vehicles (PHEVs) according to their electric range which is the distance traveled before the vehicle switches from charge depleting to charge sustaining operation. Nermy et al. [5] studied the analyzed the potential benefits and pitfalls of PHEVs. Axsen et al. [6] defined the key features to electro-chemical battery selection of electrical hybrids to be energy storage capacity, specific energy, energy density, battery calendar life, cycle life, safety, and thermal management requirements, cost, usable SOC, and recharge time. A good alternative is the use of integrated starter generator (ISG) which offers the engine improvement of transient response as well as reduction of emission and fuel consumption [1].

Kobeler et al. [7] patented a power management logic that is based on multiple inputs in an attempt to optimize the power consumption of an automotive vehicle as an alternative to cruise control. The system may be manually engaged by the operator at any point of time, compensates for missing input data through estimation, monitoring of operator commands, vehicle operations and the provided input data. One important contribution is the prevention of engine flooding logic which enhances fuel consumption in case of heavy legged drivers. Tamor [8] attempted to minimize complexity and reduce the cost of a PHEV powertrain system by replacing electric converterless automatic transmission (ECLT) which is capable of all hybrid functions except electric only propulsion. However, the control logic causes extra consumption of fuel than in regular hybrid systems due to engine emulation. Abe [9] designed a power-split hybrid for Toyota Prius thus improving the fuel efficiency, and the exhaust emission making it better than the Insight [10] which uses parallel hybrid technology integrated motor assist. By increasing the intake air volume and improving the timing, the maximum torque and power

output have been improved. Also, they switched from pulse width modulation (PWM) switching to PWM switching in low speed range and one pulse switching in high speed range as well as provided a more compact design for the battery system.

Teratani et al. [11] installed a new Toyota hybrid system (THS) which improved fuel economy with 40%. The old THS had slow response, high vibration, and noise during starting and stopping. They managed to reduce the size of the THS. Also, they presented the control logic currently used in most ISG systems, as well as presented a sequence of steps through which the vibration and noise can be minimized. Yamaguchi et al. [12] claim priority from other patents filed in Japan in 2000 related to a power-split HEV (PSHEV) claiming originality in design for using unidirectional clutch and transmission. Boggs et al. [13] claim originality in designing a controlled engine shutdown strategy that provides engine protection to different threatening conditions as well as reducing emissions and fuel consumption. The proposed strategy suggests different approach than its counterparts such as aborting shutdown if the engine is commanded to run and the fuel injector ramping has yet to begin and disabling the ignition when engines speed is below the calibratable threshold. While this system may be advantageous in commercial vehicles, it neglects the possible power requirements of other machines that may find this strategy unfavorable.

Many researchers designed control strategies for battery control on electric hybrid vehicles in order to optimize the charging and discharging sequence of the battery throughout its life in order to increase its life span while meeting the power requirements of the hybrid vehicle. Koike and Masuda [14] made use of historic data to forecast possible control scenarios. Sakai and Kobayashi [15] attempted to improve SOC measurement from integrating the current discharged from the battery which neglects the errors due to variation in charge/discharge efficiencies by

implementing a current and voltage closed loop feedback control. Kimura and Murakami [16] introduced an index to define the quantity of charge available in the battery.

Due to energy conversion inefficiencies, sensitivity from internal and external conditions that affect battery performance, the high cost and size of electric hybrids, other hybrid options are investigated. Shen and Veldpaus [17] used a flywheel hybrid with a V-belt Continuously Variable Transmission (CVT) that partly cancels the engine inertia; hence, they called it zero inertia powertrain. Also, they studied two control concepts with the flywheel hybrid, one controls the engine and the other controls the vehicle speed. They employed feedback linearization with the engine control strategy which could cause bifurcation if the transmission and the zero inertia ratios became equal.

Schurmann and Schroder [18] replaced batteries with ultracaps (double layer capacitors) and used decentral control network that identifies operator commands and calculates the optimized values at low sampling rates. Their system is so complex that they had to calculate at low sampling rates leaving the system vulnerable to various signal misinterpretation (bias, beat...) and forcing the machine to operate at low speeds. They also used the electric motor and a flywheel to move the engine from stop up to a certain speed before starting the combustion process to increase efficiency and reduce fuel consumption and emissions by taking the engine out of the inefficient range.

Diego-Ayala et al. [19] studied the flywheel hybrid due to its low cost, efficiency, offering an easy method of determining the SOC just by measuring the rotational speed and absence of energy conversion penalties. They proposed a system with planetary gear set, brake and CVT to avoid using a wide range, less efficient CVT. However, all braking is done by regenerative

braking which is not possible in heavy machinery. While energy requirement to accelerate the vehicle increase compared to the conventional vehicle due to the additional weight, the hybrid vehicle offer better fuel economy and reduced emissions.

Cross and Brockbank [20] defined flywheel hybrid (Flybrid) systems as kinetic energy recovery systems (KERS). In 2009 Formula 1, flybrids managed to store and utilize 400kJ per lap at a maximum rate of 60kW in a 6000 kg car with power availability in the vicinity of 550 kW. The KERS system developed by Flybrid Systems LLP uses high speed carbon filament flywheel and Torotrak full-toroidal traction CVT and utilizes regenerative braking. The full-toroidal traction CVT was for its power density torques based control and ease of calibration to different power levels. The flywheel runs in vacuum for efficiency optimization and is sealed in housing as a safety measure for failure event. When the ratio of flywheel to vehicle speed exceeds the CVT capacity, one of the clutches is allowed to slip reducing the transmission efficiency. If CVT ratio too low the output clutch is disengaged and if too high then the input clutch is disengaged. The efficiency of this system is highly dependent on the control strategy implemented.

Katrasnik et al [21] analyzed the energy conversion efficiency in parallel and series HEVs using simulations as a basis for comparison. They concluded that the parallel hybrid powertrain out performs the series hybrid powertrain especially at lower average loads and their benefit over series configuration decreases as the average load increases. Karden et al. [22] studied the energy storage devices for HEVs and concluded that for the foreseeable future the Lithium-Ion batteries and Nickel metal hydride will dominate the electric hybrid market for their improved performance and smaller size compared to other storage devices. He and Hodgson [23, 24] modeled and simulated the electric hybrid vehicle built by the University of Tennessee. Their research proposed using a Lithium-ion battery as a modification from the original energy storage

device and proposed a control strategy based on the study of the battery state of charge, power output of the engine and the hybrid, and the acceleration capability of the vehicle. Stecki, and Matheson [25] discussed different configurations of hydraulic hybrid powertrains and their implementations in trucks. They summarized a list of major issues accompanying the use of hydraulic hybrid technology such as: safety, weight, drivability and performance. Donitz, et al. [26] studied pneumatic hybrid with a downsized supercharged engine. They achieved fuel savings of up to 35% using that system with dynamic programming as a supervisory control overcoming the so-called turbo lag. Regenerative braking in HEVs [27-29] considers the battery state of charge, transmission ratio, and the available regenerative braking torque to determine when to charge the battery. It can be done through the addition of auxillary braking systems such as hydraulic mechanism [27, 29], modifications to the transmission and braking mechanisms [28], or through mathematical optimization [29].

Yafu, and Cheng [30] studied mild HEVs with ISG. They used a parallel assist control strategy and modeled the system in Simulink and achieved their objective of reducing the fuel consumption. Park, and Jung [31] designed and studied three vehicle cooling system for a heavy duty tracked series HEV. While all three provided significant improvement from the original cooling system, they provided different parasitic power consumption. Tavares, et al. [32] studies a variable displacement engine with power-split hydraulic hybrid powertrain and used a predictive model control strategy. They achieved a much smoother engine operation which resulted in a better fuel economy and they are planning further investigations to their work. Montazeri-Gh and Soleymani [33] investigated the possibility of energy regeneration from active suspension in HEVs, however, that resulted in increase in fuel consumption and emission. Katrasnik [34] proposed a new analytical method for the calculation of the fuel consumption in

series and parallel HEVs at a balanced state of charge. Atkins and Koch [35] compared several powertrain configuration including downsizing engines, supercharging, fuel cell vehicles, electric vehicles and HEVs and evaluated their performance and emissions. Ogawa, et al. [36] described the work done on the development of the integrated motor assist technology developed at Honda Co. and implemented in the Civic vehicle. They reduced the emissions and fuel consumption by reducing the engine displacement, implement an idle stop strategy and recovery of regenerative energy during deceleration that is used to assist through a brushless DC motor. Flynn, et al. [37] tested flywheel hybrid technology performance in a lab environment.

Jackey, et al. [38] used hydraulic hybrid powertrain and compared it to electric hybrid powertrains. They also claim that the same design can be used successfully as pneumatic rather than hydraulic. However, their design progressively drains the storage device without sufficiently charging it and the control strategy needs improvement. Su, et al. [39] presented the design procedures for a permanent magnet brushless motor drive for HEVs that was implemented in Chevrolet Suburban. Destraz, et al. [40] studied the use of supercapacitors as energy storage devices in diesel-electric hybrid vehicles and concluded that the speed of response of the system is too slow to function properly. Evans, et al. [41] introduced the architecture of General Motors Sierra pickup truck hybrid vehicle. They used parallel electric hybrid powertrain with a rule based control based on the vehicle functions to achieve their objectives. Liang, et al. [42] developed a parametric design for HEVs that could be implemented on military vehicles or public transit buses. They also used a rule-based control algorithm based on the knowledge of the functions of different systems to achieve optimal control. Steinmaurer and Del Re [43] used an ISG with a HEV with a statistics based control to achieve task optimization in an attempt to mimic dynamic programming. He, et al. [44]

combine the CVT flywheel hybrid concept with the electric hybrid concept to benefit from the advantages of both systems, increase the amount of energy stored, and provide simultaneous charge and assist actions. Setlur, P., et al. [45] implemented a nonlinear control strategy to the CVT of a hybrid vehicle to enhance its performance through improving the CVT component performance. Kessels, et al. [46] developed an online identification method for the fuel consumption and the vehicle parameters for usage in a feedback controller that controls the energy management strategy in the vehicle. They used linear time periodic system model and analyzed the stability using Floquet theory.

Two control algorithms are most commonly investigated in literature [1]: rule-based control and dynamic programming. While the rule based control provided 22% reduction in fuel consumption mainly due to the regenerative braking, the dynamic programming algorithm provided 33% through the better coordination of the hybrid setup [1]. Sciarretta, and Guzzella [46] surveyed the control algorithms for HEVs up to 2007. Liu and Peng [48] studied the control of Toyota PSHEV using two control algorithms: Stochastic dynamic programming and equivalent consumptions minimization strategies (ECMS) [49]. To assess the performance of both algorithms, deterministic dynamic programming solutions are used as a benchmark for comparisons rather than a solution to be implemented. They used two motor/generator sets to have more efficient propulsion and regenerative braking such that one of them act as a type of CVT also known as electronic variable transmission. They validated the model through running it with a rule-based control. They optimized the control over two steps: system optimization to determine engine demand and then optimization of the engine controls. The stochastic dynamic programming (SDP) maps the SOC, vehicle speed, instantaneous power demand to the control decision, and engine power demand. The driving power demand is modeled to be generated



from stationary Markov chain. Using a cost minimizing performance measure and the SOC with a penalty factor the control strategy is solved iteratively. Paganali's ECMS is an instantaneous optimizations algorithm, however it does not account for kinematic constraints. By adding consumption, cost functions the optimal engine power map can be calculated. While both algorithms show significant fuel consumption improvements, the ECMS shows significant oscillations in the engine power commanded compared to the SDP. With ECMS frequent shifting should be prohibited by adding extra constraints between gears, while with SDP an extra input operating gear mode is needed beside the engine speed and the SOC. Also, they provided a good survey on the history of power-split systems, SDP and ECMS. Syed et al. [50] used a fuzzy logic gain scheduling algorithm with proportional–integral (PI) controllers which are conventionally used with PSHEV aiming for reduction of the overshoot and improved performance. Unlike the conventional vehicles, the PSHEV engine speed control is independent of the vehicle speed, requiring nonlinear control algorithms. By determining the engine power demand and battery feedback, the gains are scheduled via the fuzzy controller that utilizes Gaussian membership functions. The results of testing the controller on Ford Escape showed that a minimum of four rules are needed to ensure smoother engine speed.

Canova, et al. [51] studied the engine start/stop dynamics which led to an engine model that is used in a linear quadratic regulator control algorithm developed and optimized via design of experiments (DOE) methods for HEVs with integrated starter alternators. Lin, et al. [52] studied the dynamics of the Toyota Prius PHEV and developed an optimal control energy management strategy and artificial neural networks that was modified to a suboptimal controller using particle swarm optimization in order to be implemented. The optimal and suboptimal had a close match in the engine speed output but the difference in engine torque was relatively high. Hui, et al.

[53] implemented hydraulic and electric hybrid concepts on heavy hybrid vehicles with high braking energy requirements and developed a torque control strategy based on thresholds logic to control and synchronize energy flow through the vehicle; however, they did not optimize their logic and settled for the best solution out of a parameter combinations selected. Saerens, et al. [54] used a mean value model of the powertrain and the hybrid vehicle and applied Bock's direct multiple shooting method with dynamic optimization to come up with an optimal control strategy that will minimize the fuel consumption. Their simulations show that they achieved a 13% fuel consumption reduction but no experimental validation is done. Feroldi, et al. [55] implemented a control strategy based on the efficiency maps of the vehicle components. By determining the efficiency map of the individual components in the operating ranges the overall efficiency is determined and a selection is made to maximize the benefit out of the fuel thus reducing the fuel consumption. Their method succeeded in reducing the fuel consumption by up to 26%.

Gokasan, et al. [56] used sliding mode control to limit the series HEVs to the optimal efficiency operating range and compared it to PI controllers. They used two simultaneous sliding mode controllers one to control the engine speed and the other to control the engine torque. Moura, et al. [57] used SDP in PHEV power management, explored the potential of charge depletion over charging and the economy of fuel-electric usage in hybrid technology. Their approach allows for energy management control without prior knowledge of the driving cycle. Johannesson, et al. [58] developed a GPS based SDP control algorithm for HEV that utilizes the travel and location information of the HEV to manage its power sources to assess the potential benefit out of predictive controls. They compared a position-dependent controller, and a position-invariant one to an optimal control algorithm which showed a slight reduction in fuel consumption when in the

position information are taken into account. However, they also discovered that only the average travel information is needed and the high level of detail is not needed. They also used Model predictive control (MPC) for real-time implementation. Fang, et al. [59] developed a non-dominated sorting genetic algorithm based controller to avoid converting multi-objective algorithms to single objective which produces many Pareto-optimal solutions and the appropriate one can be selected.

Shupeng, et al. [60] compared Electric assist, adaptive, and genetic algorithms control strategies on all configurations of HEV. They concluded that genetic algorithm strategies provide superior results compared to electric assist, and adaptive control strategies. Quigley [61] developed a GPS based optimal control to explore the advantages of using the navigation information as a prediction method; however, he did not present any conclusive results. Ranjan, and Li [62] tested a stochastic approach to predict the SOC of the battery in HEV based on the Trip information and evaluated it using Monte Carlo approach. They validated their hypothesis in Milwaukee. Mathews, et al. [63] documented the approach used by Mississippi State University to develop a controller for HEV Chevrolet Equinox 2005.

Huag, et al. [64] used a threshold logic control strategy that is optimized continuously during operation to control a PHEV. Hui, et al. [65] developed a new configuration of hydraulic hybrid vehicles to improve the regenerative braking and came up with a fuzzy torque control strategy for the hybrid vehicle that was optimized via dynamic programming. Lei, et al. [66] divided the regenerative braking into two categories: braking and coasting and applied different control strategies to deal with each of them, thus achieving a 35% fuel consumption reduction and acceleration performance improvement. Lee, et al. [67] developed an artificial intelligence using neuro-fuzzy techniques to analyze and learn GPS data and control the hybrid vehicle to

improve fuel economy and reduce emissions. Wu, et al. [68] developed a rule-based power management strategy for hydraulic hybrid trucks and utilized dynamic programming to optimize gear shifting trajectories. They claim to achieve a fuel economy increase of 28-48%. Du, et al. [69] created a development platform for control systems of hybrid vehicles to facilitate the development process. Kleimaier, and Schroder [70] attempted online optimization of PHEV control algorithm, however, their control often produced results far from optimal. Delprat, et al. [71] developed an optimal control algorithm for hybrid vehicle and theorized that evaluating the fuel consumption should be expressed as a function of the overall SOC variation rather than taking the actual fuel consumption for a given cycle.

Fu [72] developed a methodology for real time prediction of torque availability in interior permanent magnet motors when implemented on HEVs in order to prevent torque requests at times where there is no availability, hence protecting the battery from depletion. Cacciatori, et al. [73] developed a rule based control for PHEVs and investigated the optimal trajectories via dynamic programming. They managed to achieve 10% better fuel economy using the rule based control and 14% using dynamic programming. Sinoquet, et al. [74] used ECMS and dynamic programming to develop control algorithms for hybrid vehicles and performed a parametric study on both the vehicle design and control. According to Borhan et al. [75] dynamic programming requires knowledge of the upcoming cycle while ECMS are less sensitive to computation, short sighted and sensitive to their parameters. Borhan et al. [75] linearized the models and simulated over different cycles. They modeled the system using the resistance torque, rate of SOC equations and Willan's line method. For this reason, MPC strategy for PSHEV has been developed to minimize fuel, reduce service brake use, and prevent overcharge and discharge of the battery. The MPC technique (also known as the receding horizon control)

introduced by Euler-Lagrange [75, 76]. The MPC in its essence avoids calculating the optimal solution on a global scale but more on the short term and focusing on the points around the current state making it less computationally taxing than the HJB. However, the MPC problem as it is could face stability issues [76]. One way to attempt overcoming this and decrease the computational price of MPC is by the addition of feedback linearization [77]. The energy management problem is an optimization problem of a multivariable constrained nonlinear system with the objectives of minimizing fuel, retain or improve productivity, and return the SOC to the initial state. In other words, the hybrid system control problem is a minimum time, minimum control effort, terminal control and regulator problems put together [78]. For nonlinear constrained systems, HJB equation and Pontryagin's principles of optimal control are more suitable. However, Pontryagin's methods don't have a standard method to achieve optimal solution, the manner in which they are used differ from one problem to the next and requires numerical solution of the boundary value problem which is very difficult [79]. The HJB equation is more suited for this kind of problem, however the exact solutions to this problem is very difficult and requires numerical methods [80]. Many approximations and techniques such as Chebyshev, Pseudospectral Chebyshev, and Galerkin techniques are used to approximate and solve the HJB equation, however the computational cost of implementing these methods is heavy [79-83]. MPC offers a viable alternative as it integrates optimal, stochastic, multivariable, and process control with time delay [75-77]. In the MPC approach, the optimization is performed over the future prediction horizon in discrete time domain, both input and output constraints are included in the optimization, and only the first predicted control value is sent to the system to allow for more accurate predictions through prediction error detection and computational repetition. One of the major compromises when using MPC is that the longer the horizon is, the

better the predictions are, the more stable the solution is and the more computational cost increases [76]. When using nonlinear models for prediction, it should be noticed whether the constraints and the cost function are convex or not to ensure convergence. However, the problem as a whole will be non-convex, making it difficult to optimize, if it is possible at all [77]. For this reason, system linearization around the prediction horizon is the most common procedure. However, if a nonlinear control law is to be implemented due to the system nonlinearity and in cases where model nonlinearities are too severe, it is recommended to use nonlinear approaches such as Hammerstein- Wiener, or nonlinear auto-regressive exogenous (NARX) models [84-86]. If the system nonlinearity is severe, a wavelet network NARX model could be used to model the system via identification [85]. If the machine model linearization is possible, a state space formulation could be derived to enable the use of controller auto-regressive moving-average (CARIMA) model [87]. Generalized predictive control (GPC) predicts the plant's outputs over several steps based on future control assumptions in order to minimize the cost function over the prediction horizon [88, 89]. This method utilizes the CARIMA model but can also use a regular state space model [90] and aims to apply a control action that will minimize a finite horizon quadratic cost function. By minimizing the cost function considering the constraints (which may result some changes in the cost function), the control action is obtained [87, 91-93]. However, only the first estimated value will be sent to the plant and then the calculations will be repeated. It should be noted that with the increase in dimensionality and number of constraints, the system stability may get compromised. For this reason, many researchers working in the field of model predictive control started researching methods to enhance the robustness of the controls as well as the stability [94-96]. Jain, et al. [97] performed a review on statistical pattern recognition techniques in literature. Giannotti, et

al. [98] performed a multistep trajectory pattern mining using spatio-temporal pattern mining, however their technique requires previous knowledge of the data so it is more suited to post work analysis. Chen, et al. [99] used GPS and odometer data for pattern recognition of the vehicle to estimate repetitive patterns over time. Abed, et al. [100] used genetic algorithm techniques for pattern recognition with a success ratio of 95%. Hybrid technology have been studied and implemented in passenger vehicles and trucks, yet close to none literature can be found about hybrids in construction equipment. Only one paper [101] could be found covering the implementation of power split hybrid electric vehicle (PSHEV) technology in small wheel loaders and using a classic proportional–integral–derivative controller (PID) to control the system.

### **1.3. Thesis Outline**

The test bed machine investigated in this work is Caterpillar's (CAT) 966K series medium wheel loader (MWL) [102]. However, the procedures used are general such that they are applicable to other machines. Chapter 1 contained an introduction to the thesis in the form of the problem statement, literature review and thesis outline. Chapter 2 describes the machine and its operation as well as the mathematical model and software used to model the machine. Chapter 3 describes the control strategies under investigation. Chapter 4 discusses the results obtained through this investigation. Chapter 5 presents the conclusions reached from this investigation.

## **2. MEDIUM WHEEL LOADERS AND HYBRID TECHNOLOGY**

This chapter introduces the test machine (Fig. 4), machine model, and the hybrid technology implemented on the machine. This chapter describes the software tools adopted to create a complete virtual machine and environment model. The use mathematics based simulation for the development phase is known as virtual product development (VPD) which is more than developing on actual machines from the start. For this purpose, accurate virtual models with relatively high fidelity are needed to attempt mimicking the actual machine. However, replicating every aspect of the machine in virtual reality is impossible due to unpredicted factors and physical inaccuracies and reliability issues. Therefore, once the VPD is completed a prototype/test-bed must follow. The machine model was developed using the physics based mathematical equation and embedded in S-functions in Simulink [103-105].

### **2.1. Medium Wheel Loader**

To explain the MWL, the operations that the wheel loaders perform must be explained. The general cycle definitions provided by Caterpillar performance monitoring group are provided in table I. Note that the time is the total cycle time in seconds and distance in meters. These definitions are the guidelines for identifying and distinguishing the cycles from one another. There are five general cycles: truck-loading, load-and-carry, pile dressing, roading, and miscellaneous. Both the truck-loading and the load-and-carry are cycles that involve digging, moving earth from one location to another and dumping it at the new location. The truck-loading is loading a truck or a hopper with earth and is categorized into two major cycles: aggressive truck-loading (ATL), and moderate truck-loading (MTL).



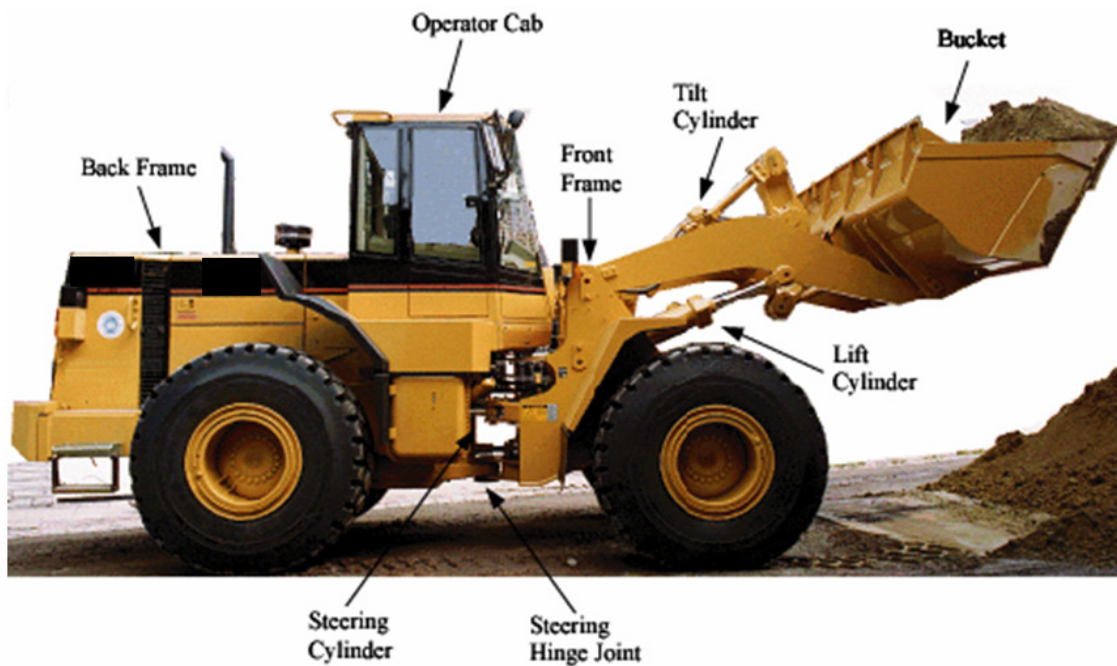


Figure 4: Medium Wheel Loader.

TABLE I MEDIUM WHEEL LOADERS WORK CYCLES DEFINITIONS

General Category	Cycle	Travel Distance (m)	Time/Distance
Specific Loading Cycles	Tight Aggressive Truck-loading	Less than 30	Less than 1
	Tight Moderate Truck-loading	Less than 30	Greater than 1
	Open Aggressive Truck-loading	50±10	Less than 0.9
	Open Moderate Truck-loading	50±10	Greater than 0.9
	Short Load-and-carry	150±10	Undefined
	Long Load-and-carry	Greater than 300	Undefined
Travel Distance-Based Cycles	All Tight Cycles	Less than 40	Undefined
	All Mid-Range cycles	40- 90	Undefined
	All Load-and-carry	Greater than 90	Undefined
Others	Pile Dressing	undefined	Undefined
	Roading	undefined	Undefined
	Miscellaneous	undefined	Undefined

ATL is characterized by its speed and the machine is operated with the engine at full throttle at all times. Moderate truck-loading (MTL) can be as fast as or slower than ATL but the operator varies engine speed command and may never reach full throttle. The load-and-carry cycles is moving dirt to a hopper far away from the pile and is defined by the travel distance into short and long. Pile dressing is moving the earth in the pile around to make it ready for the previous cycles. Rading is driving the loader from one location to another without being involved in any of the previous cycles. Miscellaneous is any other functions done by the loader that does not fall into the previous ones. There are five main systems (Fig. 5) in loaders, namely engine, powertrain, hydraulics, controllers, and chassis (frame and linkages). The engine is the primary source of energy for this machine from which all power requirements are withdrawn. The torque provided by the engine is split between two the powertrain which is responsible for the motion of the loader and the hydraulics which is responsible for mainly linkages operations and possibly braking, cooling fan motoring, vibration damping and steering. The controllers are the coordinators between all these functions and the operator. The loader systems and the machine model (Fig. 6) are discussed next.

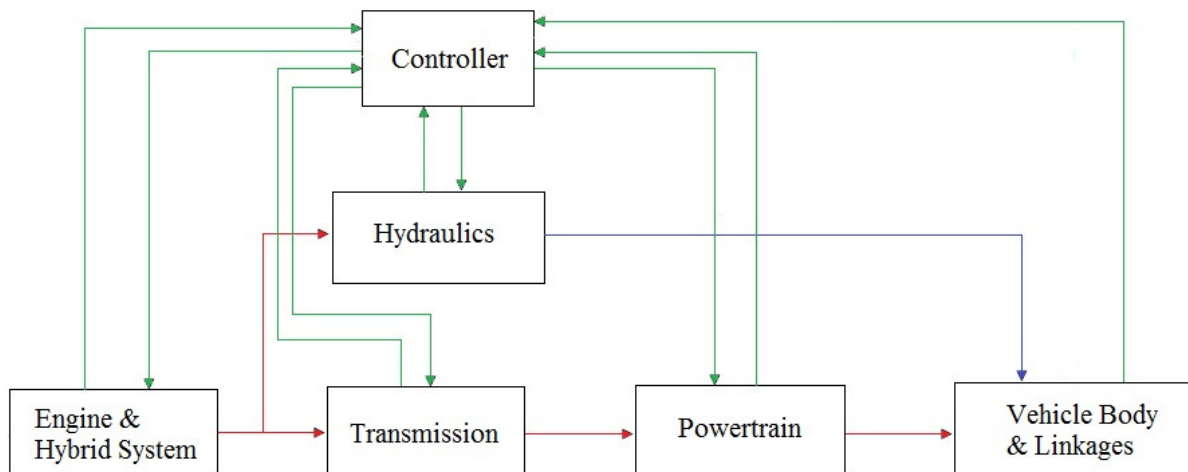


Figure 5: Wheel loader block diagram.

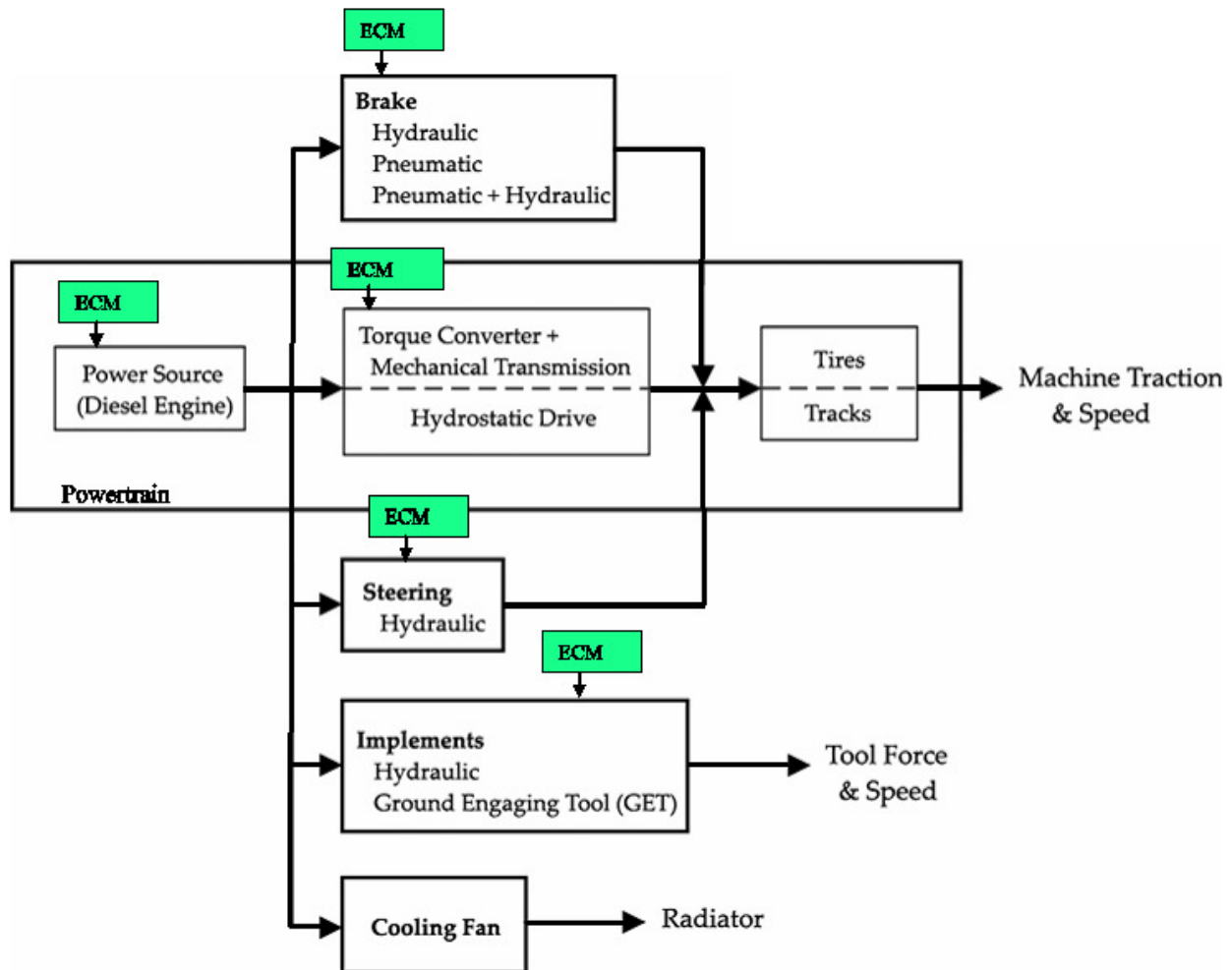


Figure 6: Wheel loader systems [2].

### 2.1.1. Engine

The original engine (Fig. 7) on this machine is a four stroke turbocharged after cooled injection diesel 9 liters engine [106], with power rating (Fig. 8) of about 224-261 kW at 1800-2200 rpm and compression ratio of 17:1 (Table II). . The downsized engine is a four stroke turbocharged after cooled injection approximately 7 liters diesel engine, with average power rating (Fig. 9) of 140-225 kW at 1800-2200 rpm and compression ratio of 16.5:1[107].



Figure 7: Wheel loader engine [102].

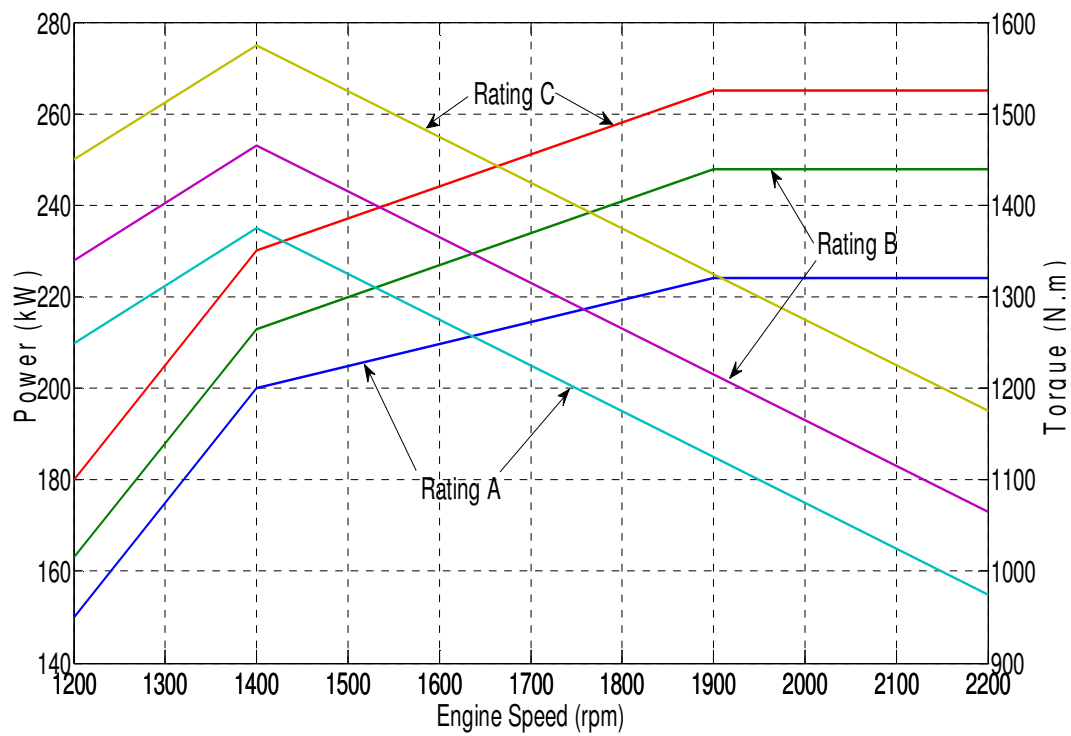


Figure 8: Rated 9 Liters engine lug curve and power rating (from [106]).

**TABLE II - ENGINE RATING**

Rating	Peak Power (kW) at 2200 rpm	Peak Torque (Nm) at 1400 rpm
A	224	1369
B	242	1483
C	261	1597

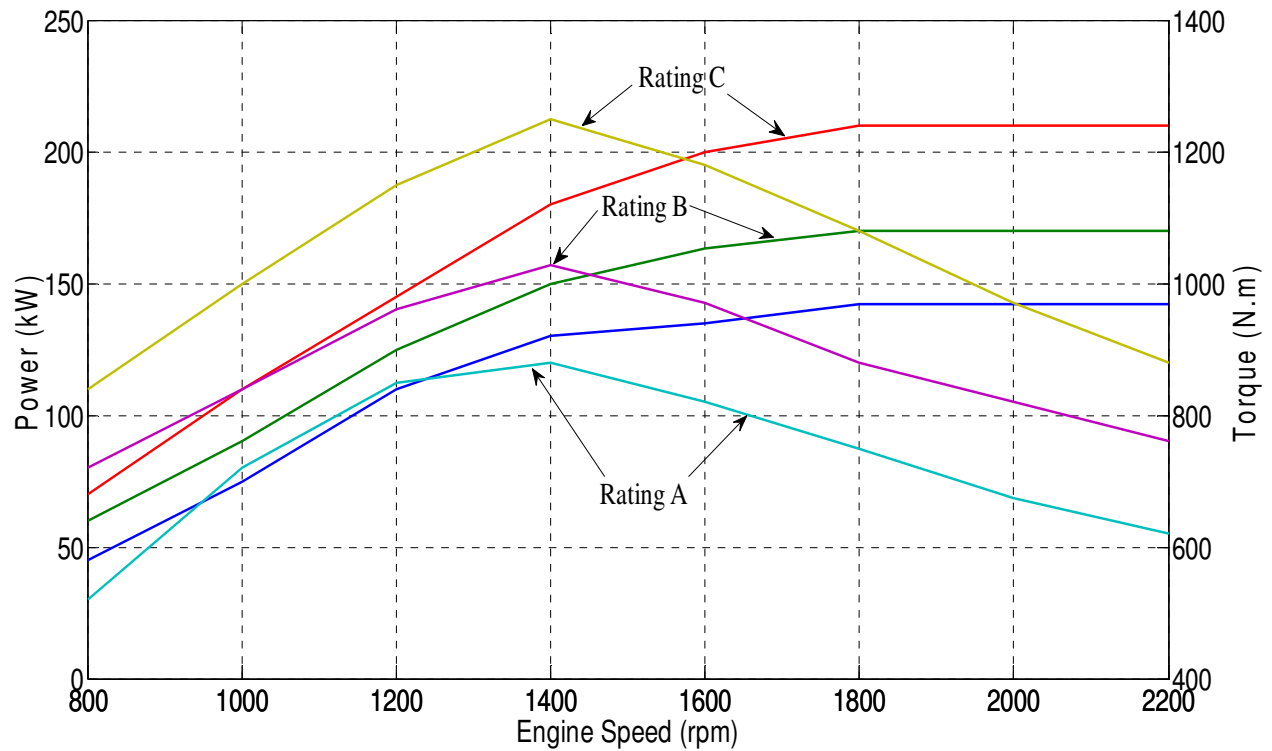


Figure 9: Rated 7 Liters engine lug curve and power rating (from [106]).

The output gross power from the engine is not the actual available power to the wheel loader main systems due to power consumptions from accessories such as the alternator, muffler, emission control, and cooling system [108]. Thus, the power losses (6-14%) must be accounted for when calculating the net available power to the powertrain and the hydraulics. Unlike automotive engines, the diesel engine speed in construction equipment is limited to about 2300 rpm for increasing torques due to the need for higher torque values at lower machine speeds, desire for longer engine life and reduced fuel consumption. The engine dynamic model allows for the calculation of the torque and speed along the lug curve and calculating the engine fuel consumption via the brake fuel consumption (BSFC) map (Fig. 10). The region between every 2 contour lines in the BSFC map represents an area of 50 grams per minute fuel consumption difference between the two contours. The most efficient range is that that lies above the 150 contour line which means that the engine is burning between 200 and 250 grams per minute at the given torque and speed. With hybrid implementation this engine downsizing to 7 liters allowing the engine to run in a more efficient zone and making the hybrid system more cost effective will be investigated.

### **2.1.2. Powertrain**

The main function of the powertrain is to transfer the torque from the engine to the wheels to create the necessary rimpull for the motion through a series of speed reductions and torque multiplications. The powertrain of a wheel loader consists of wheels, axle reductions (simple gear train) and either a torque converter (TC) and transmission or Continuously Variable Transmission (CVT). Both configurations will be discussed; however, the mathematical model is based on the TC while the testbed has a CVT implemented to observe the maximum fuel reduction and efficiency increase obtainable from combining different systems.

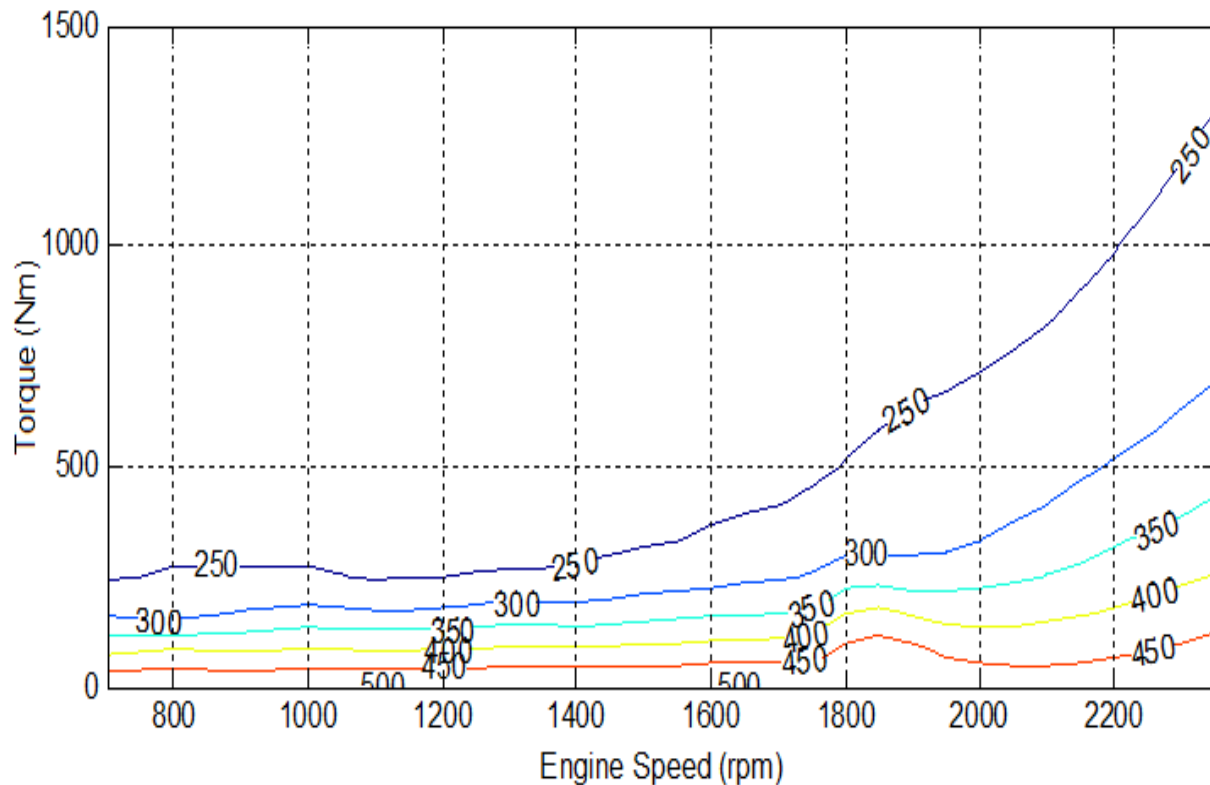


Figure 10: Brake specific fuel consumption map.

#### **2.1.2.1. Torque Converter and Transmission**

A TC is a hydro-dynamic coupling which transfers torque between its input and output while absorbing the difference in speed, hence, it is the evolution from clutches. The difference in speed between input and output is absorbed and dissipated in the oil inside the TC in the form of heat. The main components of a TC (Fig. 11<sup>1,2</sup>) are the impeller, turbine, and stator.

<sup>1</sup> Nice, Karim. "How Torque Converters Work" 25 October 2000. HowStuffWorks.com. <<http://auto.howstuffworks.com/auto-parts/towing/towing-capacity/information/torque-converter.htm>> 02 July 2012.

<sup>2</sup> <http://vmttec4844.blogspot.com/>

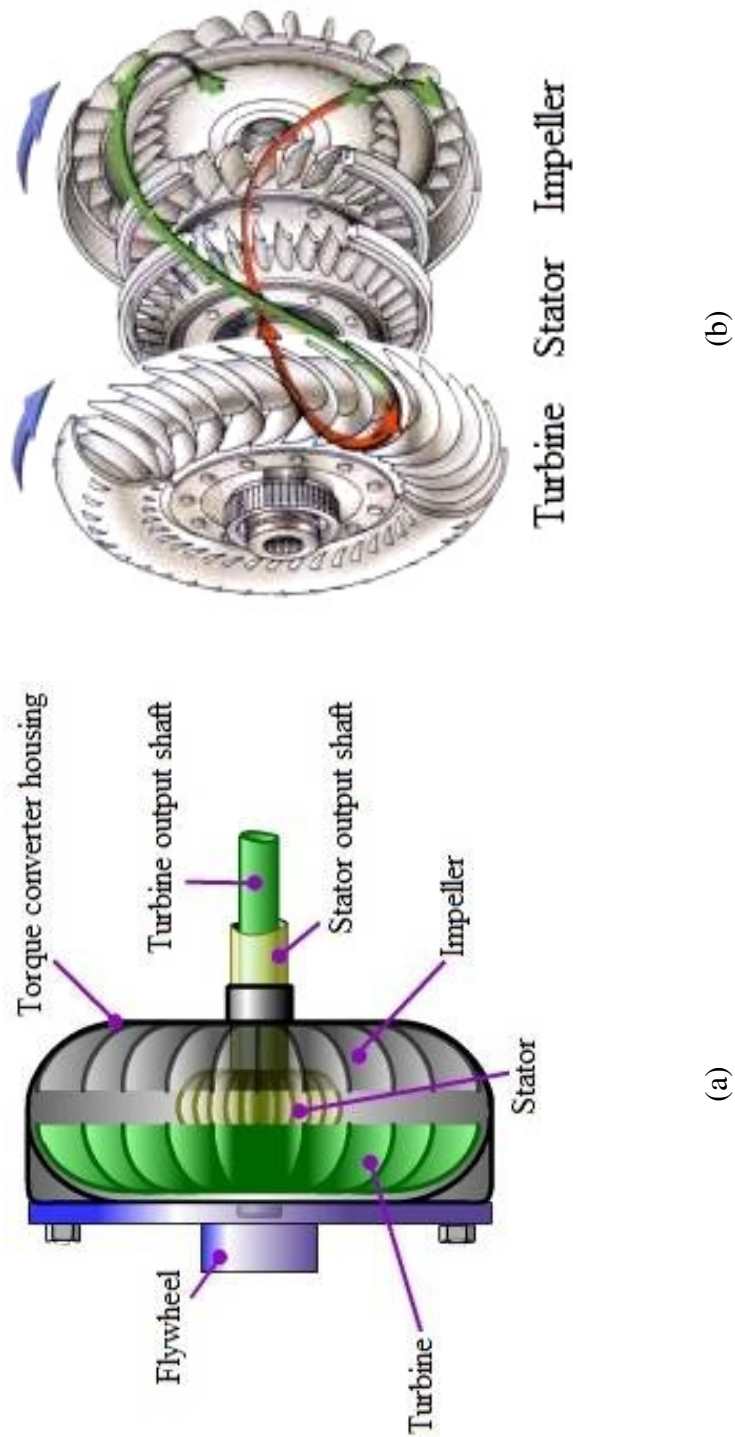


Figure 11: Torque converter<sup>3,4</sup>.

<sup>3</sup> Nice, Karim. "How Torque Converters Work" 25 October 2000. HowStuffWorks.com. <<http://auto.howstuffworks.com/auto-parts/towing/towing-capacity/information/torque-converter.htm>> 02 July 2012.

<sup>4</sup> <http://vmttec4844.blogspot.com/>



The analysis of the TC dynamics is not within the perspective of this work, however, the mathematical modeling basis will be presented. The two main defining characteristics of the TC are the primary torque  $T_p$  which is the torque of the impeller rated at a certain speed  $N_{rated}$  (usually 1700 rpm) and the torque ratio  $T_r$  which is the ratio between the output turbine torque and the input impeller torque.

$T_r$  is also function of the speed ratio  $S_r$  which is the ratio between the output turbine speed and the input impeller speed. Through the knowledge of  $T_p$ ,  $S_r$ , the rated and the input speed  $N_i$ . The input torque  $T_i$  can be calculated at various speeds using the following equation and figure 11:

$$T_i = T_p \left|_{S_r} \left( \frac{N_i}{N_{rated}} \right)^2 \right. \quad (2.1)$$

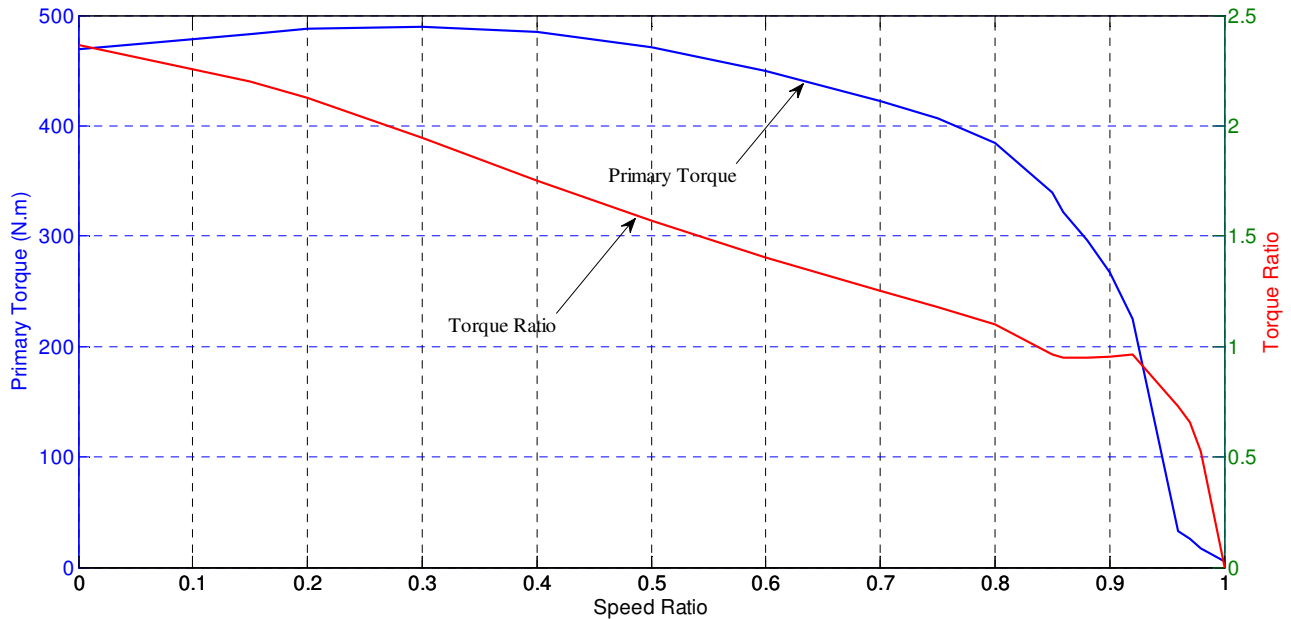


Figure 12: Torque converter characteristics.

The torque converter is followed by a gearbox which reduces the output speed to a desired range for the machine ground velocity. The gearbox is constituted of several planetary gear trains (Fig. 13<sup>5</sup>) connected together via brakes and clutches that determines the final reduction ratio. The explanation of how the mechanism works is not within the scope of this work, however, detailed explanation is available in literature [108]. The regular gear train in wheel loaders has four forward speeds, four reverse and one neutral (Table III). The dynamic transmission model is based on multiple look up tables for the gear combinations and clutches' pressures.

**TABLE III - TRANSMISSION GEAR RATIOS**

<b>Gear shift</b>	<b>Gear ratio</b>
4F	-0.77
3F	-1.36
2F	-2.44
1F	-4.66
N	0
1R	4.22
2R	2.21
3R	1.23
4R	0.70

#### **2.1.2.2. Continuously Variable Transmission**

A CVT is a transmission that can change steplessly through gear ratios, thus, giving smoother performance, and avoiding jumps between gearshifts and providing better fuel economy. There are many types of CVT configurations such as the full toroidal, variable belt drive and the hydrostatic.

<sup>5</sup> <http://www.caranddriver.com/photos-09q4/309587/2010-bmw-activehybrid-x6-automatic-transmission-and-electric-motor-diagram-photo-310275>

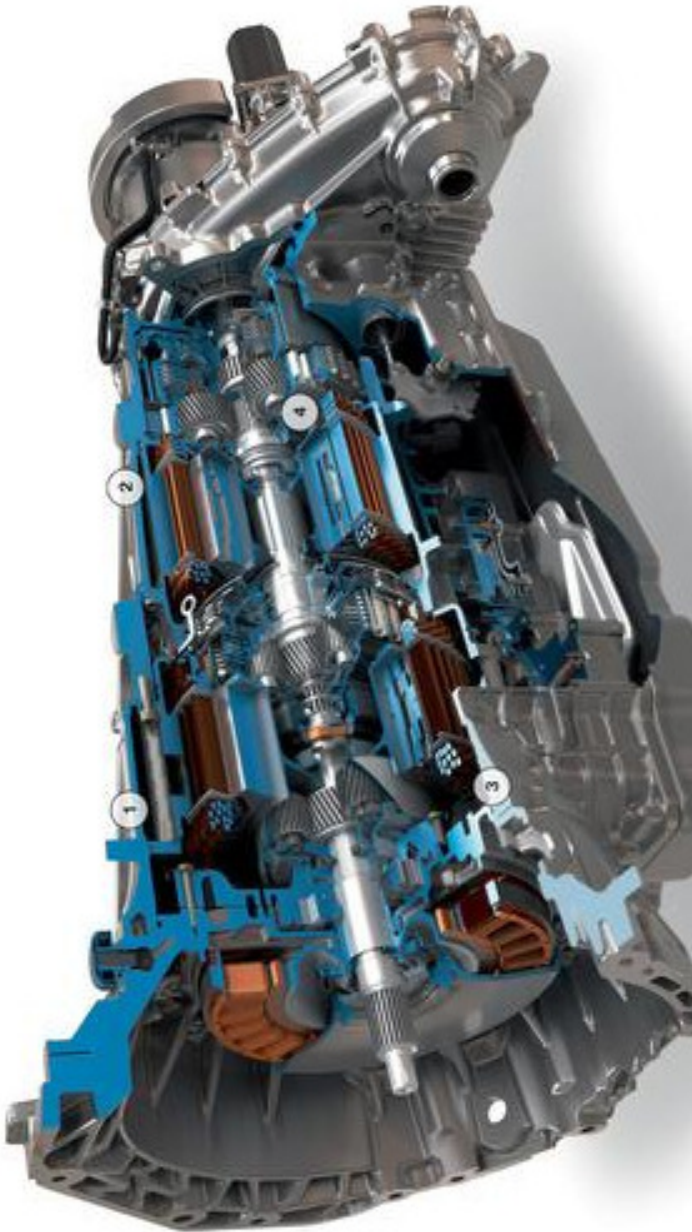


Figure 13: Planetary gearbox<sup>6</sup>.

<sup>6</sup> <http://www.caranddriver.com/photos-09q4/309587/2010-bmw-activehybrid-x6-automatic-transmission-and-electric-motor-diagram-photo-310275>

The hydraulic parallel path variable (also known as the hydro-mechanical CVT) being used is not a hydrostatic one while it contains one in its system. The hydraulic parallel path variable (HPPV) (Fig. 14<sup>7</sup>) consists of three systems (Fig. 15): mechanical transmission and hydrostatic CVT (Fig. 16) parallel to each other to avoid using a wide range, less efficient CVT [19] and a synchro system to add both outputs together. At a low speeds, power is transmitted hydraulically, and at a high speed, power is transmitted mechanically. Between these extremes, the transmission uses both hydraulic and mechanical means to transfer power. The mechanical path is a mechanical transmission that enables gear shifting and is covered in literature [108]. In the hydrostatic CVT, the engine operates variable-displacement pumps to vary the fluid flow into hydrostatic motors and the fluid flow is converted back into rotational motion.

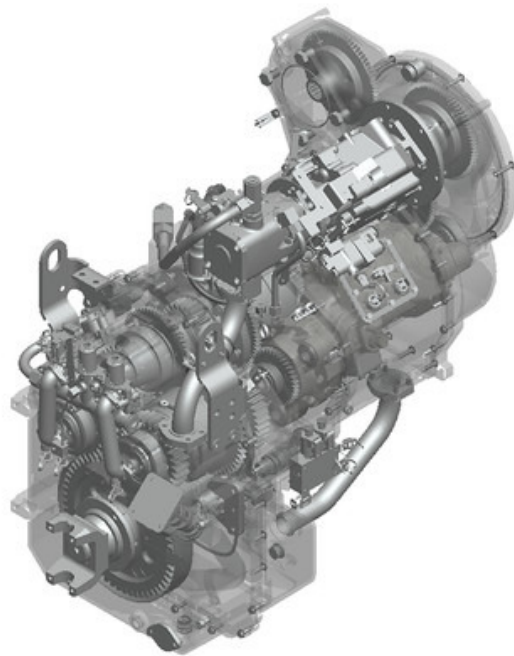


Figure 14: Hydraulic parallel path variable<sup>8</sup>.

---

<sup>7</sup> <http://www.oemoffhighway.com/article/10829058/a-shift-away-from-shifting>

<sup>8</sup> <http://auto.howstuffworks.com/cvt4.htm>

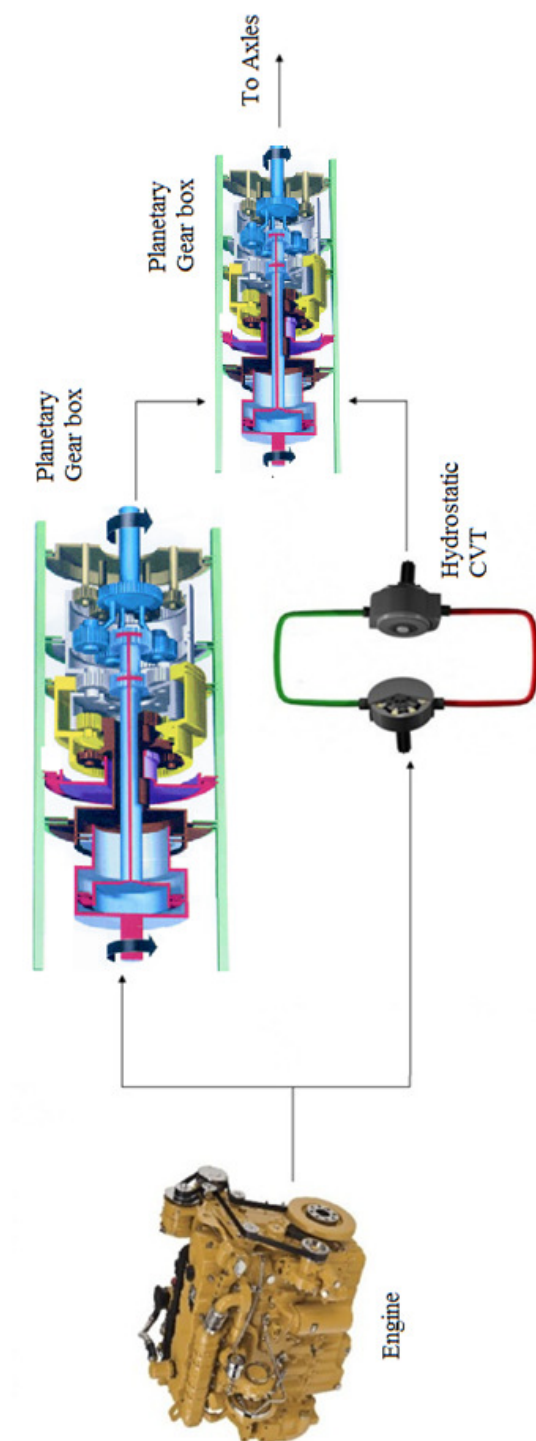


Figure 15: Hydraulic parallel path variable System.

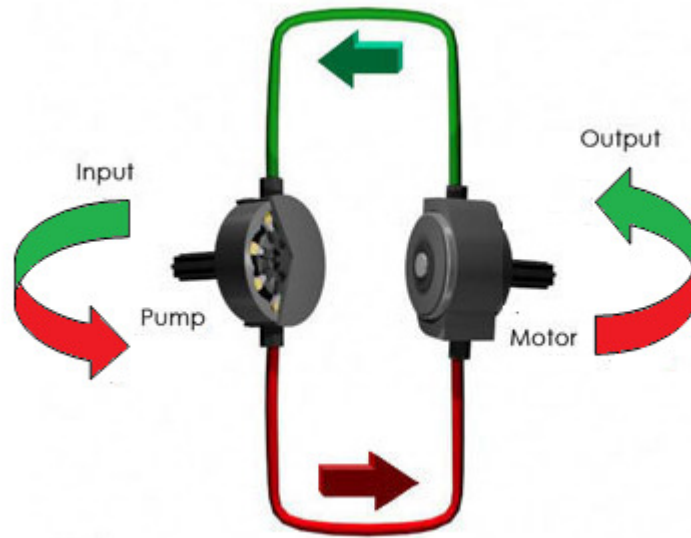


Figure 16: Hydrostatic continuously variable transmission.

### 2.1.3. Implement Hydraulics

MWL hydraulics system is closed center load sensing hydraulics system. This system is common trend in MWL as it avoids dissipation of energy as it adapts the amount of flow provided by the pump to the real needs of the machine, minimizing the losses unlike tandem center systems. It is not within the scope of this thesis to give a full review of this type of hydraulic system; however, a brief description for the hydraulic circuit of the MWL will be given.

The key features of this system are the following:

- Load sensing hydro-mechanical axial piston pump.
- Closed center proportional valve with post-compensation.
- Both tilt (tilting of the bucket) and lift (arm lever lift) have the same priority.

The load sensing system compares the pump pressure at the output to the cylinder pressures and adjusts the pump's swash plate based on that feedback in order to provide the correct amount of

flow and maintain a certain pressure differential (Fig. 17<sup>9</sup>). A shuttle valve senses the highest between the two tilt and lift pressures and that pressure is the one sent out through feedback for comparison. The following equation governs the angle of the pump's swash plate [2]:

$$\theta_{cmd} = \theta_{offset} + K(\Delta P_{cmd} - (P_s - P_L)) \quad (2.2)$$

where  $\theta_{cmd}$  is the commanded swash plate angle,  $\theta_{offset}$  is the swash plate angle offset from the desired position,  $K$  is a gain,  $\Delta P_{cmd}$  is the desired pressure differential,  $P_s$  is the pump outlet pressure, and  $P_L$  is the load pressure. A pressure limiting control system in the pump called the high pressure cut-off or pressure compensator whose function is to limit the maximum system pressure by reducing pump displacement to zero when the set pressure is reached. A traditional load sensing hydraulic circuit is shown in figure 18<sup>10</sup>. The post compensation (Fig. 19) regulates the amount of flow sent to the tilt and lift based on the pressure feedback from both valves such that the valve with the higher pressure receives more flow than that with the lower pressure, i.e. it maintains a constant pressure drop. The spool movement of a compensator valve is governed by the following relationship:

$$\Delta x_s = \frac{1}{K_{spring}}(p_s A_s - p_l A_l) \quad (2.3)$$

---

<sup>9</sup> <http://www.mobilehydraulictips.com/efficient-mobile-hydraulic-systems/>

<sup>10</sup> <http://www.nautical-structures.com/products/hydraulic-power-and-controls/load-sensing-hydraulic-system.html>

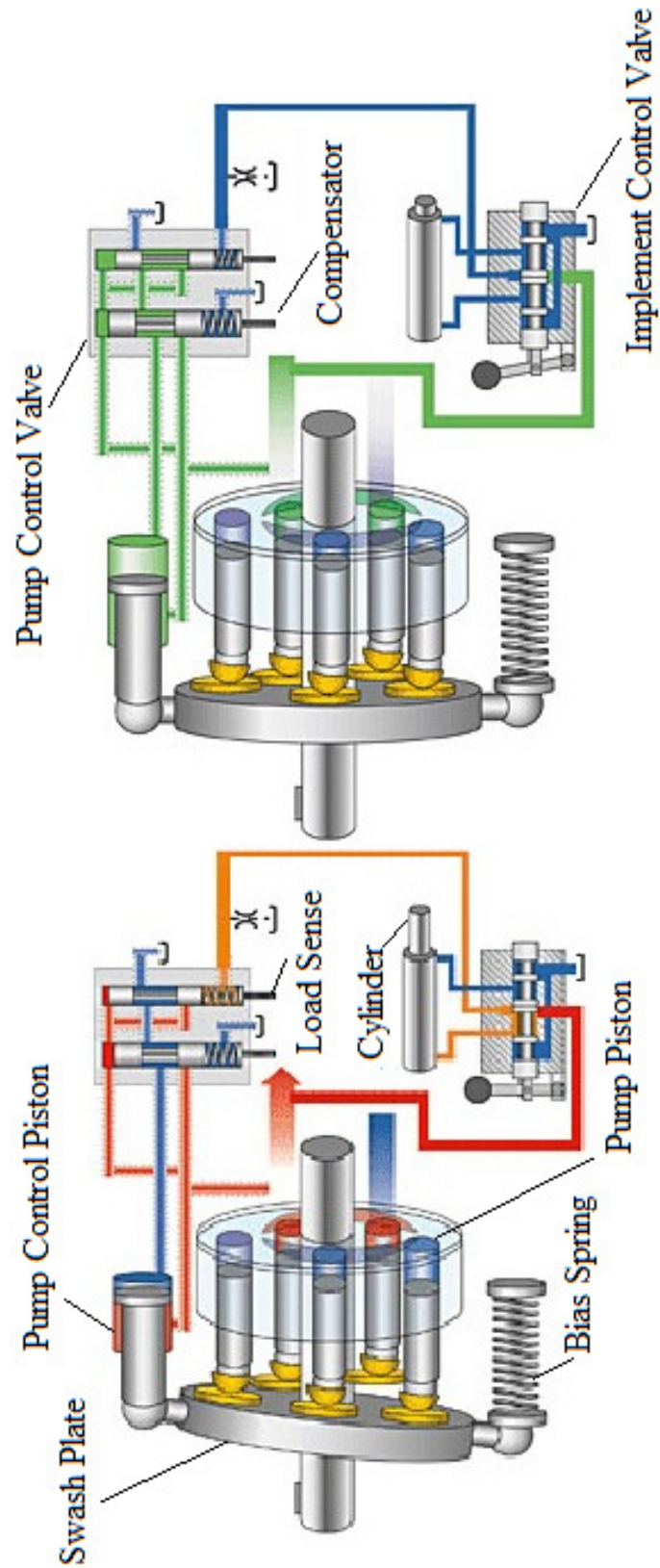


Figure 17: Load sensing axial piston pump with swash plate<sup>11</sup>.

<sup>11</sup> <http://www.mobilehydraulictips.com/efficient-mobile-hydraulic-systems/>



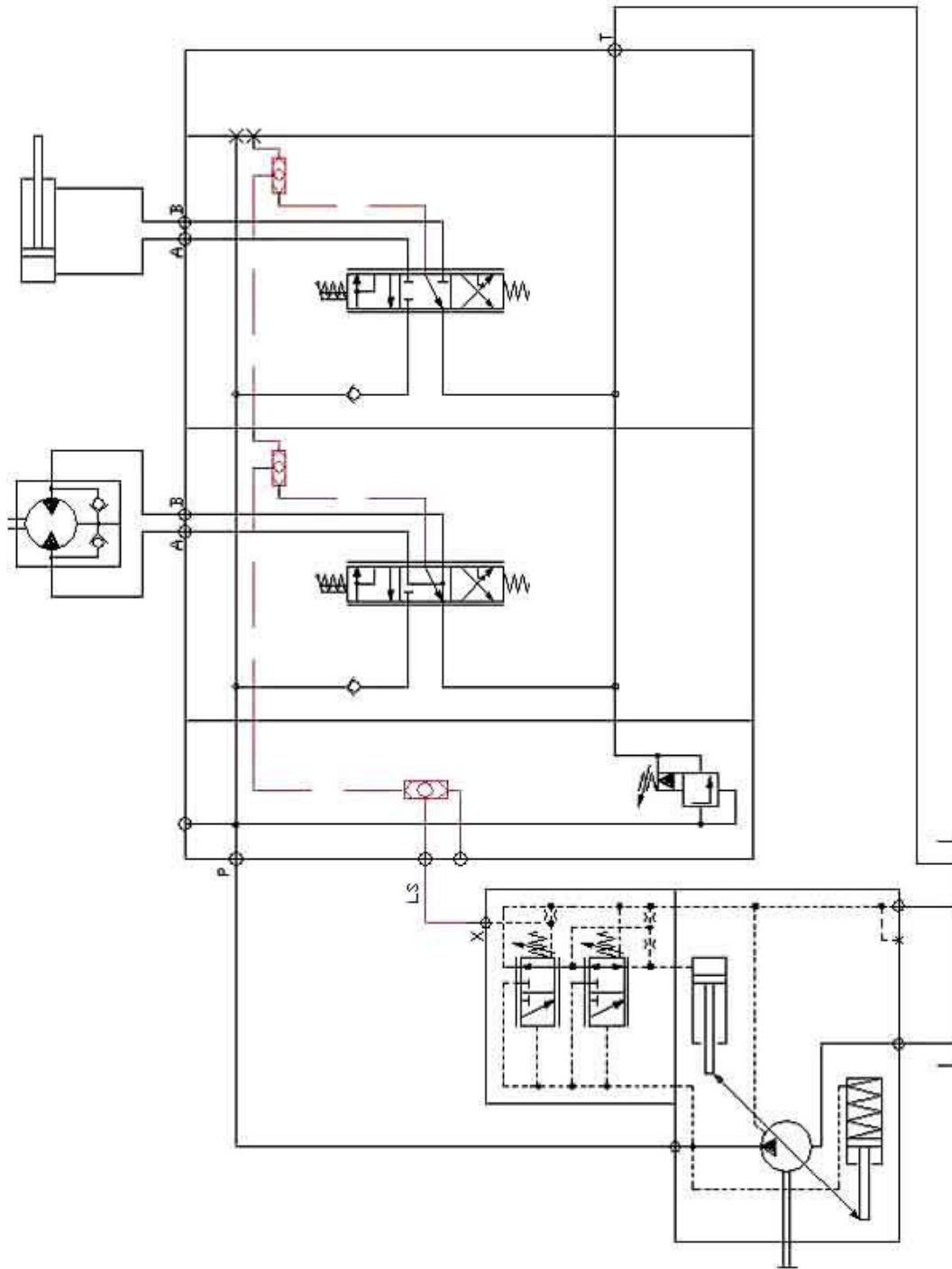


Figure 18: Traditional load sensing hydraulic circuit<sup>12</sup>.

<sup>12</sup> <http://www.nautical-structures.com/products/hydraulic-power-and-controls/load-sensing-hydraulic-system.html>

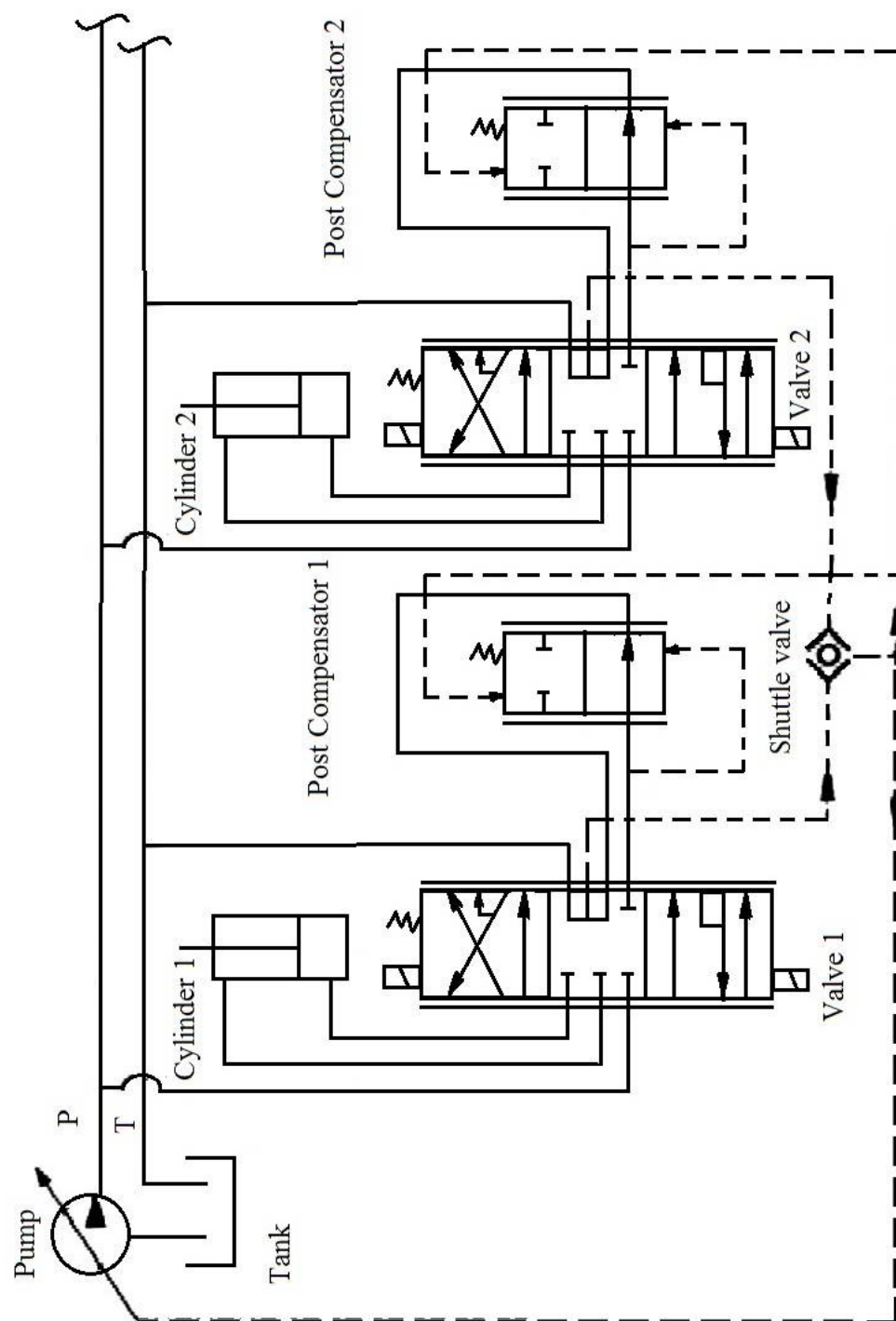


Figure 19: Post compensator configuration in multifunction hydraulic circuit [2].

Four equations govern the hydraulics system. These equations are the dynamics and static hydraulics and the hydro-mechanical equations which are listed below

$$Q = \frac{V}{\beta} \frac{dP(t)}{dt} \quad (2.4)$$

$$Q = C_d A \sqrt{\frac{2\Delta P}{\rho}} \quad (2.5)$$

$$Q = A \frac{dx(t)}{dt} \quad (2.6)$$

$$F = PA \quad (2.7)$$

where  $\beta$  is the Bulk modulus,  $Q$  is the volumetric flow rate,  $P$  is the pressure,  $\rho$  is the oil density,  $C_d$  is the valve coefficient,  $A$  is the valve opening area and  $x$  is the displacement of the piston.

#### **2.1.4. Chassis**

The chassis is the body and linkages of the machine and it is governed by the mechanical kinematic constraints and dynamics which can be represented using multibody dynamics approaches. The discussion of these approaches is out of scope of this work and will not be presented.

#### **2.2. Hybrid Technology**

There are three main hybrid concepts and energy storing devices in hybrid vehicles being implemented and tested: electric, hydraulic, and mechanical hybrids. Both the electric and

hydraulic concepts employ energy conversion concepts. The MWL test bed has all three concepts implemented on it (Fig. 20) to compare between their performance and cost.

### 2.2.1. Electric Hybrid

The electric hybrid concept (Fig. 21, 22) is to convert the regenerative mechanical energy to electrical energy via an electric generator. The electric energy is then stored in electro-chemical batteries, pending reuse via an electric motor on power demand. The implemented electric hybrid graphics is shown in figure 23. The electric hybrid consists of a motor/generator (ISG) combo, inverter that requires a separate cooling system, and a Lithium-Ion battery. The Li-I battery was selected as it is the most promising rechargeable battery technology available, and is widely used in electric hybrid technology [109]. The battery SOC can be calculated using the following equation:

$$SOC = SOC_0 - \int \frac{i(t)}{Q(i(t))} dt \quad (2.8)$$

where  $Q(i(t))$  is the ampere-hour capacity of the battery at current rate  $i$ . While the electric hybrid is the most expensive, due to its maturity is receiving the most investment in all mobile industries. With the engine downsize, the Heinzmann integrated starter generator (ISG) system costs come to neutral. The diesel engine is the primary power plant, electric hybrid constitute the energy bumper. The ISG adds power to powertrain from the battery when power assist is needed, and stores the energy to the battery from the powertrain when there is power-storage opportunity exists. The electric hybrid cooling cycle passes through all the components where the coolant fluid goes through the shunt tank into radiator, through the pump, inverter, battery and ISG and then back to radiator.

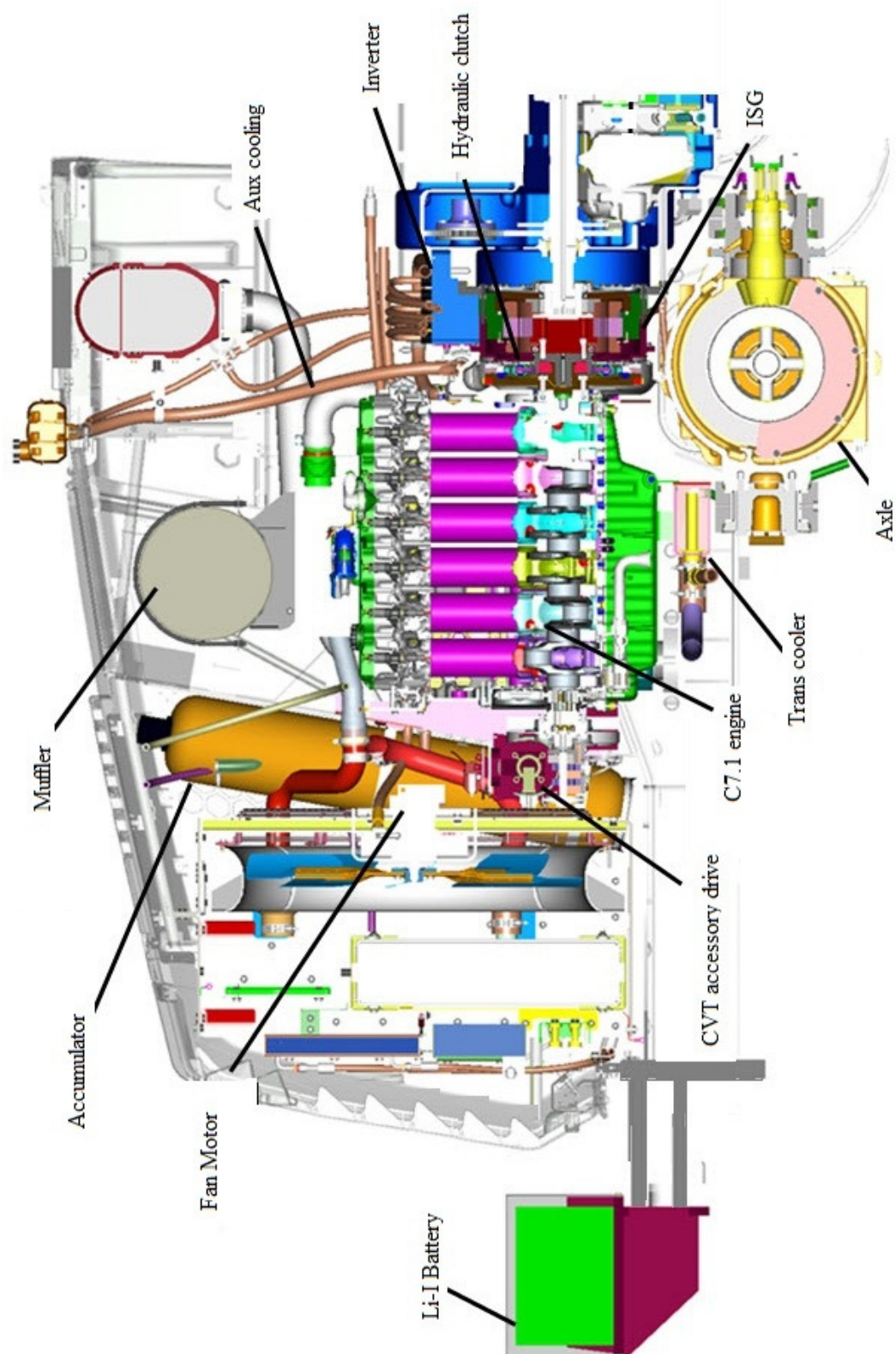


Figure 20: Test bed hybrid concepts implementation.

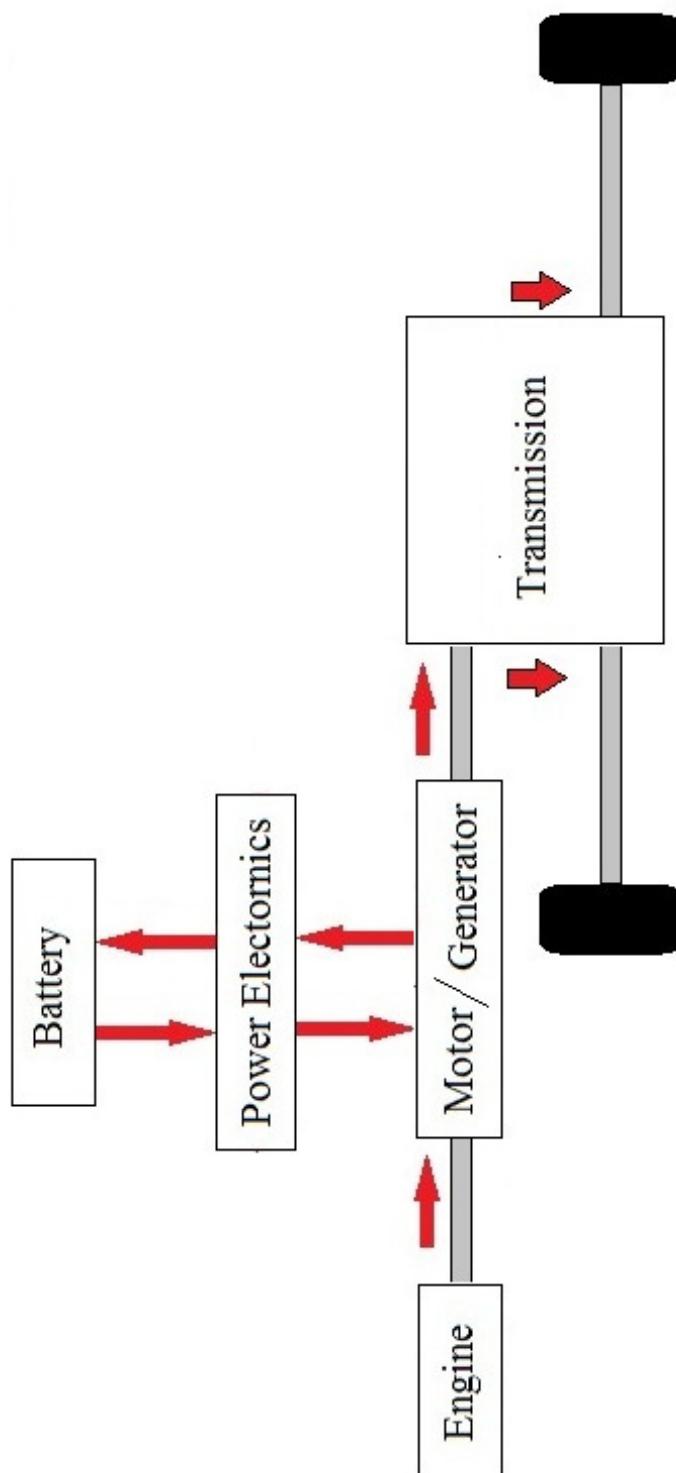


Figure 21: Electric hybrid concept.

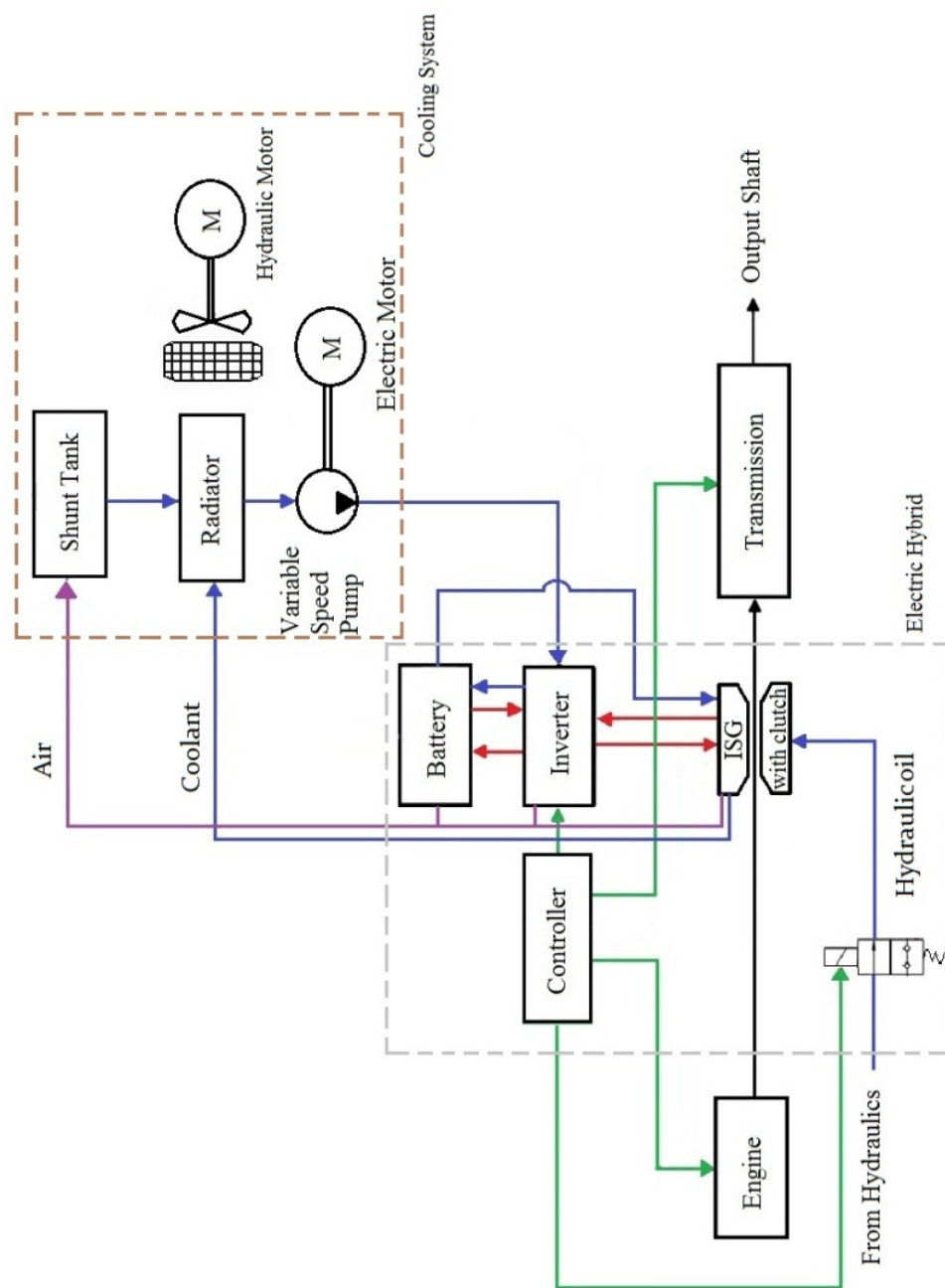


Figure 22: Electric hybrid powertrain for wheel loader.

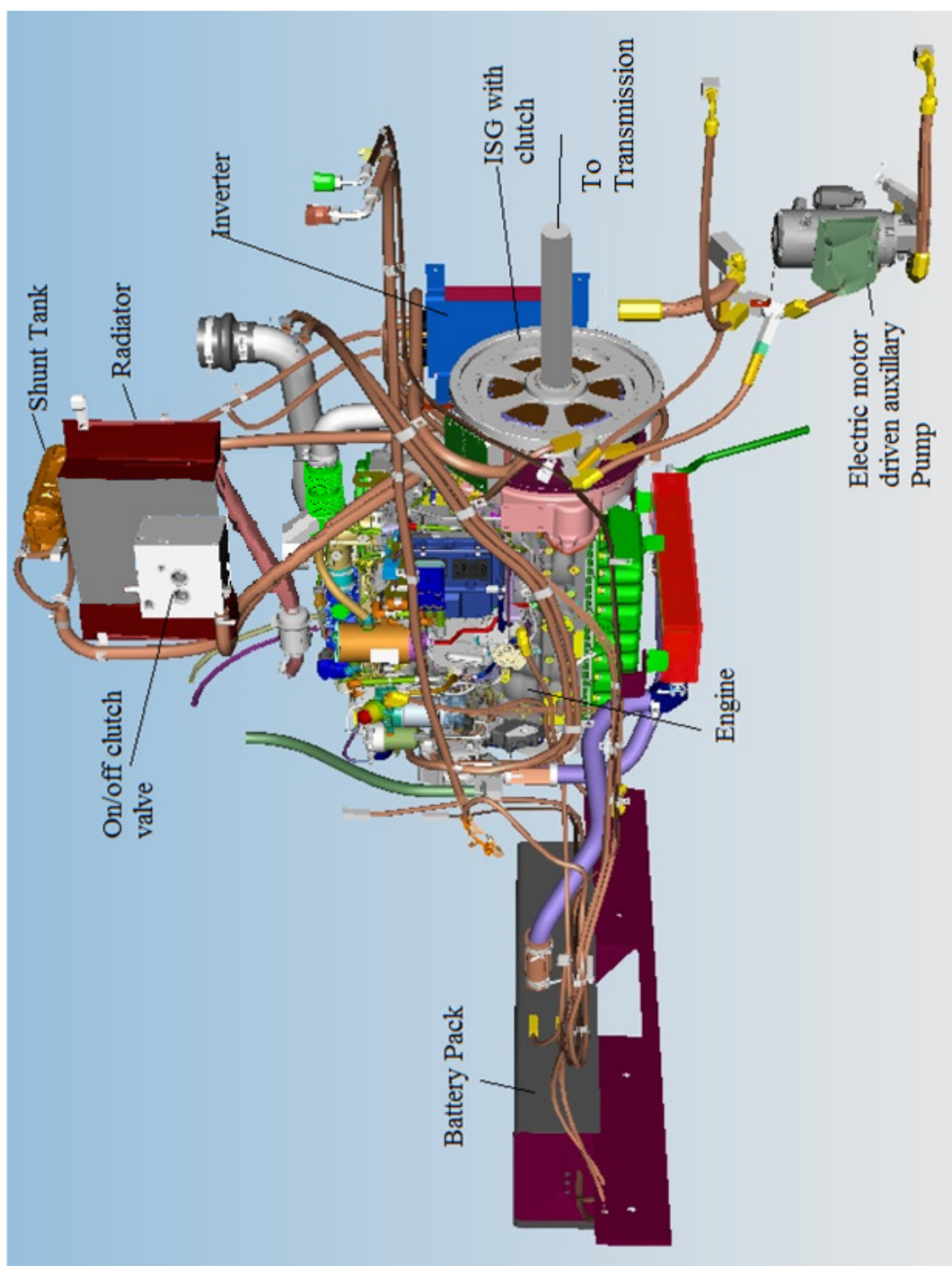


Figure 23: Electric hybrid powertrain for wheel loader prototype.



Also, the shunt tank is connected to all the hybrid parts to allow air bubbles to escape and to the radiator to allow coolant to expand and supply excess fluid.

### **2.2.2. Hydraulic Hybrid**

The hydraulic hybrid concept (Fig.24, 25) is to convert the regenerative mechanical energy to a pressurized fluid flow in order to store it in high pressure accumulators, and reuse it by either back conversion to mechanical energy via a hydraulic a motor or as hydraulic energy based on the power demands of the machine.

Figure 26 shows the hydraulic hybrid circuit. For the hydraulic hybrid implementation the originally combined braking and cooling fan circuits are separated and the hydraulic hybrid is connected to the fan circuit. During charging the high pressure accumulators, high-pressure oil is provided via the implement pump during implement pump retarding (Fig. 27) and the fan circuit is powered by the engine.

During discharging (Fig. 28), the hydraulic oil flows from the accumulators, hence, powering the hydraulic motor which turns the fan. When accumulators are discharging the torque at the variable displacement pump is added to the engine output decreasing the engine load through adjusting the pump's swash plate angle. The pump's swash plate angle controls the torque at pump/motor output shaft, through which the load of the engine can be increased or decreased. Note that the fan is allowed to go in reverse to blow out accumulated dirt. Figure 29 shows the implemented hydraulic hybrid graphics. For compact design, most of the valves are built into one block or included with the pump block.

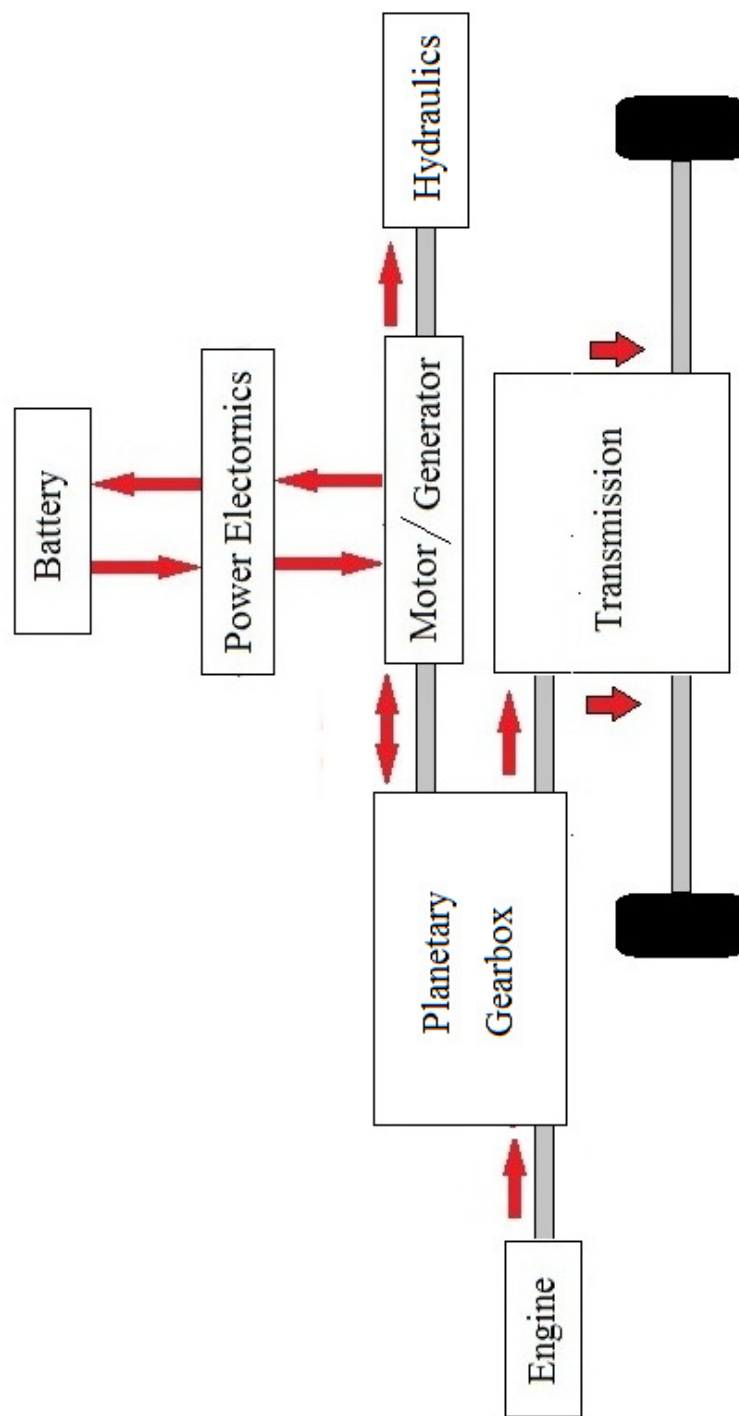


Figure 24: Hydraulic hybrid concept.

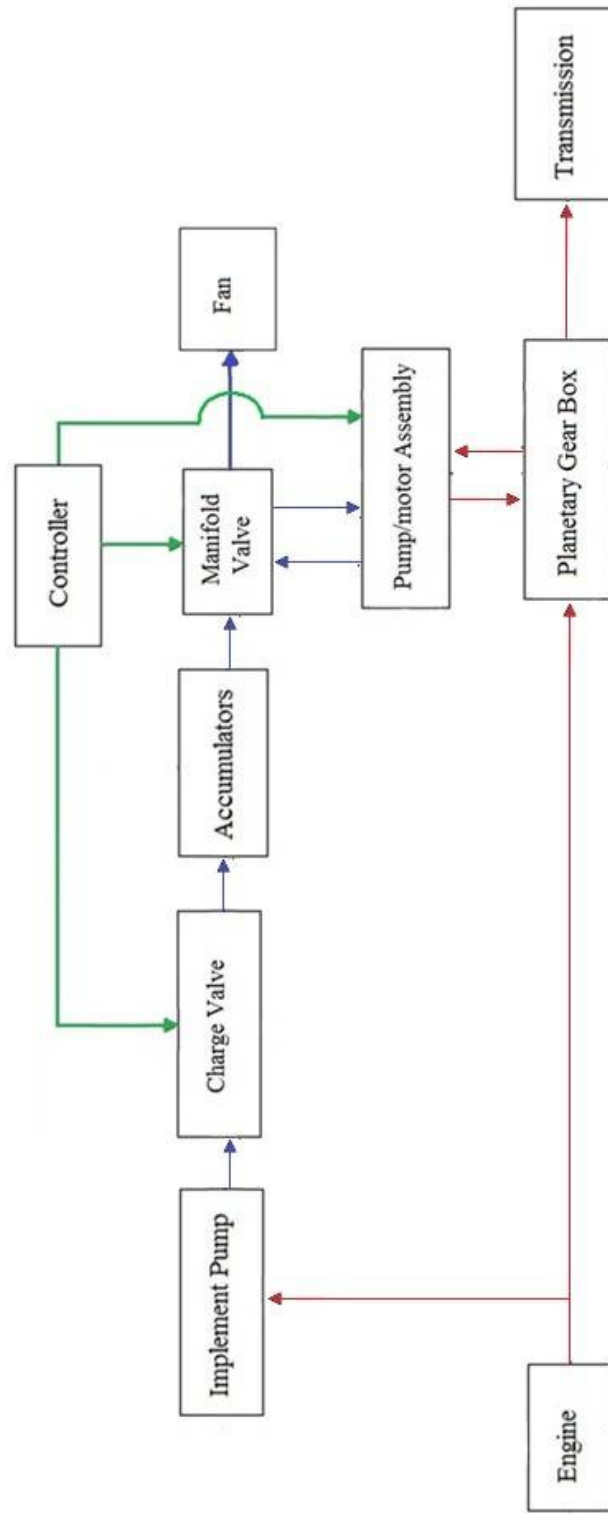


Figure 25: Hydraulic hybrid powertrain for wheel loader block diagram.

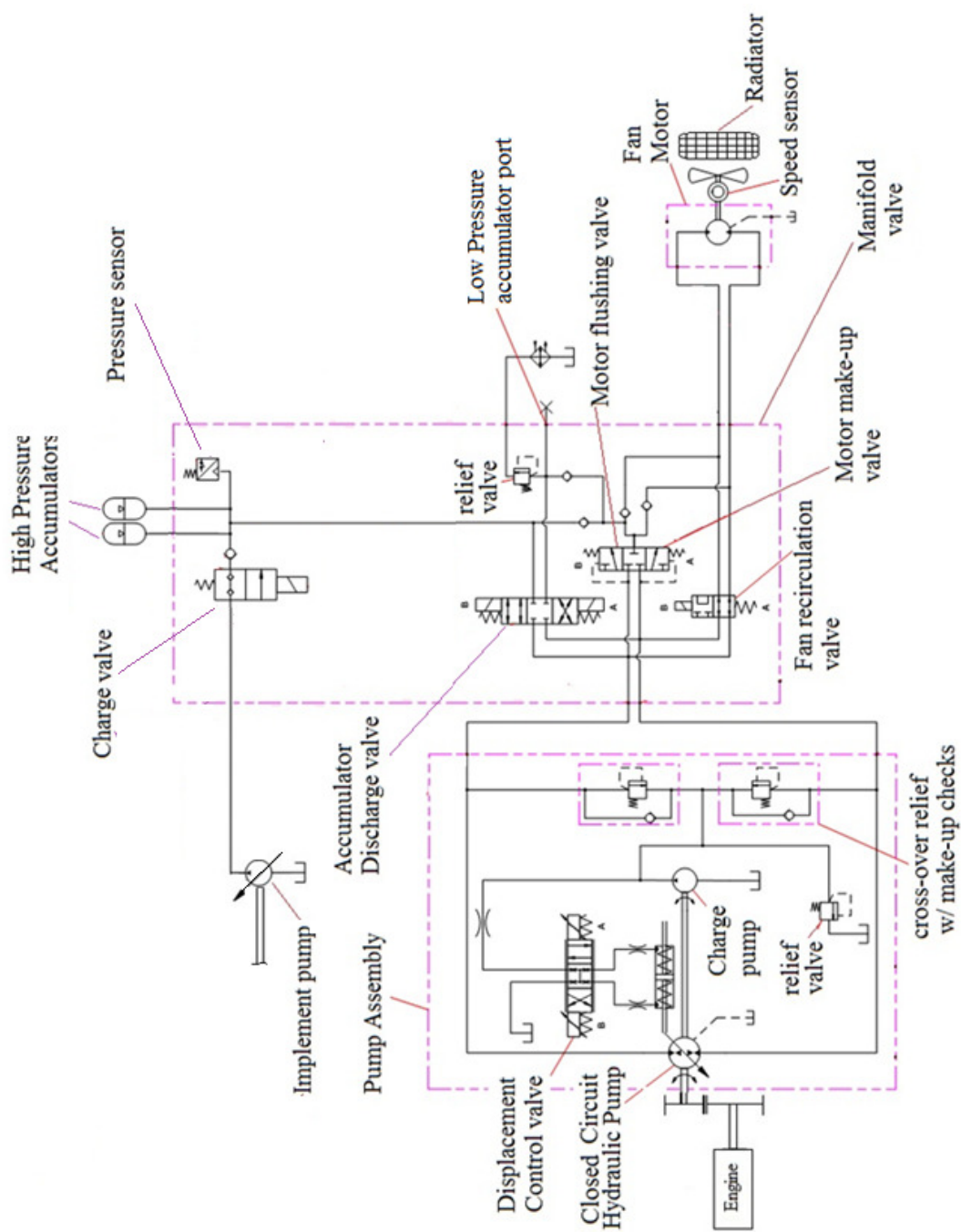


Figure 26: Hydraulic hybrid circuit.

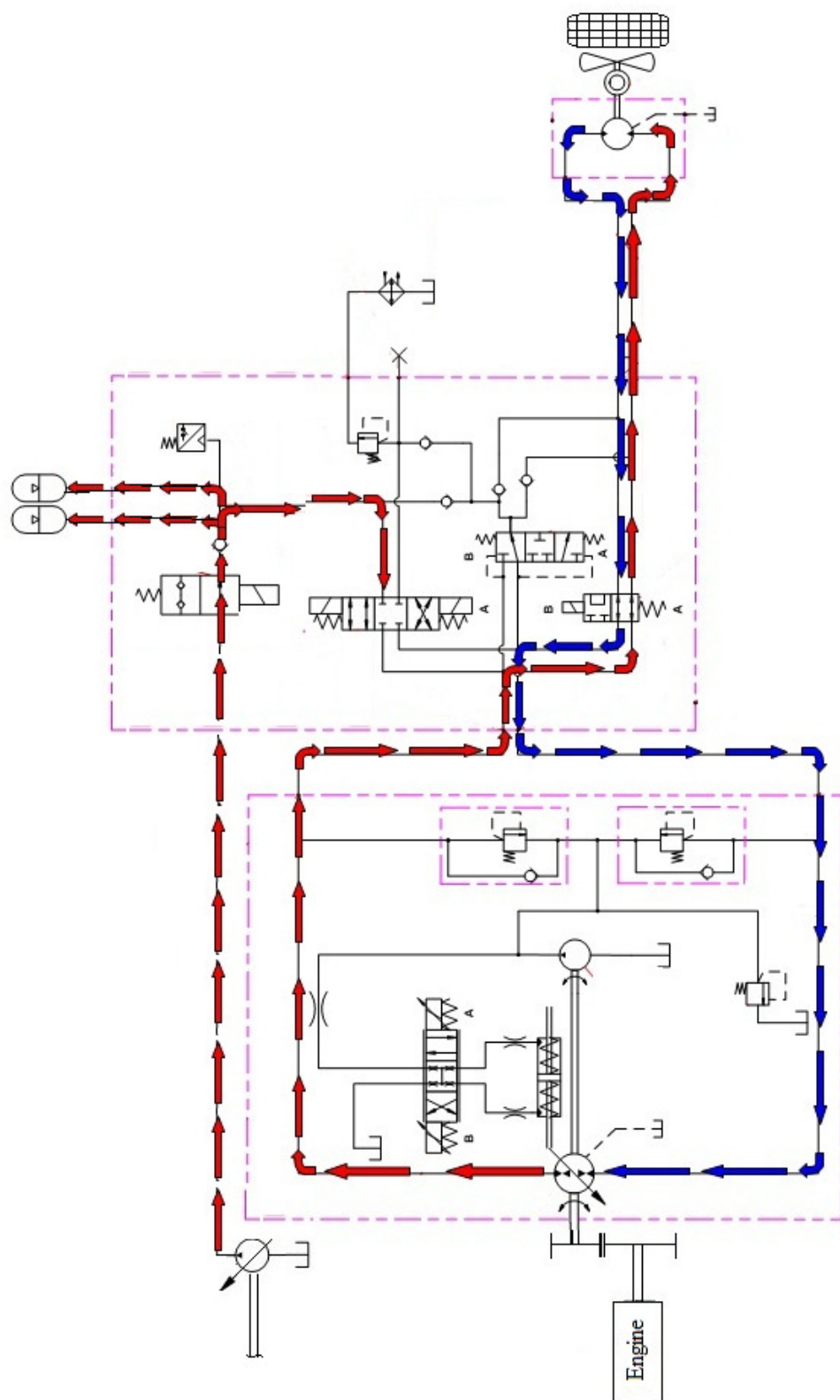


Figure 27: Hydraulic hybrid circuit charging.

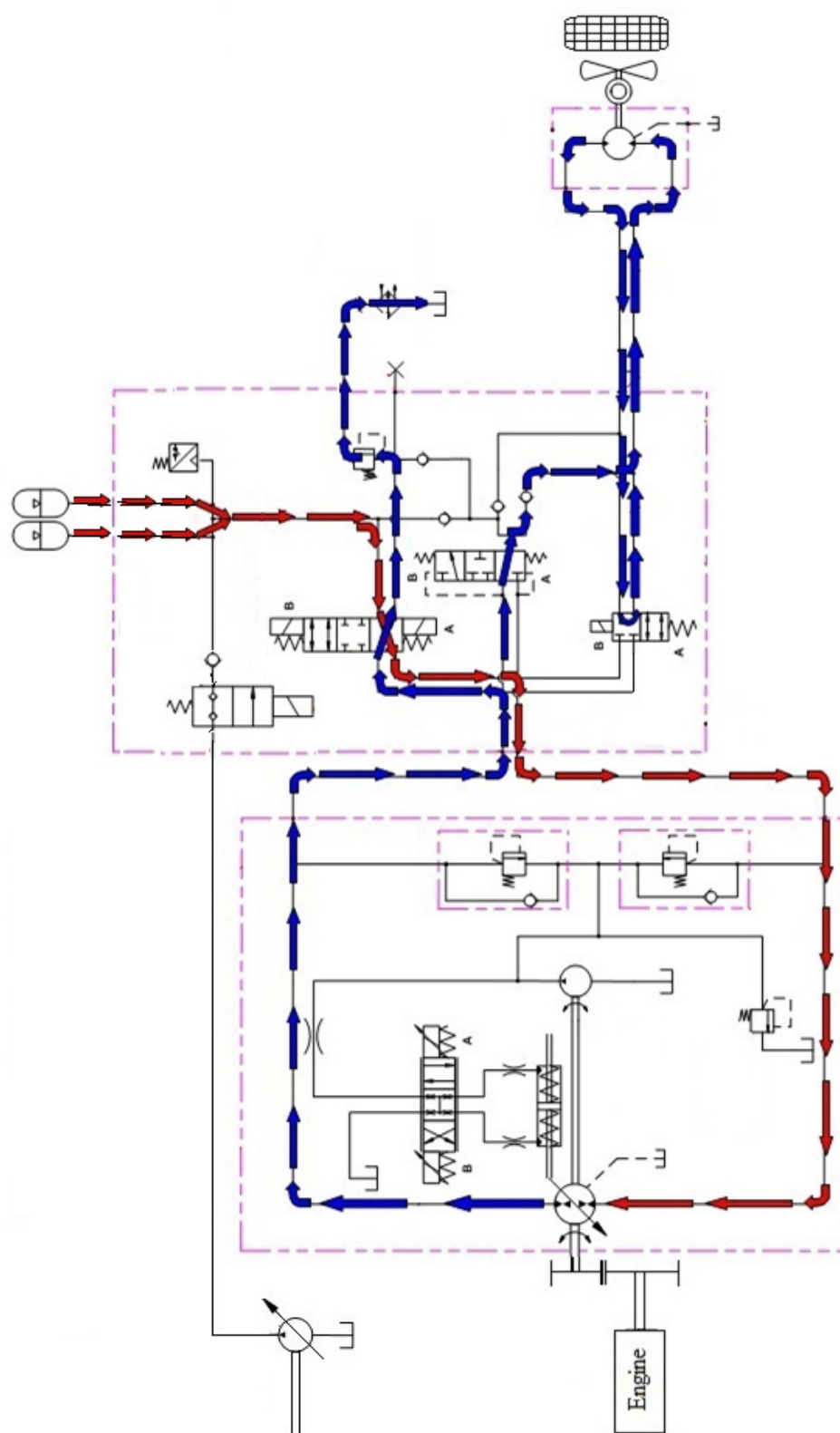


Figure 28: Hydraulic hybrid circuit discharging.

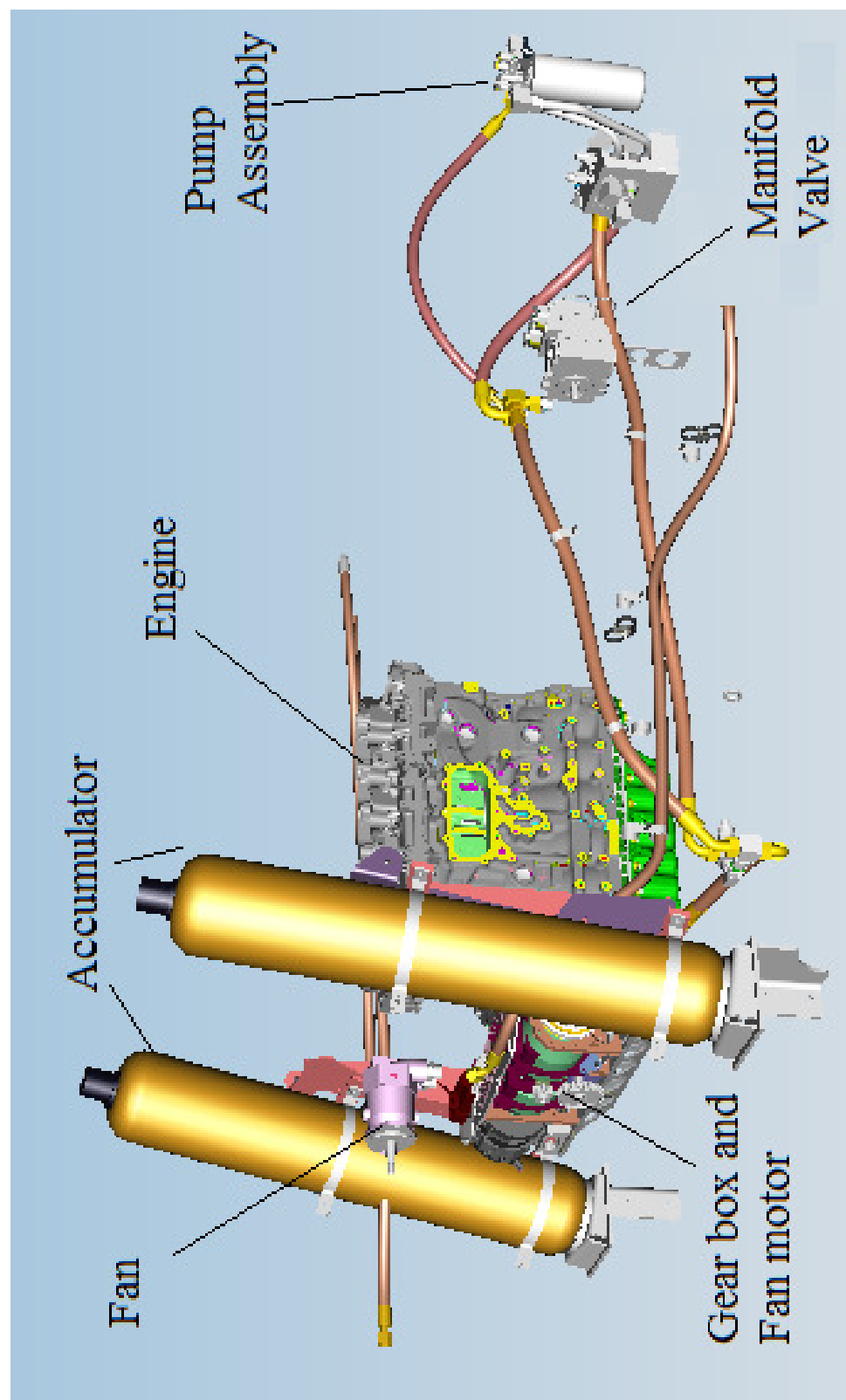


Figure 29: Hydraulic hybrid concept.

### 2.2.3. Flywheel Hybrid

The flywheel hybrid (Fig.30, 31) stores the regenerative energy as a kinetic energy in a rotating flywheel. The stored energy is directly proportional to the product of the flywheel energy and the speed of rotation of the flywheel squared. The energy relation is governed by the following equation:

$$E = \frac{1}{2} J_f \omega_f^2 \quad (2.9)$$

Where  $E$  is the energy stored in the flywheel,  $J_f$  is the flywheel mass moment of inertia in  $\text{kgm}^2$ , and  $\omega_f$  is the flywheel rotational speed in rad/s. This equation enables the storage of massive amount of energy in a small flywheel by rotating it at very high speeds, thus, achieving compact design. The flywheel is attached to a toroidal CVT (Fig.32) to allow control of the flow of energy in and out of the storage device (Fig.33<sup>13</sup>) via torque control. Flybrid self-steer to achieve whatever ratio stress is required to realize the requested torque. Flywheel energy storage promises to be the least expensive that it does not require downsizing the engine to be cost effective unlike the hydraulic and electric hybrids as well as the lightest and most compact solution. Jaguar Land-Rover and Porsche have announced intentions of implementing flybrid technology. To reduce losses, the housing in which the flywheel rotates is held at low pressure of 0.1kPa. Figure 34 shows the flybrid concept.

---

<sup>13</sup> <http://auto.howstuffworks.com/cvt3.htm>



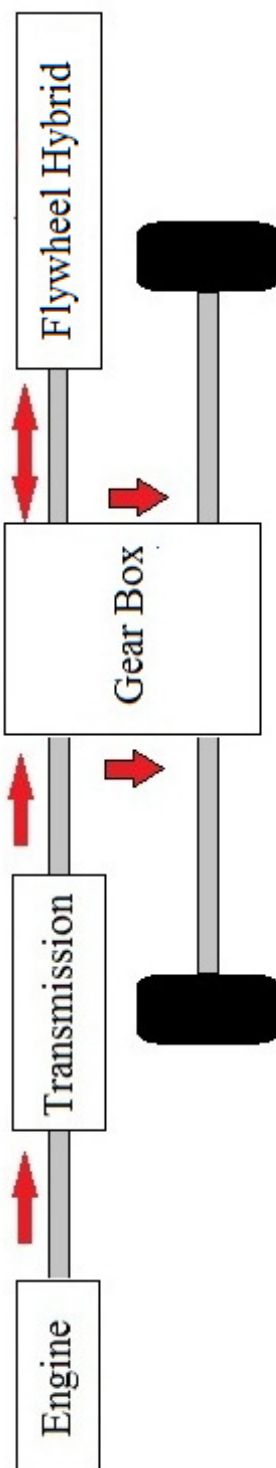


Figure 30: Flywheel hybrid block concept.

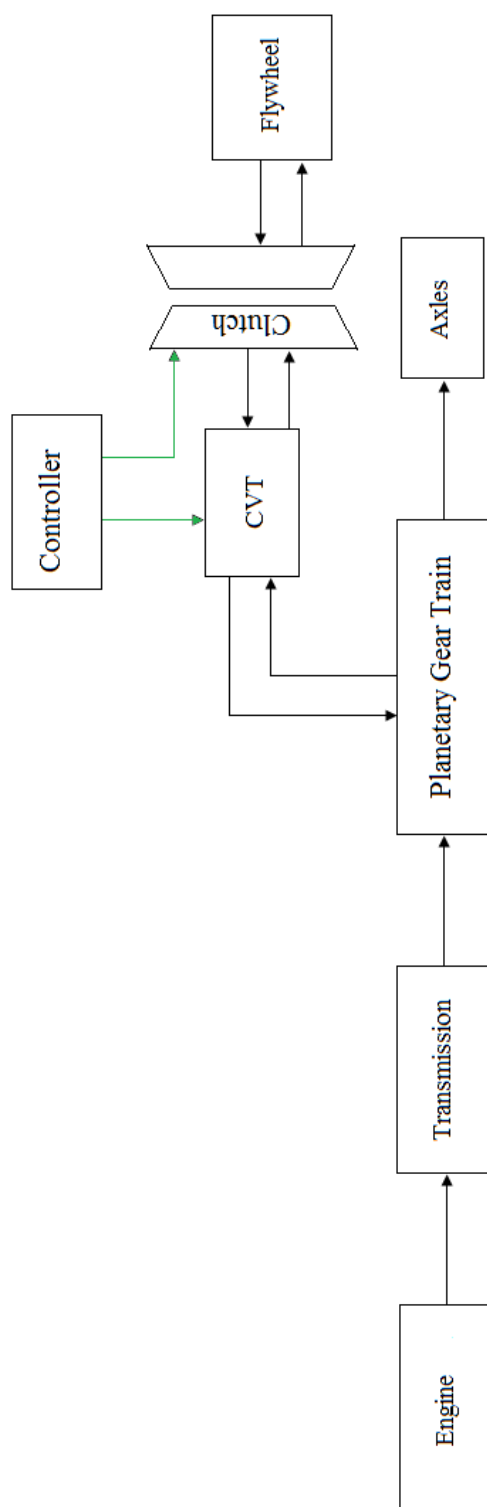


Figure 31: Flywheel hybrid block diagram.

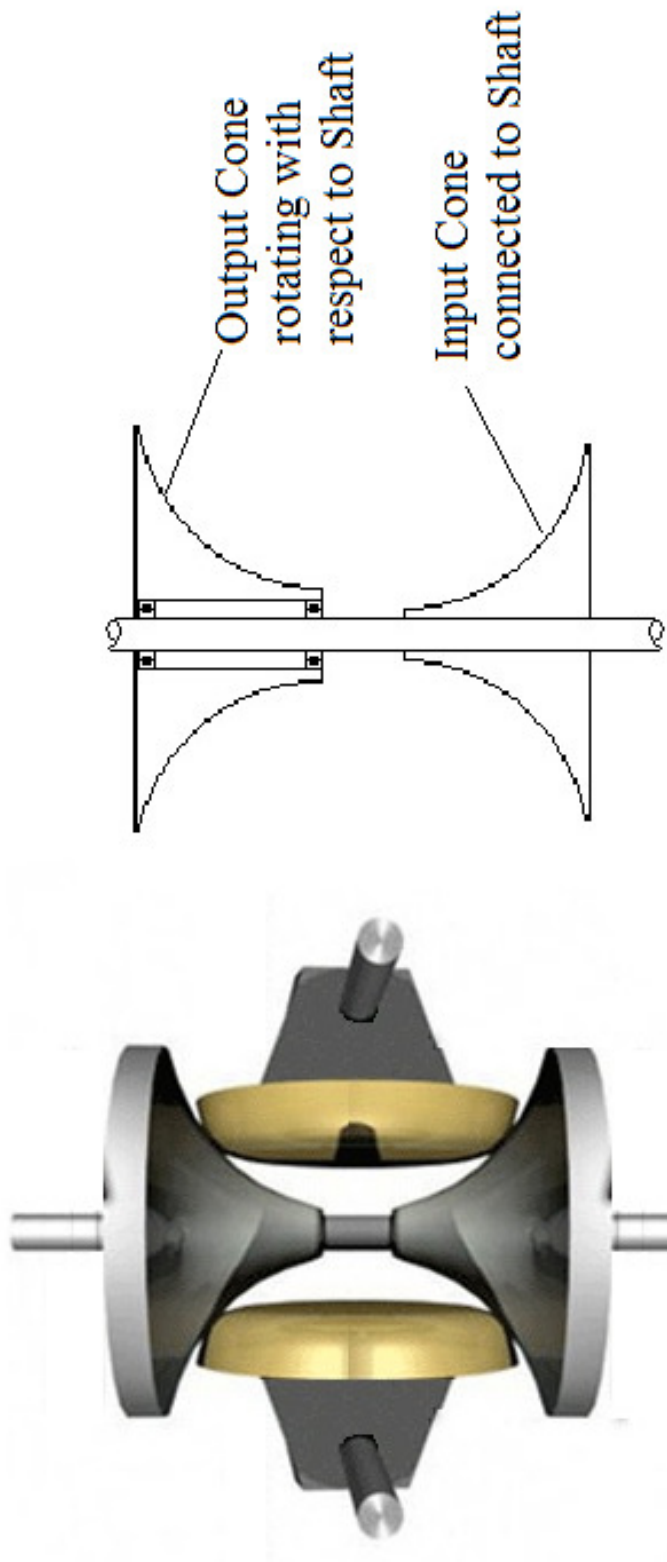


Figure 32: Toroidal CVT Concept<sup>14</sup>.

<sup>14</sup> <http://auto.howstuffworks.com/cvt3.htm>

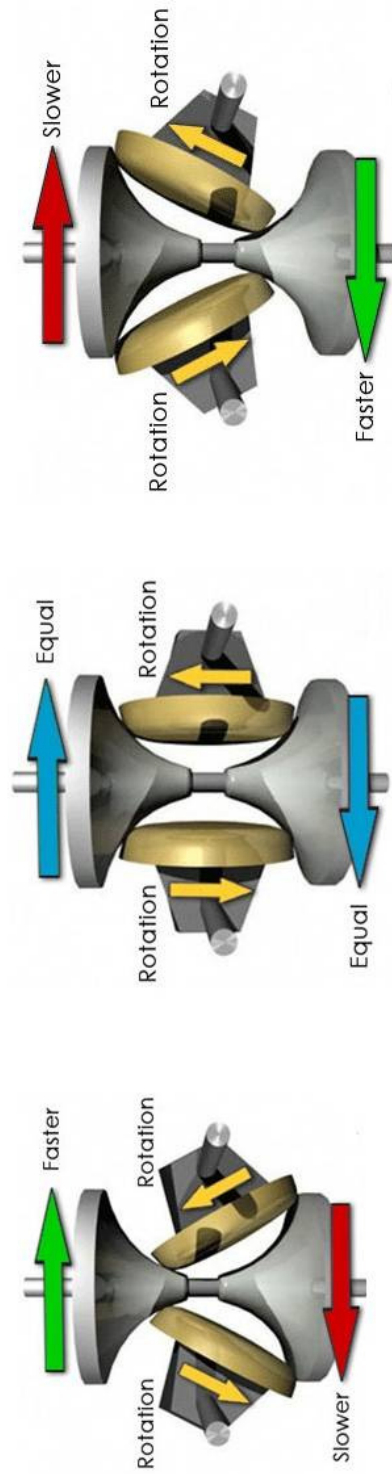


Figure 33: Toroidal CVT Principle<sup>15</sup>.

<sup>15</sup> <http://auto.howstuffworks.com/cvt3.htm>



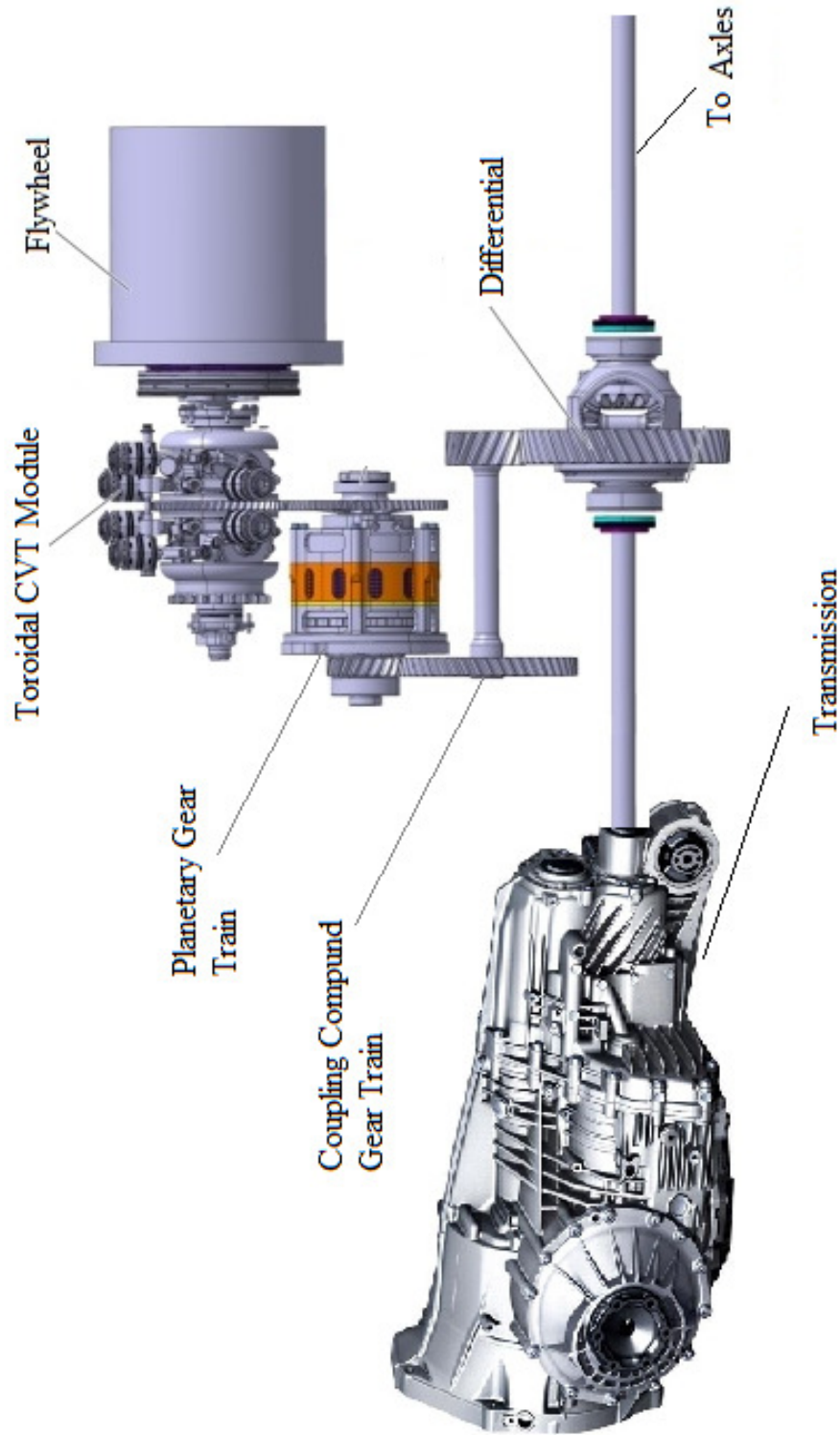


Figure 34: Flywheel hybrid<sup>16</sup>.

<sup>16</sup> [http://reviews.cnet.com/8301-13746\\_7-20068342-48.html](http://reviews.cnet.com/8301-13746_7-20068342-48.html)

### **3. CONTROL STRATEGIES**

In this chapter, the proposed control strategy will be introduced. The control strategy under investigation is a rule-based control. Based on the analysis and the results it will be determined if gain scheduling via GPS tracking and cycle recognition algorithm will be needed. Since the ISG is the benchmark of all hybrids due to full maturity, it will be used to design the control strategies.

#### **3.1. Rule-based Control**

The rule-based control (Fig.35) is easy to implement on the machine. The gains of this controller are tuned to different cycles to minimize the fuel consumption, bring the final SOC closest to the initial SOC, minimize the cycle time, and regulate the minimum engine speed to be close to 1000 rpm or higher. These gains are mapped to the cycles they are optimized for and stored in the memory. Whenever a cycle is identified, the gains are set in the control logic. The upper level Simulink diagram is shown (Fig.36). Two methods are used to identify the cycle: GPS location and cycle identification. If the machine recognizes the path, the controller gains will automatically be set, otherwise, the machine will wait until it finishes one cycle on that path, identifies the cycle, map the path to the gains, and set the controller gains.

##### **3.1.1. Cycle Model**

The cycle model is built to mimic the commands of the real operator sent to the different machine systems as well as the work area. In total, there are four different cycles and hence four different operator models used in this investigation: ATL, MTL, short load-and-carry (SLC) and long load-and-carry (LLC).

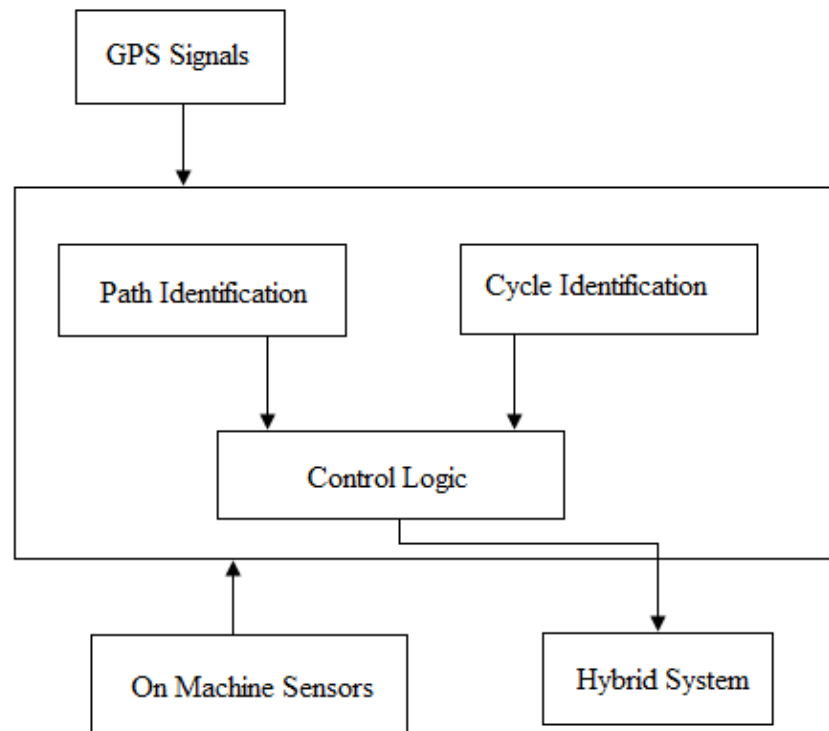


Figure 35: Rule –based control block diagram.



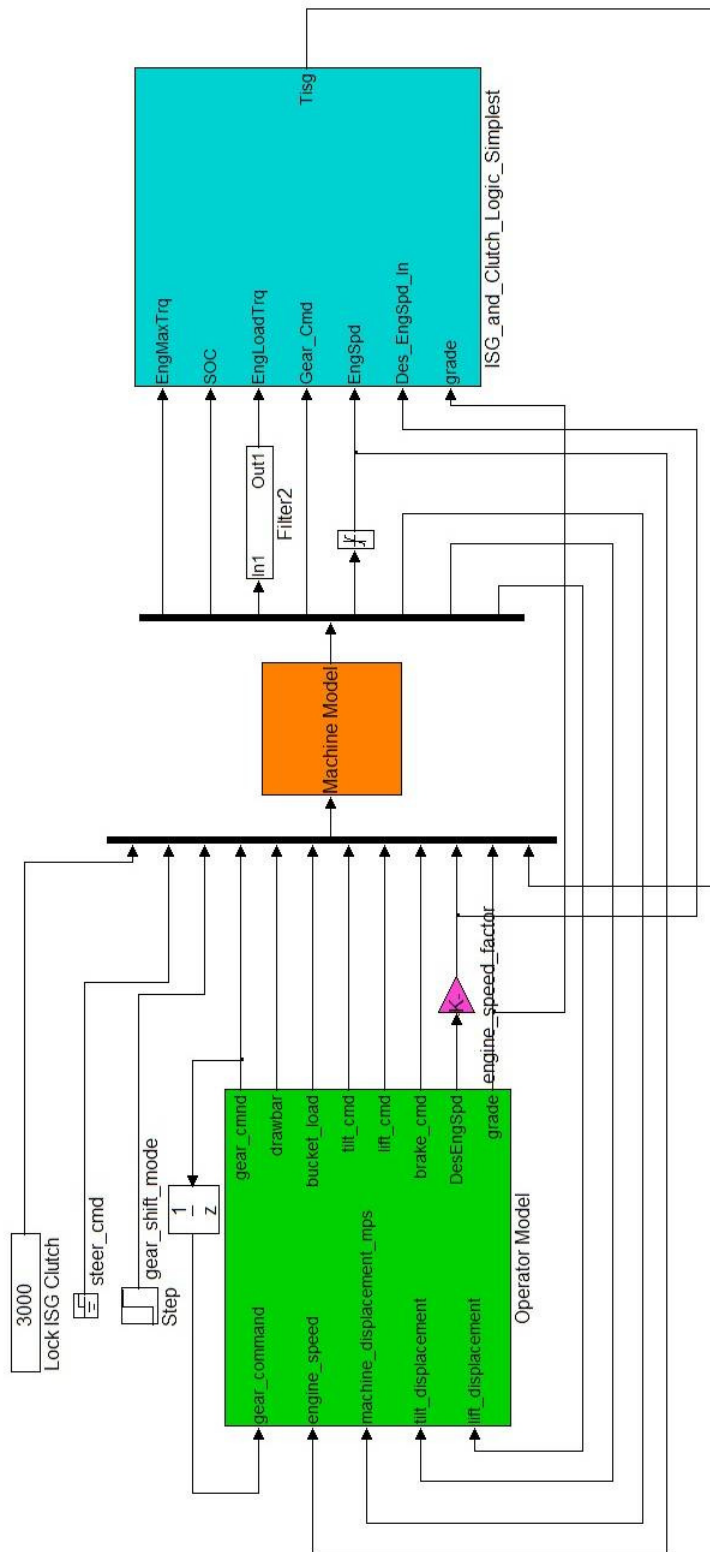


Figure 36: Rule –based control upper level Simulink diagram.

Table IV shows the input and output signals to the operator model.

**TABLE IV OPERATOR MODEL SIGNALS**

<b>Cycle Model Input Signals</b>	<b>Cycle Model Output Signals</b>
Engine speed (rpm)	Desired Engine Speed (rpm)
Gear Command	Gear Command
Lift Displacement (m)	Lift Command
Tilt Displacement (m)	Tilt Command
Machine Ground Velocity (m/s)	Brake Command
	Bucket Load
	Grade
	Drawbar

The cycle model (Fig.37) is modeled as if statement with multiple possible output scenarios based on time and distance along the cycle. Each output from each if statement corresponds to a group of time and distance based operator commands to the machine (Fig.38, 39). The sequence of these commands will result in the machine operations that will lead to completing the cycle.

### **3.1.2. Rule-based Logic**

The rule-based control (Fig.40) is designed based on knowledge of machine functions and system of the machine. Table V shows the input and output signals to the controller.

**TABLE V RULE-BASED LOGIC SIGNALS**

<b>Input Signals</b>	<b>Output Signals</b>
Engine speed (rpm)	ISG Torque
Desired Engine Speed (rpm)	
Engine Load Torque (Nm)	
Engine Maximum Torque (Nm)	
SOC	
Gear Command	
Grade	

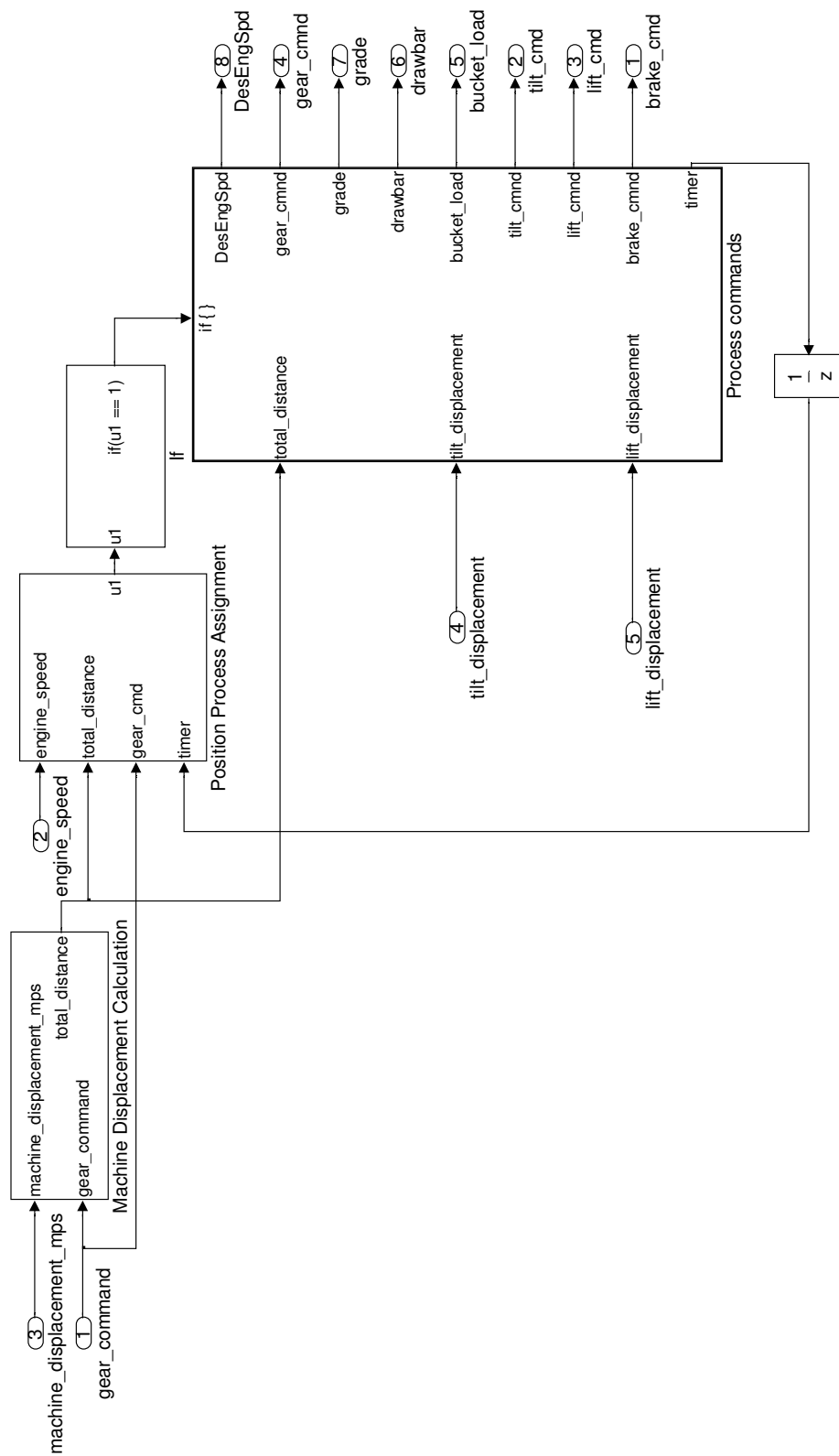


Figure 37: Cycle model Simulink diagram.

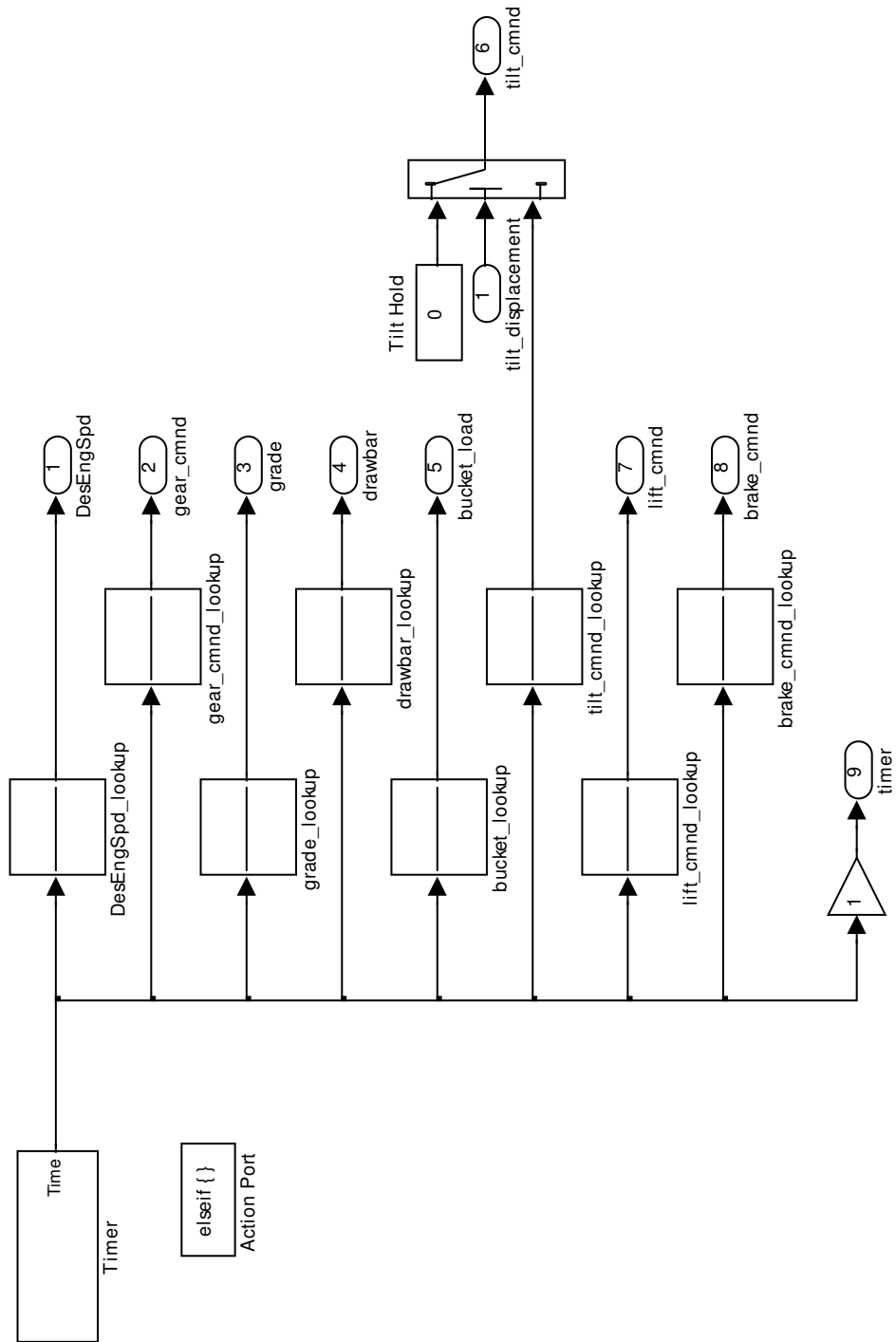


Figure 38: Time Based commands Simulink diagram.

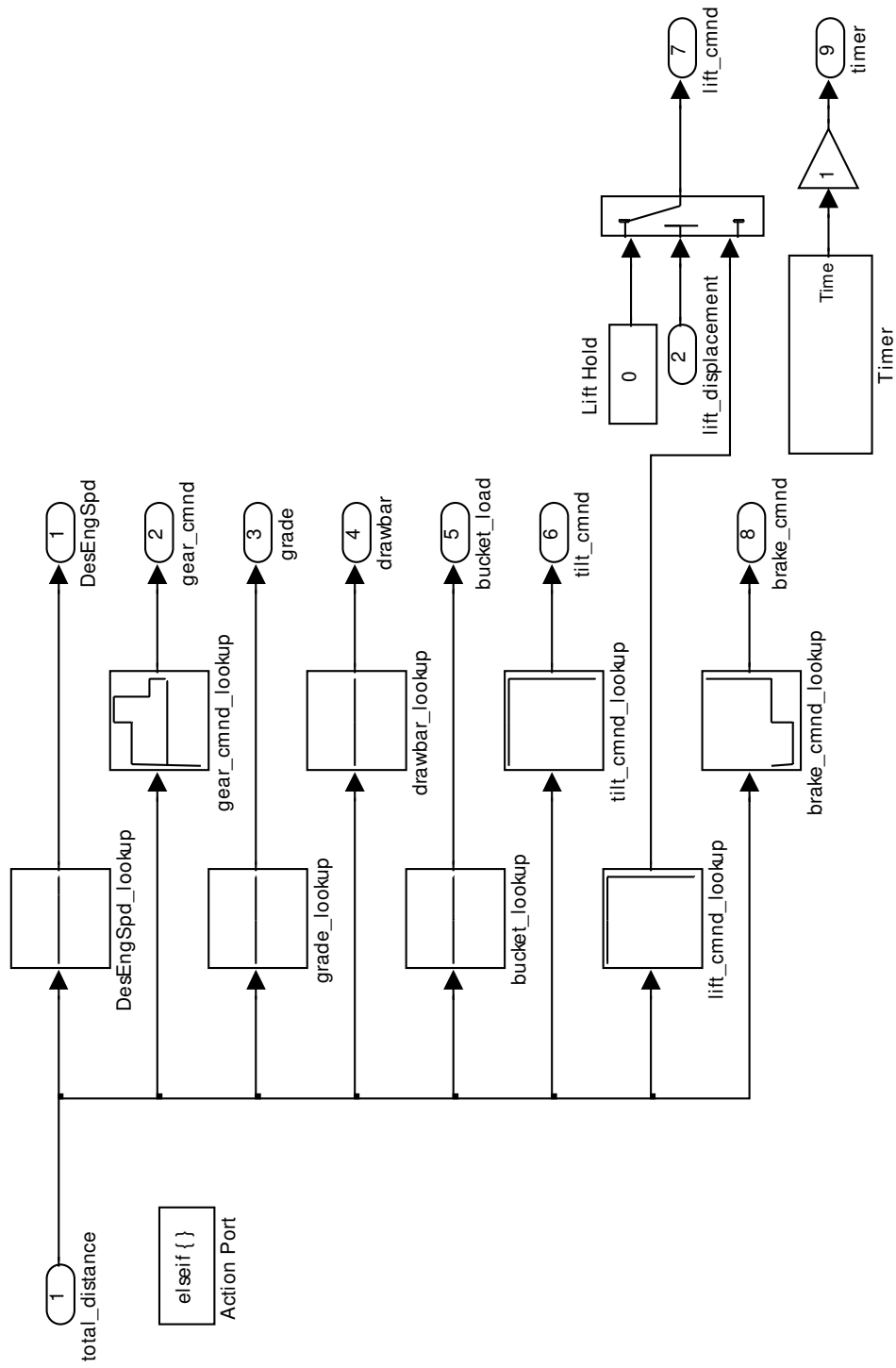


Figure 39: Distance Based commands Simulink diagram.

Figure 40: Rule-based control logic Simulink diagram.

This control is torque based control that will send out desired torque to the ISG and based on this the generator-motor action will be determined. To decide whether to charge or assist multiple factors are considered. These factors are represented by gains and thresholds that will enable reaching the decision. These gains and thresholds are tuned for different cycle to achieve optimum robust results based on the criteria listed earlier. The gains tuned in this logic are: delay timer, assist threshold, charge threshold, low SOC threshold, idle charge torque, ISG torque required threshold, engine speed factor, assist/charge threshold offset, and the idle charge SOC threshold.

To reach this decision the first step is to multiply the engine torque limit by three of the gains and compare the results to the engine load torque. These gains are the assist threshold, charge threshold, and hysteresis factor. Another gain exists to assist with that decision is the low SOC threshold which is biased to charging when the SOC drops below it. For low SOC mode, the more aggressive (charge bias) assist/charge thresholds should be arrived at by taking the standard values and offsetting them by assist/charge threshold offset.

This along with comparing the engine speed and torque demand with the actual will determine the torque demand out of the engine. This step determines if the engine is capable of supplying the demanded power on its own, need assistance from the hybrid, or has excess power to be used for charging. If the engine is idle and the SOC is less than the idle SOC charge threshold then a charge command is issued. Charging is also enforced when the retard engine speed threshold is exceeded. With any gear up-shift or if the engine deceleration rate exceeds the engine deceleration rate threshold, assist is triggered.

The gain tuning process is an iterative and time consuming process. The target from this process is to obtain an optimal set of parameters for robust design such that with inaccuracies or slight changes in the gain values do not affect the performance and in the same time achieve the optimal possible solution. Four approaches are commonly used to achieve this goal: build-test-fix, one factor at a time, full factorial, and fractional factorial. The build-fix-test approach is inadequate as it is not possible to know whether true optimum has been achieved. One factor at a time allows for the understanding of the effect of each parameter on the system but it does not help in understanding the effect of parameter interactions and the optimal value reached could be inaccurate. The full factorial investigates all possible combinations and thus covers both the effect of each parameter on the system as well as parameter interaction, however, this approach is very time consuming as the number of parameters increase due to the high number of combinations that exists as the number of parameters increases. The orthogonal array experiments only requires a fraction of the full factorial combinations through which the same result can be achieved by using the analysis of the variance (ANOVA) thus making it the most suitable for tuning the nine gains. A predictive model based on the ANOVA is then formulated through which an estimate of the optimal set of interactions is determined and tested. By repeating this process over time, the desired optimal robust solution can be obtained for each cycle [110]. The target optimization is to minimize the cycle time, the consumed fuel, and reach a battery SOC of 50-55%



### 3.1.3. Gain Scheduling

The key process for the gain scheduling is the identification of the cycle being performed. For this purpose two key algorithms are developed: GPS pattern recognition (Fig.41) and cycle identification. The pseudo code for the GPS pattern recognition is:

- Initialize parameters.
- Read GPS sensor data.
- Find the nearest coordinates to the read data.
- If the difference between the read and stored data within tolerances.
  - Get mapped cycles.
    - If multiple cycles available.
      - Get gains of last performed cycle in this location.
    - Otherwise.
      - Get cycle gains.
  - If current gains not equal to read gains.
    - Set controller gains.
- Otherwise.
  - Store GPS locations, keep current gains and start cycle identification algorithm.
  - If cycle is identified.
    - Map gains to path.
  - If current gains not equal to read gains
    - Set controller gains.
- Repeat.

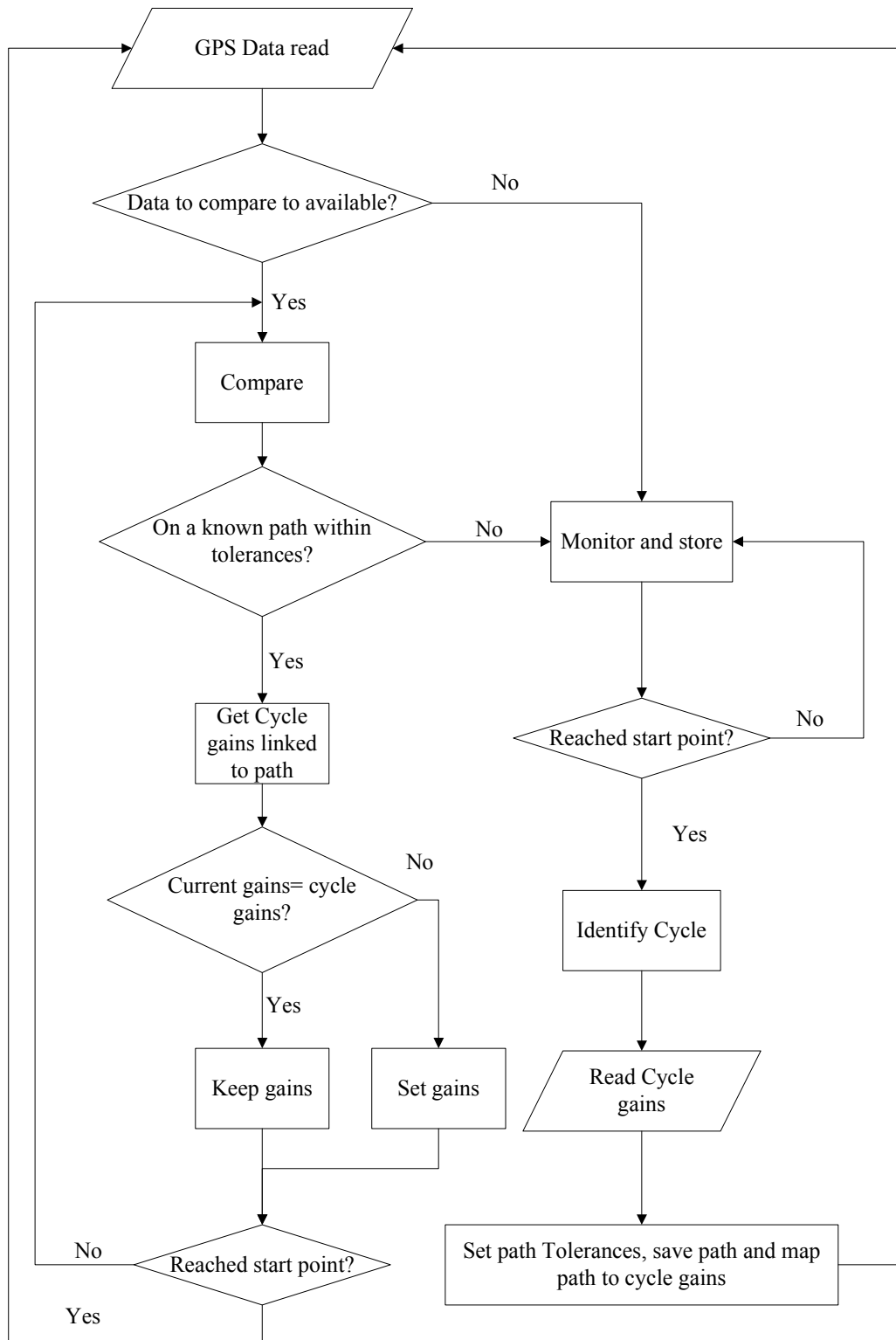


Figure 41: GPS gain scheduling algorithm.

The Pseudo code for the cycle identification is [111]:

- Initialize parameters.
- Read sensors data.
- If travel is initialized
  - If loading cycle or pile dressing initialized
    - Travel loaded
  - Otherwise
    - Travel empty.
- Otherwise
  - If idle
    - Machine is stopped
  - Otherwise.
    - If travel empty was true
      - Check for dig or scrape
    - Otherwise
      - Check for dump
- If a cycle is completed.
  - Get cycle time and distance
  - Compare distance, travel/distance, and sequence of operation to database
  - If cycle is known
    - Cycle identified
  - Otherwise
    - Miscellaneous.

- If cycle aborted
  - Restart

## 4. RESULTS

In this chapter, the machine model validation as well as the results obtained during this work will be presented. The validation results will show that the used machine model is in good correlation with the real life machine. The results obtained will show that when the engine is downsized, the hybrid system is implemented, and its control logic gains optimized, the gain scheduling via GPS tracking and cycle recognition algorithm will not be needed. Also, the results with the regular engine will show that the fuel consumption reduction is not significant and may lead to some performance reduction.

### 4.1. Model Validation

The model validation is performed by obtaining machine data from the real life wheel loader and giving the same operator commands to the machine model. If the model is in good correlation, the machine model behavior will be in good correlation with the real machine behavior. In the previous chapter table IV presented the necessary commands to the machine in the midst of the inputs and outputs to the cycle model. Figure 42 to 45 show the lift, tilt, brake, and gear commands sent by the operator to the machine that are implemented in the cycle model. Figure 46 shows both the real and simulated machine velocities. The general speed pattern is the same and is in good correlation. The differences between them could be attributed to the use of approximate dynamics in the different machine systems. Figure 47 shows the desired engine speed sent by the operator to the machine and implemented in the cycle model, the real machine engine speed and the simulated engine speed.

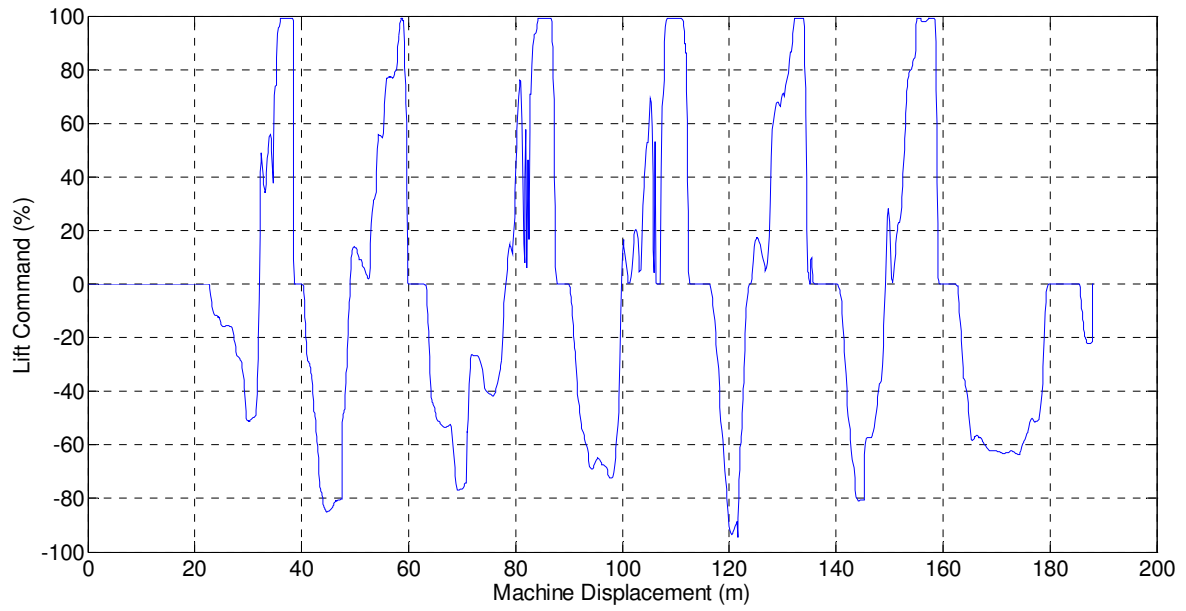


Figure 42: Validation lift command.

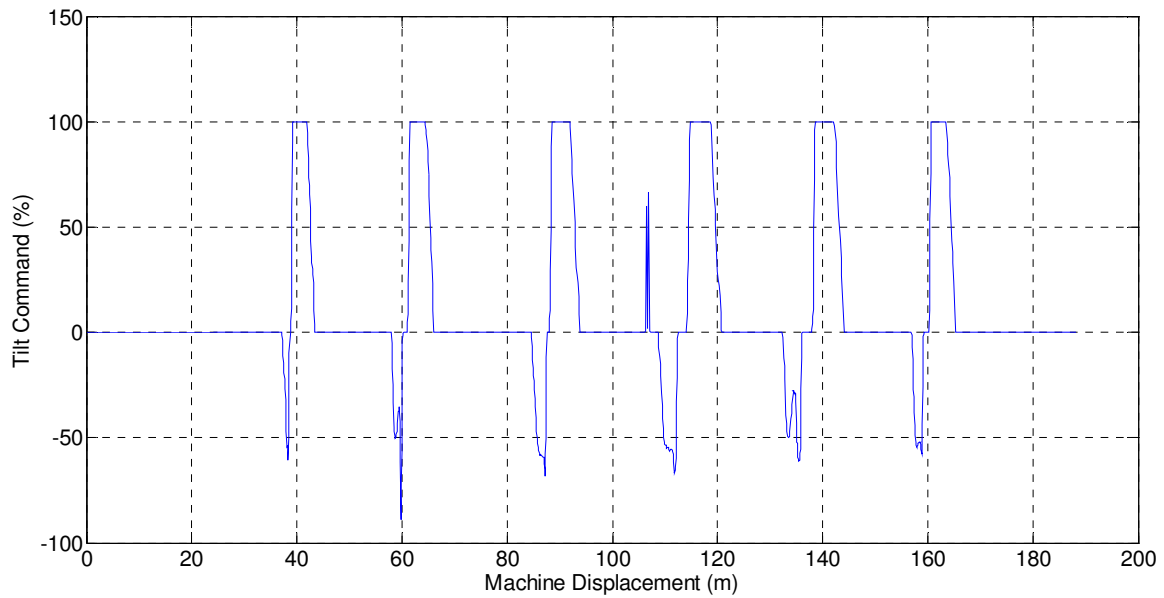


Figure 43: Validation tilt command.

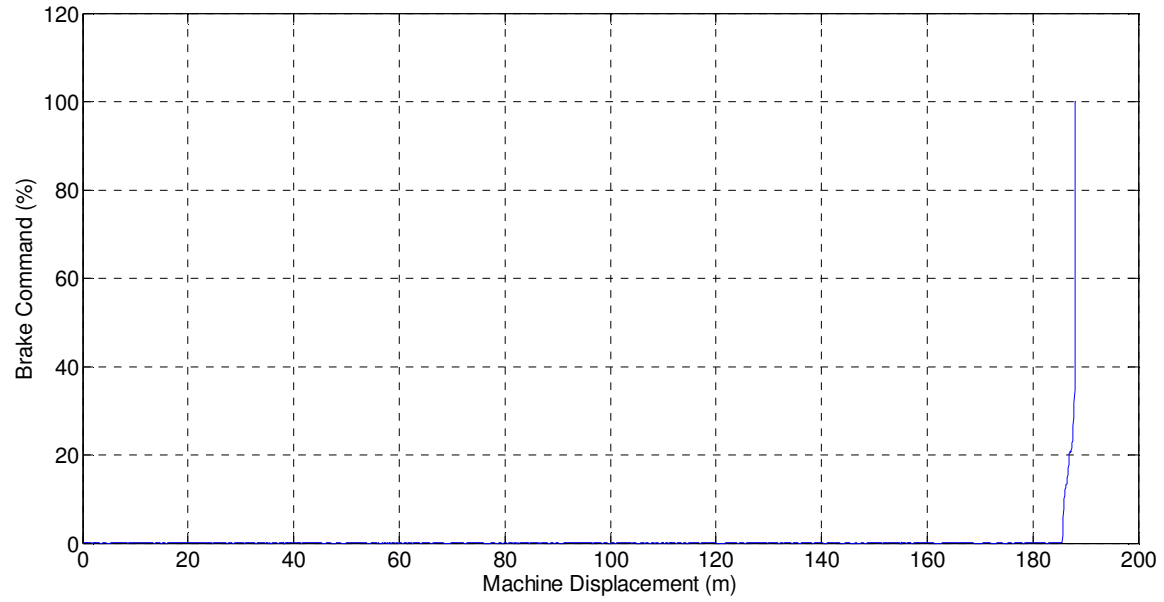


Figure 44: Validation brake command.

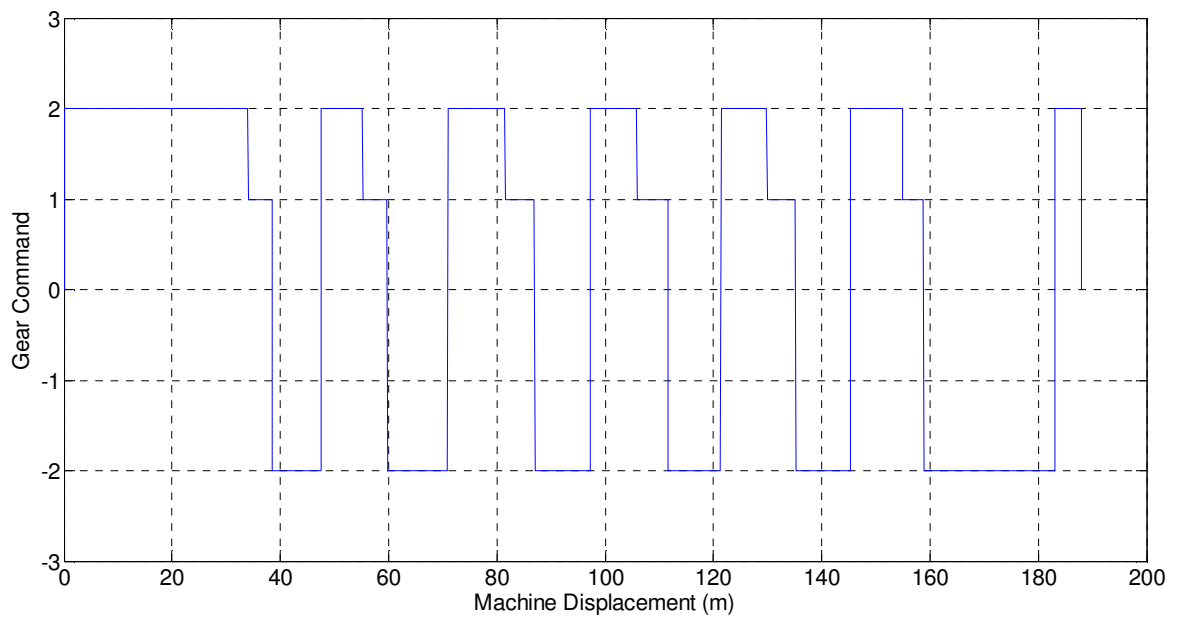


Figure 45: Validation gear command.

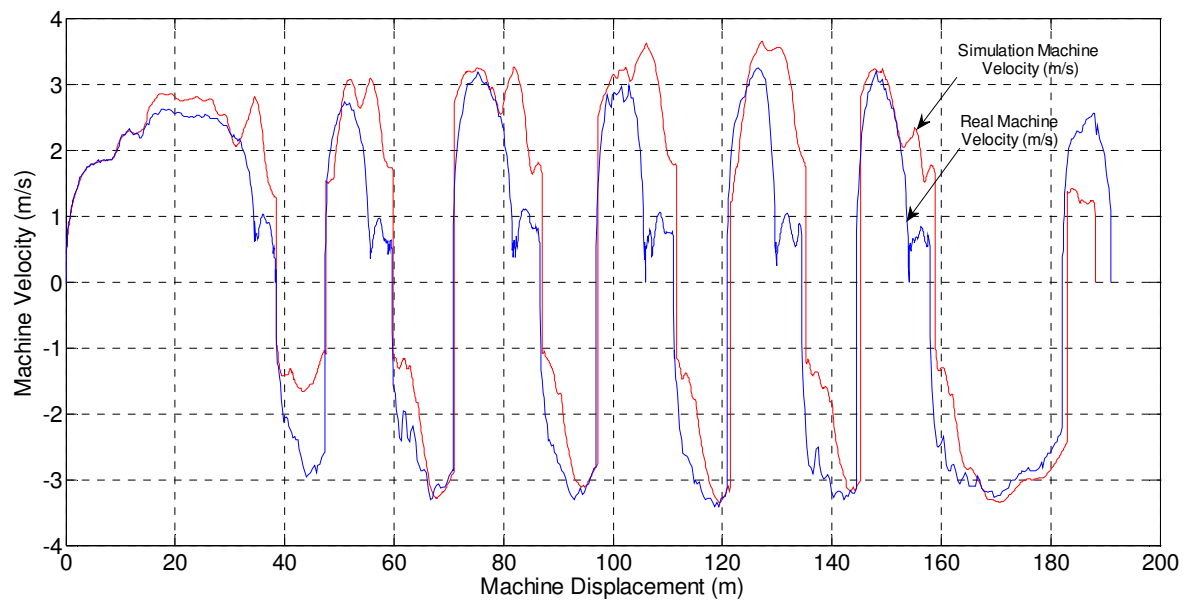


Figure 46: Validation machine velocity.

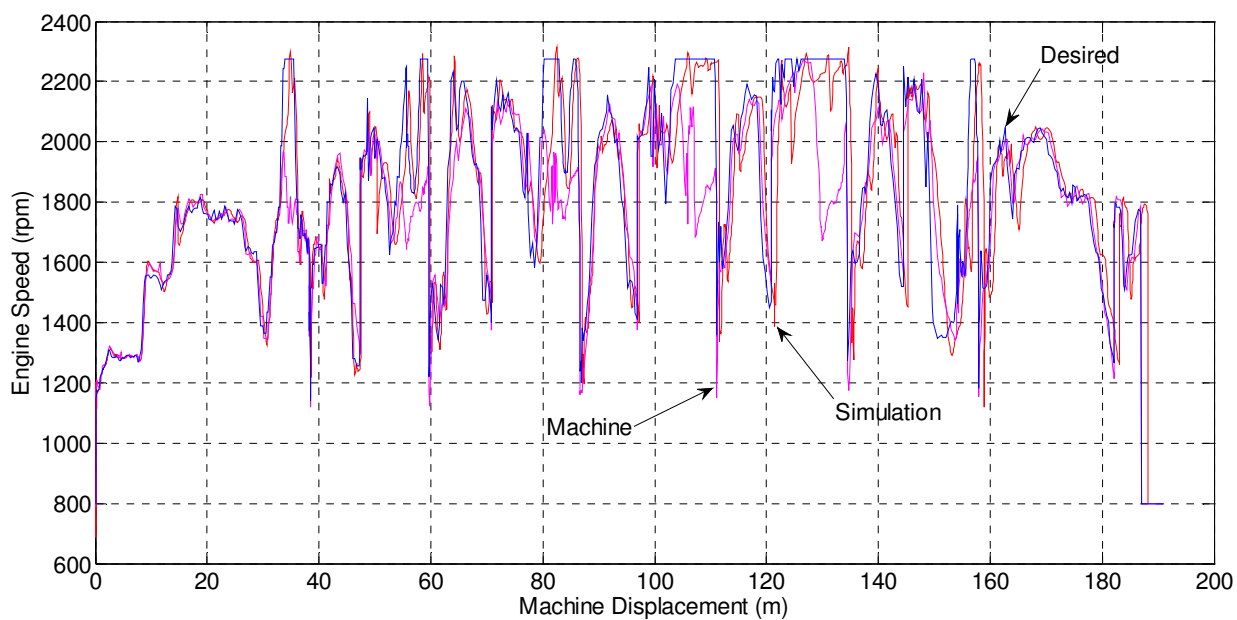


Figure 47: Validation engine speed.



From the figure it is clear that the modeled engine speed response to the desired engine speed command matches to a great extent the actual engine speed response, and the differences could be attributed to the use of approximation and estimated numbers in various points in the model including the load on the machine. Figure 48 shows the torque converter output speed if the real machine and the machine model. The approximation of the torque converter behavior using lookup tables and the unmodeled dynamics are the direct cause of the seen differences. However, the difference in behavior does not affect the machine as a whole. Figure 49 shows the amount of fuel consumed by the machine versus that estimated by the machine model. The general trend of the fuel consumption is the same and the difference in the end point is minimal. Thus, it can be concluded that the machine model has a very good correlation to the real machine. Figure 50 shows the overall error percentage between the simulation and the real machine results.

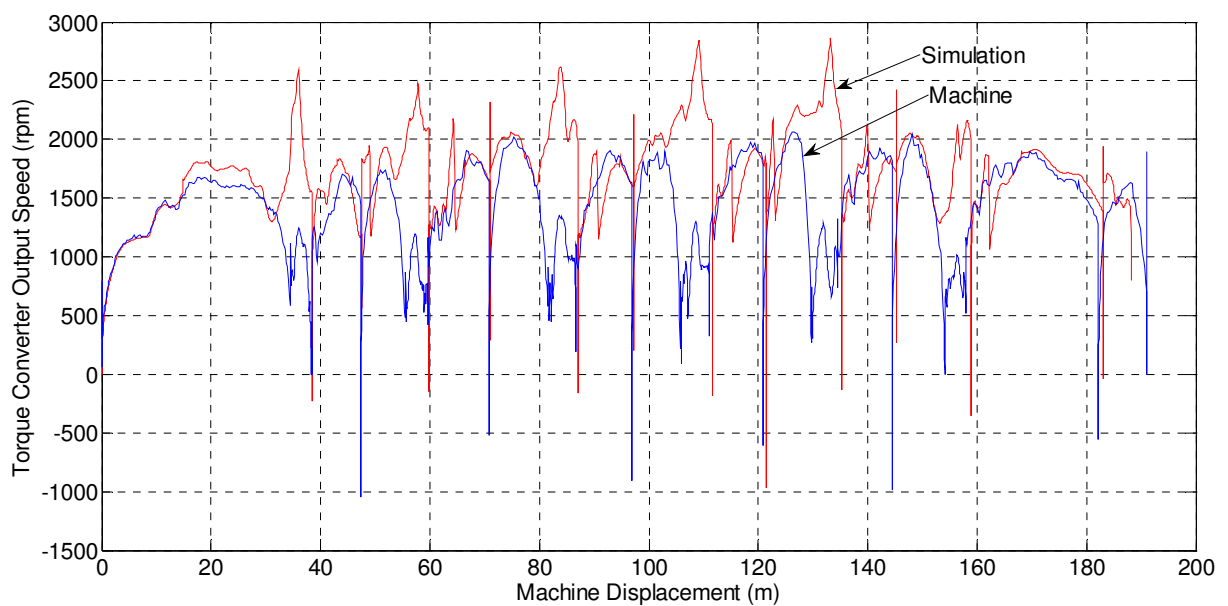


Figure 48: Validation torque converter output speed.



Figure 49: Validation consumed fuel.

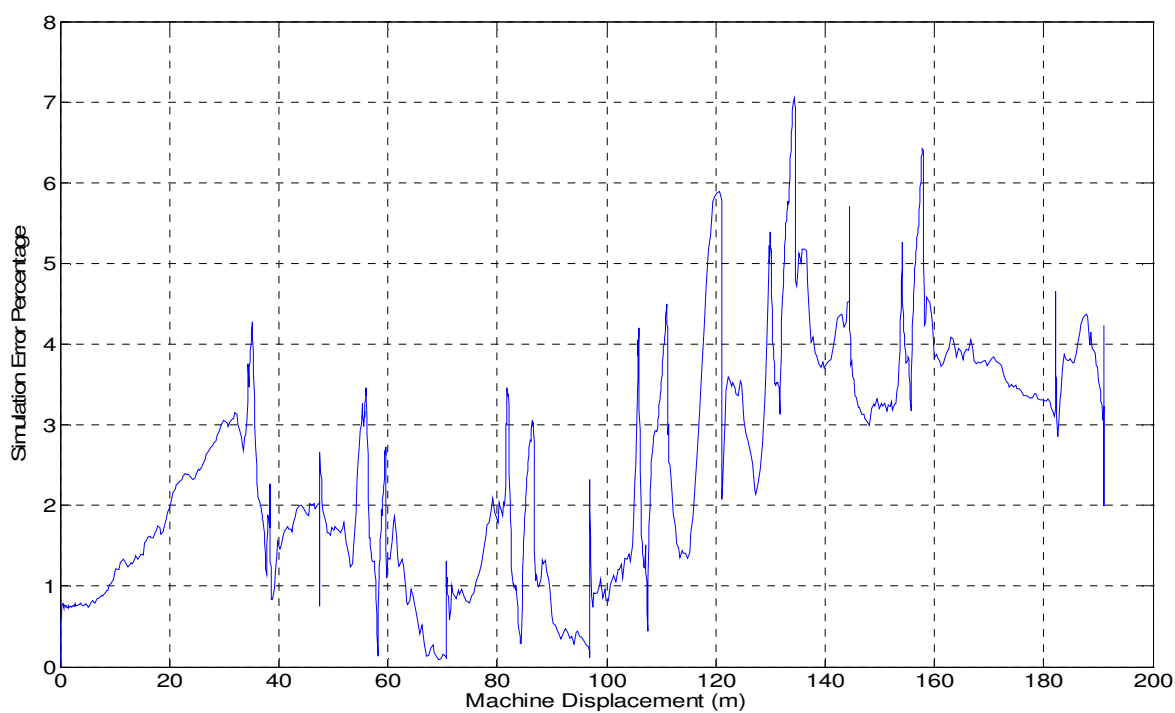


Figure 50: Simulation error percentage.

## **4.2. Results with the 7 Liters Engine**

### **4.2.1. Aggressive Truck Loading Cycle**

The aggressive truck loading (ATL) cycle is a short distance and fast cycle. It involves the loader moving between a pile where it digs to carry its load and a truck where it dumps the load. This process is normally done while the machine is at full throttle meaning that the engine is requested to run at its maximum speed constantly. Figure 51 shows the typical ATL cycle on a medium wheel loader. The typical cycle starts with the machine at rest and starts moving towards a pile. The machine rams the pile and the operator starts moving the arm and bucket slowly while forcing the machine in more to ensure that an appropriate amount of load is carried while not stalling the machine. The operator retracts from the pile moving the arm and bucket all the way up clear from the pile and then moves towards the truck raising the arm all the way up. At the truck the operator moves the bucket to dump the load in the back of the truck. The operator raises the bucket back up while moving away from the truck. When the machine has cleared the truck the operator lowers the arm and bucket to their initial position, and moves back to the starting point or commence to do another cycle. Figure 52 and table VI compare between the baseline regular and the optimized hybrid wheel loader for the ATL cycle. The optimal values for the controller gains are shown in table VII. From the obtained results it is shown that maintaining productivity while decreasing the fuel consumption by 20% can be achieved by switching to the downsized hybrid machine. It is also shown that the ATL cycle does not require a lot of charge from the battery. Figure 53 shows the total torque the machine requires, the torque supplied by the engine, and that supplied by the hybrid system during the ATL cycle.

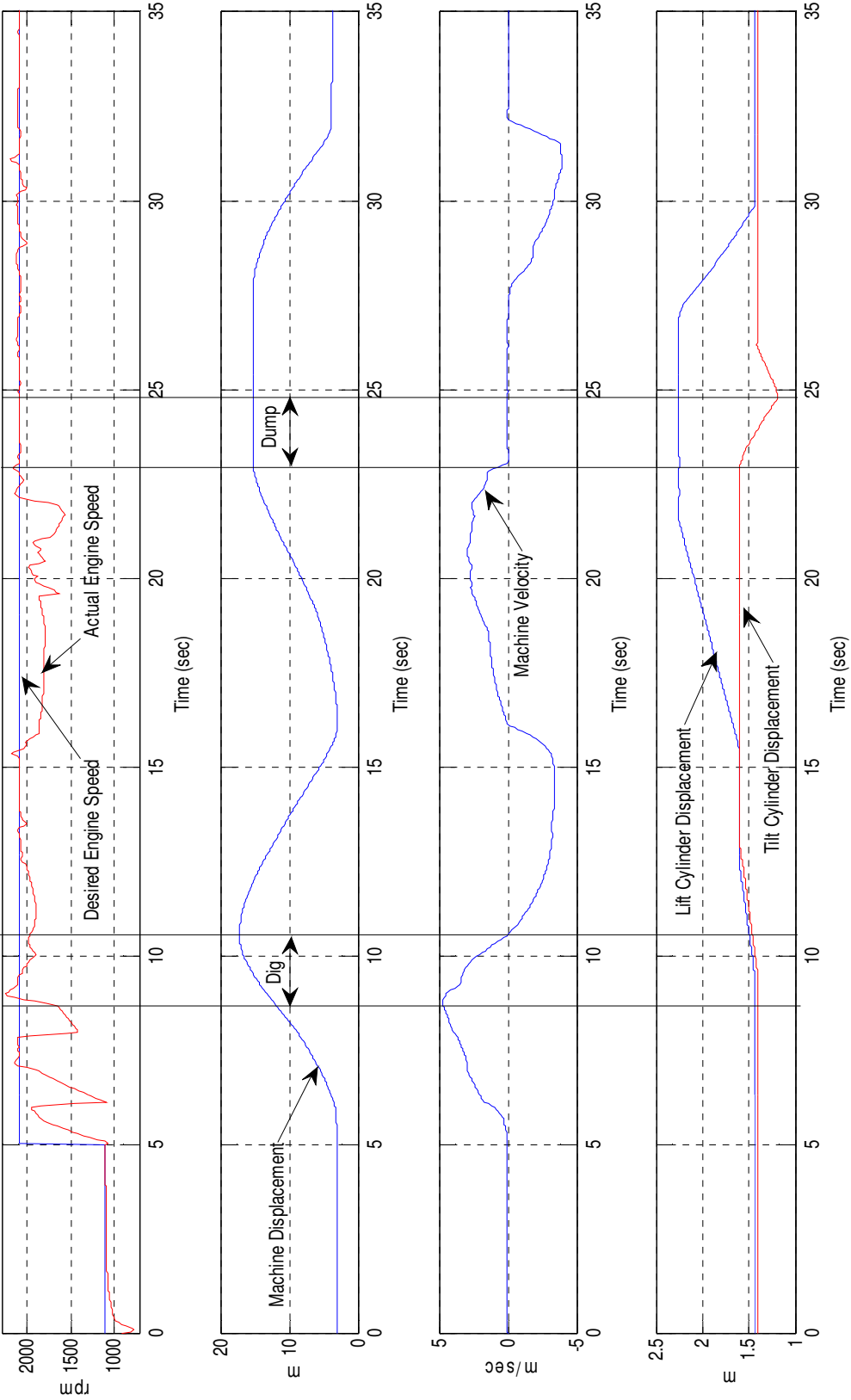


Figure 51: Aggressive truck loading cycle.

**TABLE VI AGGRESSIVE TRUCK LOADING BASELINE AND HYBRID COMPARISON**

<b>Machine</b>	<b>Cycle Time (sec)</b>	<b>Fuel (grams)</b>	<b>Productivity (%)</b>	<b>Fuel consumption (%)</b>
Baseline	32.15	344.6		
Hybrid	32.1	275.7	0.16	-20

**TABLE VII AGGRESSIVE TRUCK LOADING OPTIMIZED GAINS**

<b>Parameter</b>	<b>Value</b>
Timer	0
Assist Threshold	0.5
Charge Threshold	0
Low SOC Threshold	0
Idle Charge Torque	0
ISG Torque Required Threshold	145.82
Engine Speed Factor	1.4
Assist Charge Threshold Offset	0
Idle Charge SOC Threshold	1

From figure 54, it can be deduced that the hybrid system contributes to about 14% of the total torque needed by the machine.

#### **4.2.2. Moderate Truck Loading Cycle**

The moderate truck loading (MTL) cycle share a lot of similarities to the ATL cycle and follows the same cycle sequence. One notable difference is that the loader is not required to run at full throttle all the time, which makes it relatively a more relaxed cycle, hence consuming more time. Figure 55 shows the typical MTL cycle on a medium wheel loader. Figure 56 and table VIII compare between the baseline regular and the optimized hybrid wheel loader for the MTL cycle. The optimal values for the controller gains are shown in table IX. From the obtained results it is shown that maintaining productivity while decreasing the fuel consumption by 26.5% can be achieved by switching to the downsized hybrid machine.

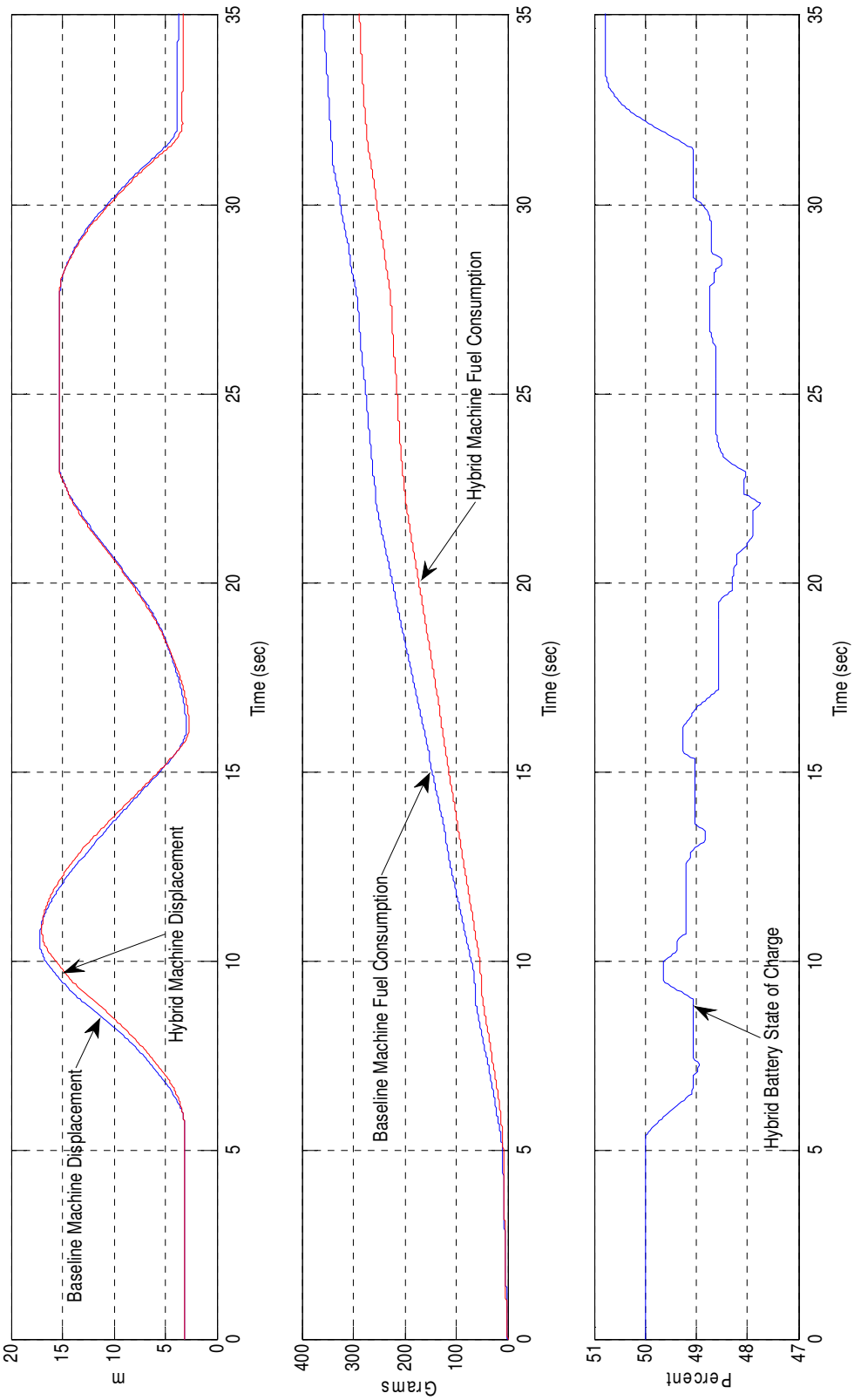


Figure 52: ATL hybrid versus baseline.

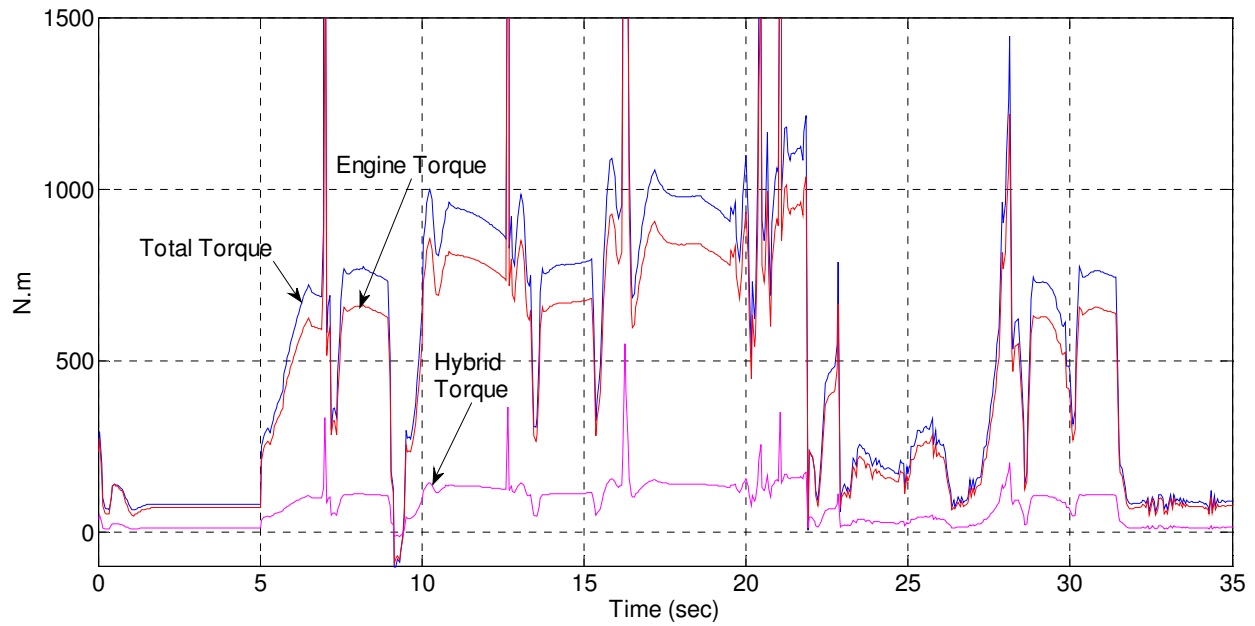


Figure 53: Hybrid machine ATL torque values.

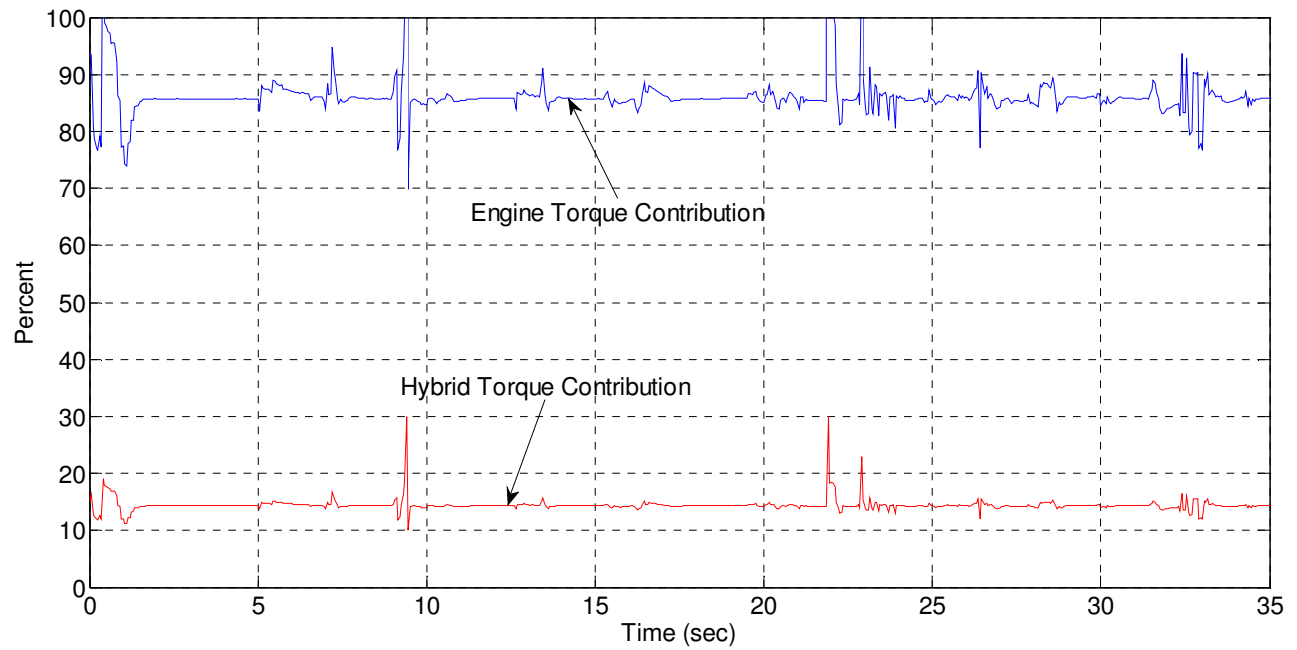


Figure 54: Engine and hybrid system ATL torque contribution.

**TABLE VIII MODERATE TRUCK LOADING BASELINE AND HYBRID COMPARISON**

<b>Machine</b>	<b>Cycle Time (sec)</b>	<b>Fuel (grams)</b>	<b>Productivity (%)</b>	<b>Fuel consumption (%)</b>
Baseline	37.7	413.17		
Hybrid	37.5	303.9	0.53	-26.45

**TABLE IX MODERATE TRUCK LOADING OPTIMIZED GAINS**

<b>Parameter</b>	<b>Value</b>
Timer	0
Assist Threshold	1.05
Charge Threshold	0.5
Low SOC Threshold	0.3
Idle Charge Torque	350
ISG Torque Required Threshold	42
Engine Speed Factor	1.35
Assist Charge Threshold Offset	0.25
Idle Charge SOC Threshold	0.5

Figure 57 shows the total torque the machine requires, the torque supplied by the engine, and that supplied by the hybrid system during the MTL cycle. From figure 58, it can be deduced that the hybrid system contributes to about 17% of the total torque needed by the machine.

#### **4.2.3. Short Load and Carry Cycle**

The short load and carry (SLC) cycle is a short distance load and carry cycle. It involves the loader moving between a pile where it digs to carry its load, transporting the load over distance to a hopper or truck where it dumps the load. Figure 59 shows the typical SLC cycle on a medium wheel loader. The typical cycle starts with the machine at rest and starts moving towards a pile. The machine rams the pile and the operator starts moving the arm and bucket slowly while forcing the machine in more to ensure that an appropriate amount of load is carried while not stalling the machine. The operator retracts from the pile moving the arm and bucket all the way up clear from the pile and then drives the machine some distance towards the truck or the hopper raising the arm all the way up as the machine approaches the truck or hopper.



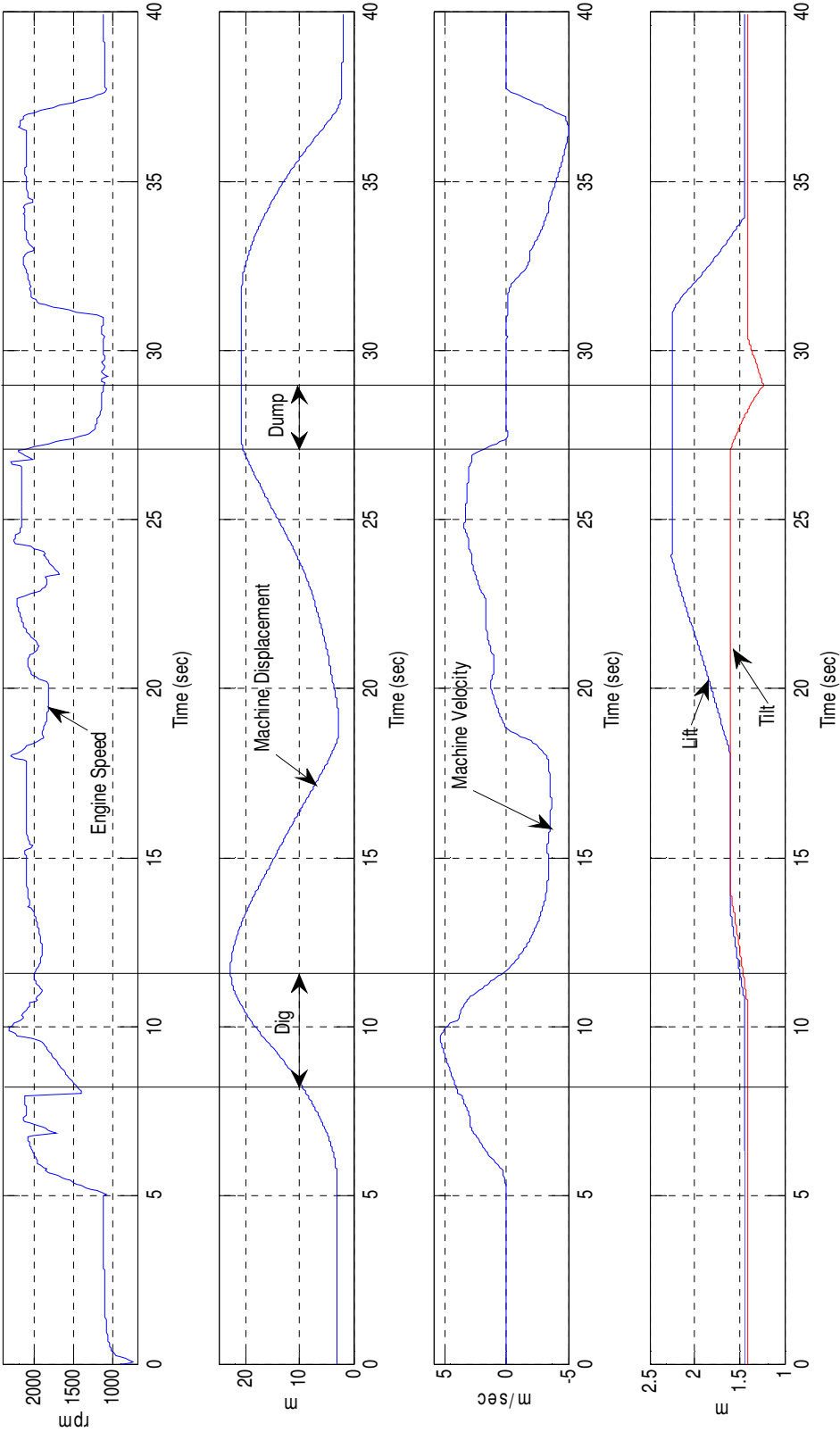


Figure 55: MTL hybrid versus baseline.

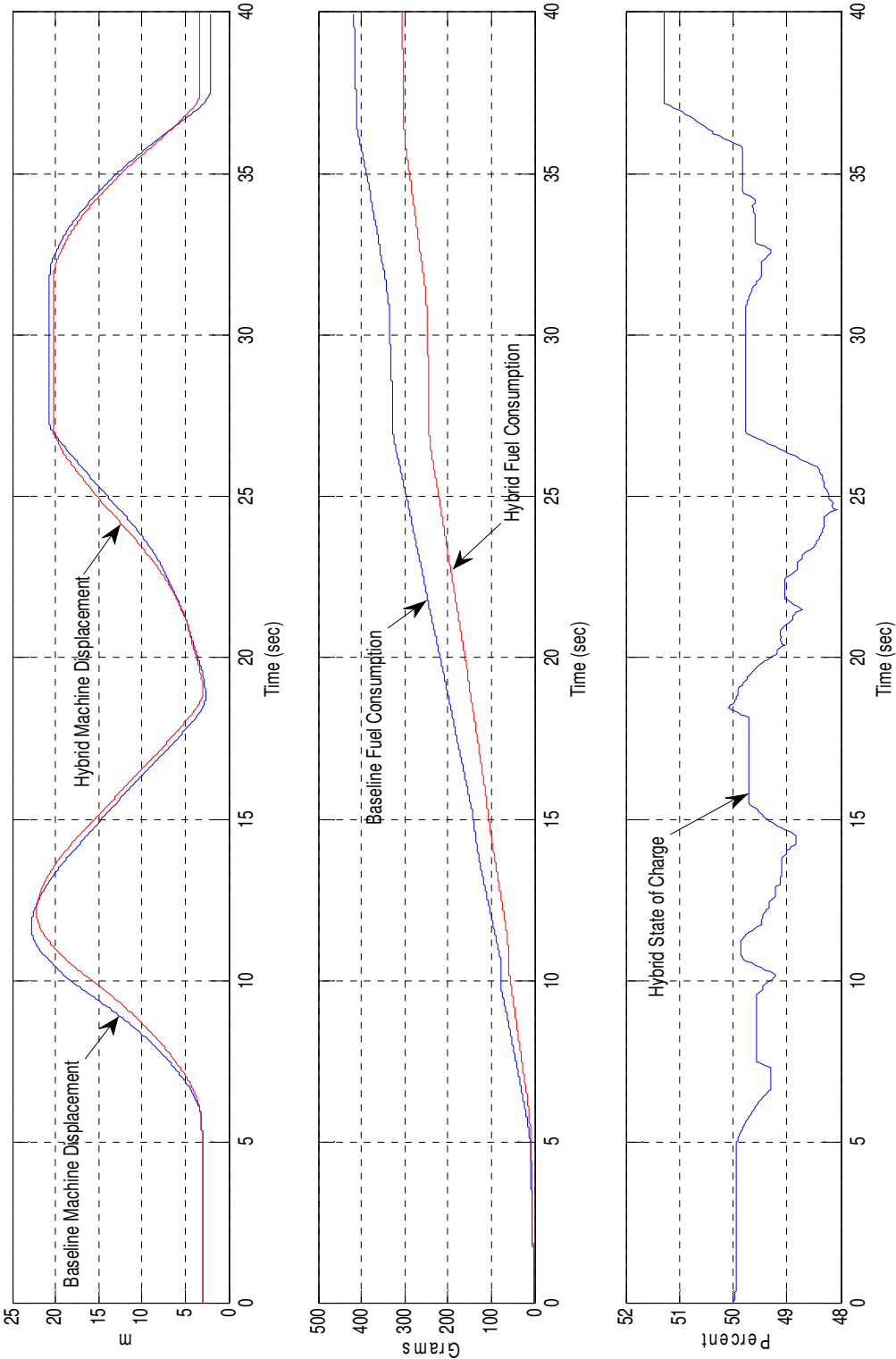


Figure 56: Moderate truck loading cycle.

At the truck or hopper the operator moves the bucket to dump the load in the back of the truck or on the hopper. The operator raises the bucket back up while moving away from the truck or hopper. When the machine has cleared the truck or hopper the operator lowers the arm and bucket to their initial position, and moves back to the starting point or commence to do another cycle. Figure 60 and table X compare between the baseline regular and the optimized hybrid wheel loader for the SLC cycle. The optimal values for the controller gains are shown in table XI. From the obtained results it is shown that increasing productivity by 7.7% and decreasing the fuel consumption by 28% can be achieved by switching to the downsized hybrid machine. Figure 61 shows the total torque the machine requires, the torque supplied by the engine, and that supplied by the hybrid system during the SLC cycle.

**TABLE X SHORT LOAD AND CARRY BASELINE AND HYBRID COMPARISON**

<b>Machine</b>	<b>Cycle Time (sec)</b>	<b>Fuel (grams)</b>	<b>Productivity (%)</b>	<b>Fuel consumption (%)</b>
Baseline	69.25	793		
Hybrid	63.9	569.7	7.73	-28.16

**TABLE XI SHORT LOAD AND CARRY OPTIMIZED GAINS**

<b>Parameter</b>	<b>Value</b>
Timer	0.95
Assist Threshold	1
Charge Threshold	0.16
Low SOC Threshold	0.22
Idle Charge Torque	350
ISG Torque Required Threshold	65
Engine Speed Factor	1.37
Assist Charge Threshold Offset	0.32
Idle Charge SOC Threshold	1

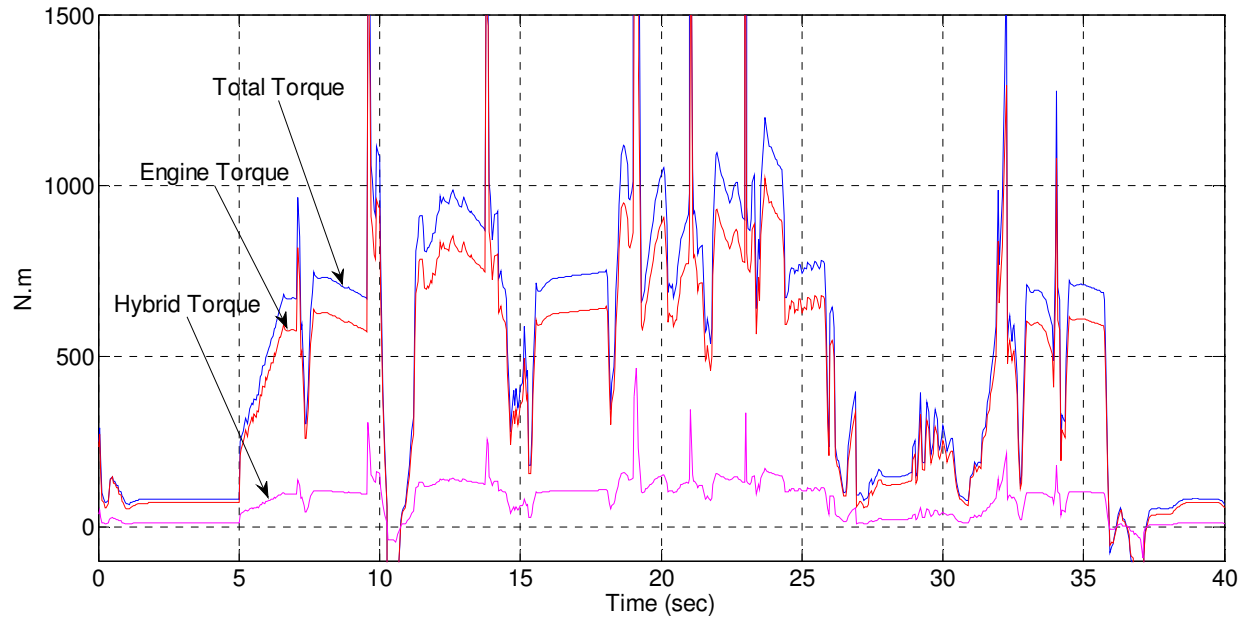


Figure 57: Hybrid machine MTL torque values.

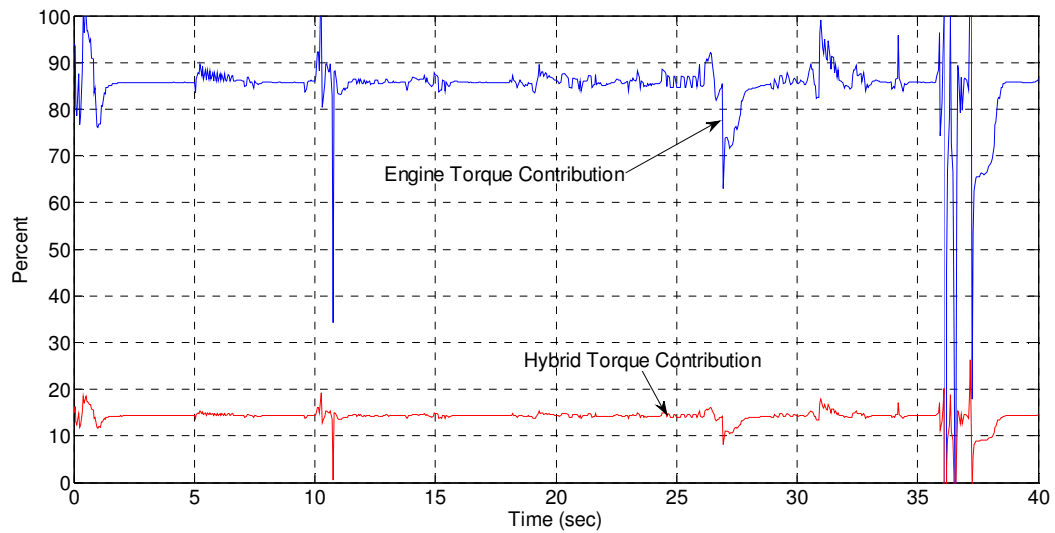


Figure 58: Engine and hybrid system MTL torque contribution.

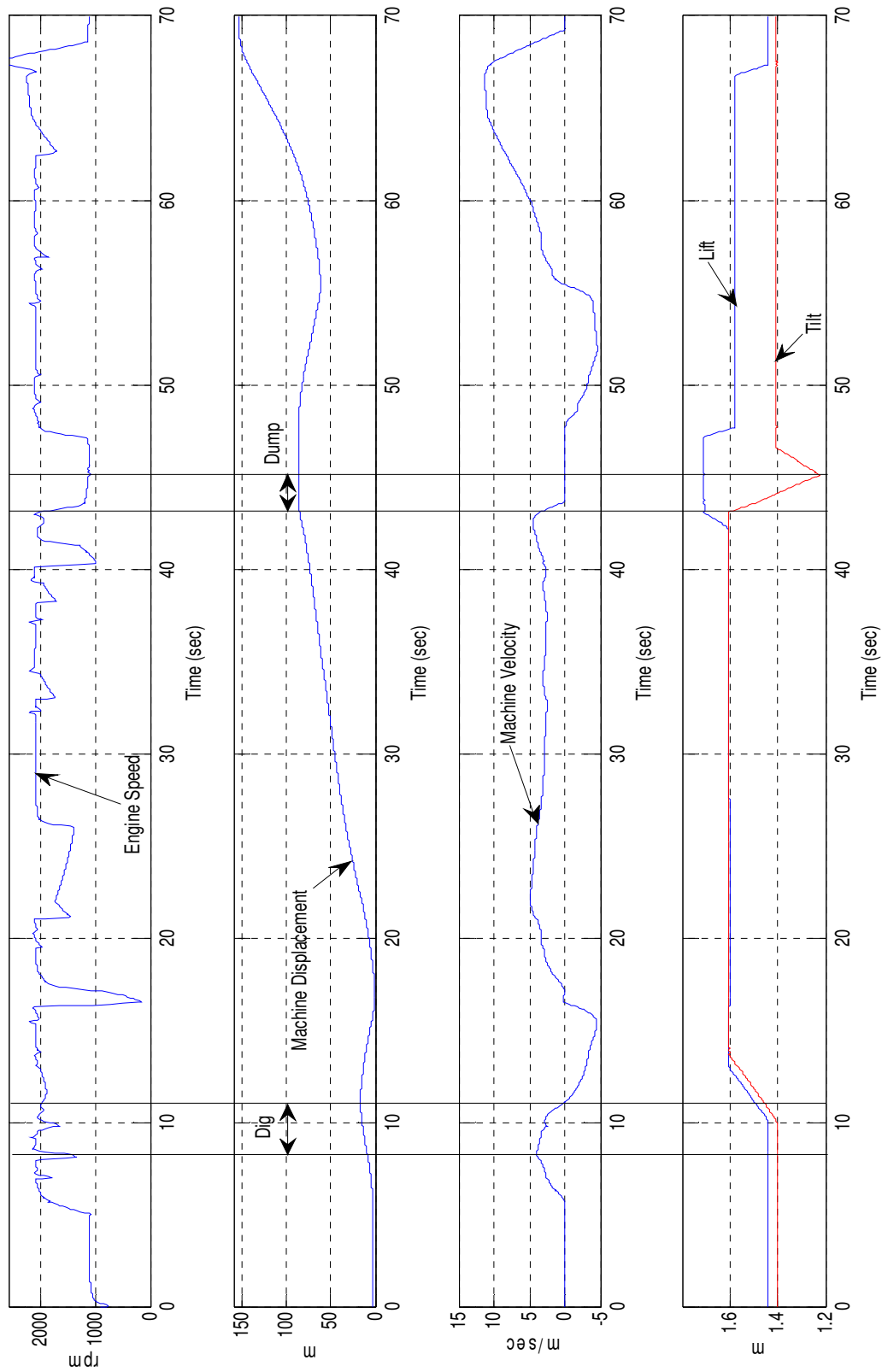


Figure 59: SLC hybrid versus baseline.

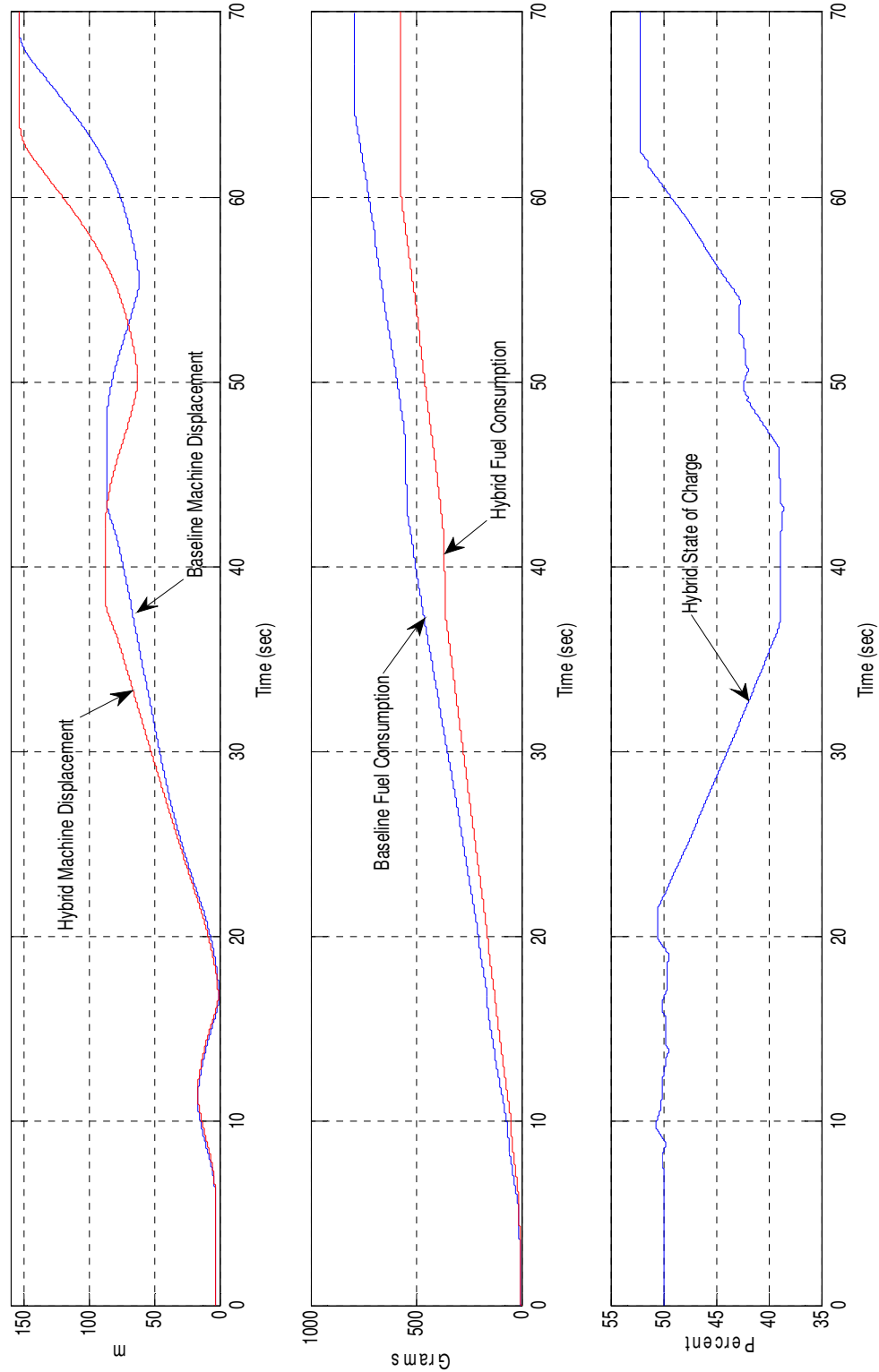


Figure 60: Short load and carry cycle.

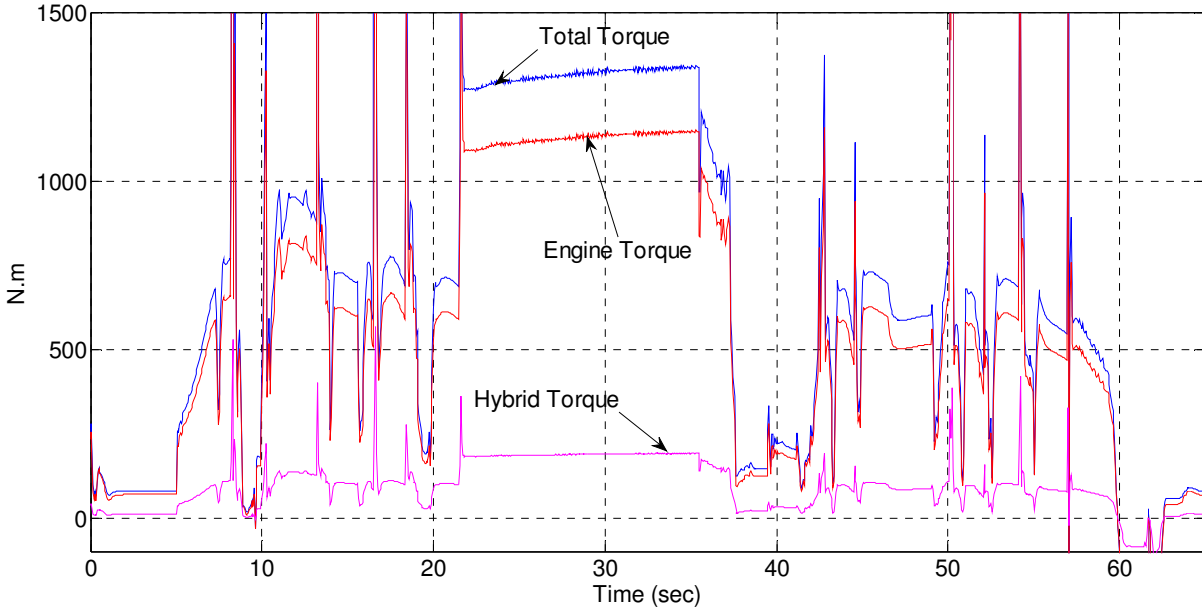


Figure 61: Hybrid machine SLC torque values.

From figure 62, it can be deduced that the hybrid system contributes to about 14% of the total torque needed by the machine.

#### 4.2.4. Long Load and Carry Cycle

The long load and carry (LLC) cycle is a long distance load and carry cycle. It involves the loader moving between a pile where it digs to carry its load, transporting the load over distance to a hopper or truck where it dumps the load. Figure 63 shows the typical LLC cycle on a medium wheel loader. The typical cycle starts with the machine at rest and starts moving towards a pile. The machine rams the pile and the operator starts moving the arm and bucket slowly while forcing the machine in more to ensure that an appropriate amount of load is carried while not stalling the machine. The operator retracts from the pile moving the arm and bucket all

the way up clear from the pile and then drives the machine some distance towards the truck or the hopper raising the arm all the way up as the machine approaches the truck or hopper. At the truck or hopper the operator moves the bucket to dump the load in the back of the truck or on the hopper. The operator raises the bucket back up while moving away from the truck or hopper. When the machine has cleared the truck or hopper the operator lowers the arm and bucket to their initial position, and moves back to the starting point or commence to do another cycle. Figure 64 and table XII compare between the baseline regular and the optimized hybrid wheel loader for the long load and carry (LLC) cycle. The optimal values for the controller gains are shown in table XIII. From the obtained results it is shown that increasing productivity by 16% and decreasing the fuel consumption by 32.6% can be achieved by switching to the downsized hybrid machine.

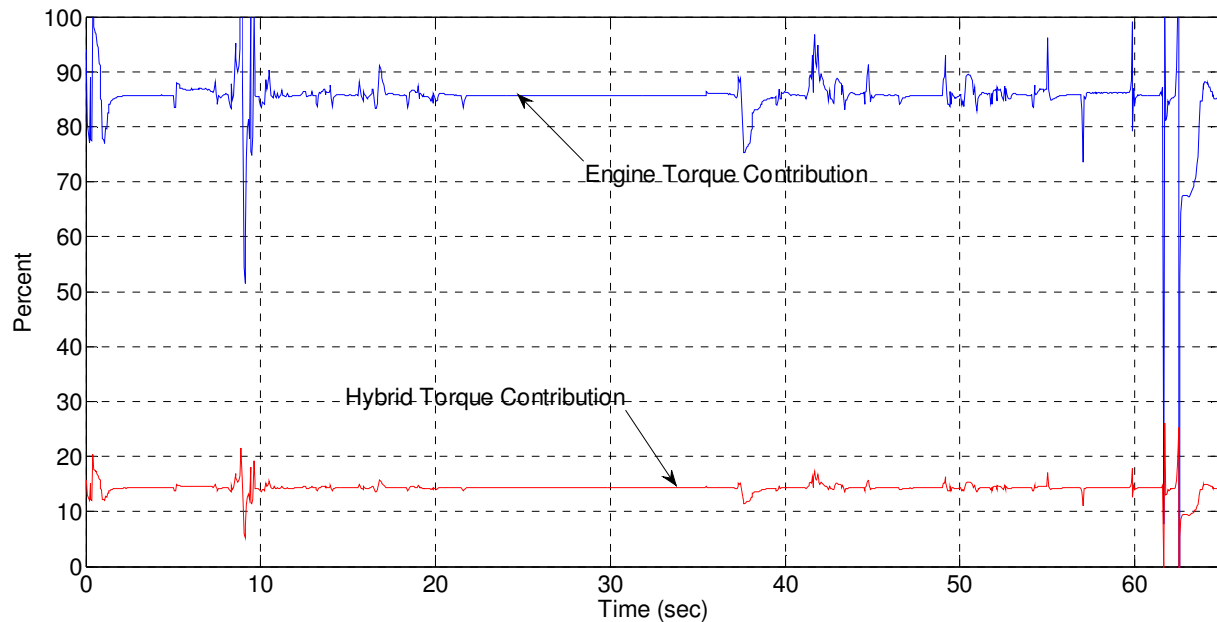


Figure 62: Engine and hybrid system SLC torque contribution.



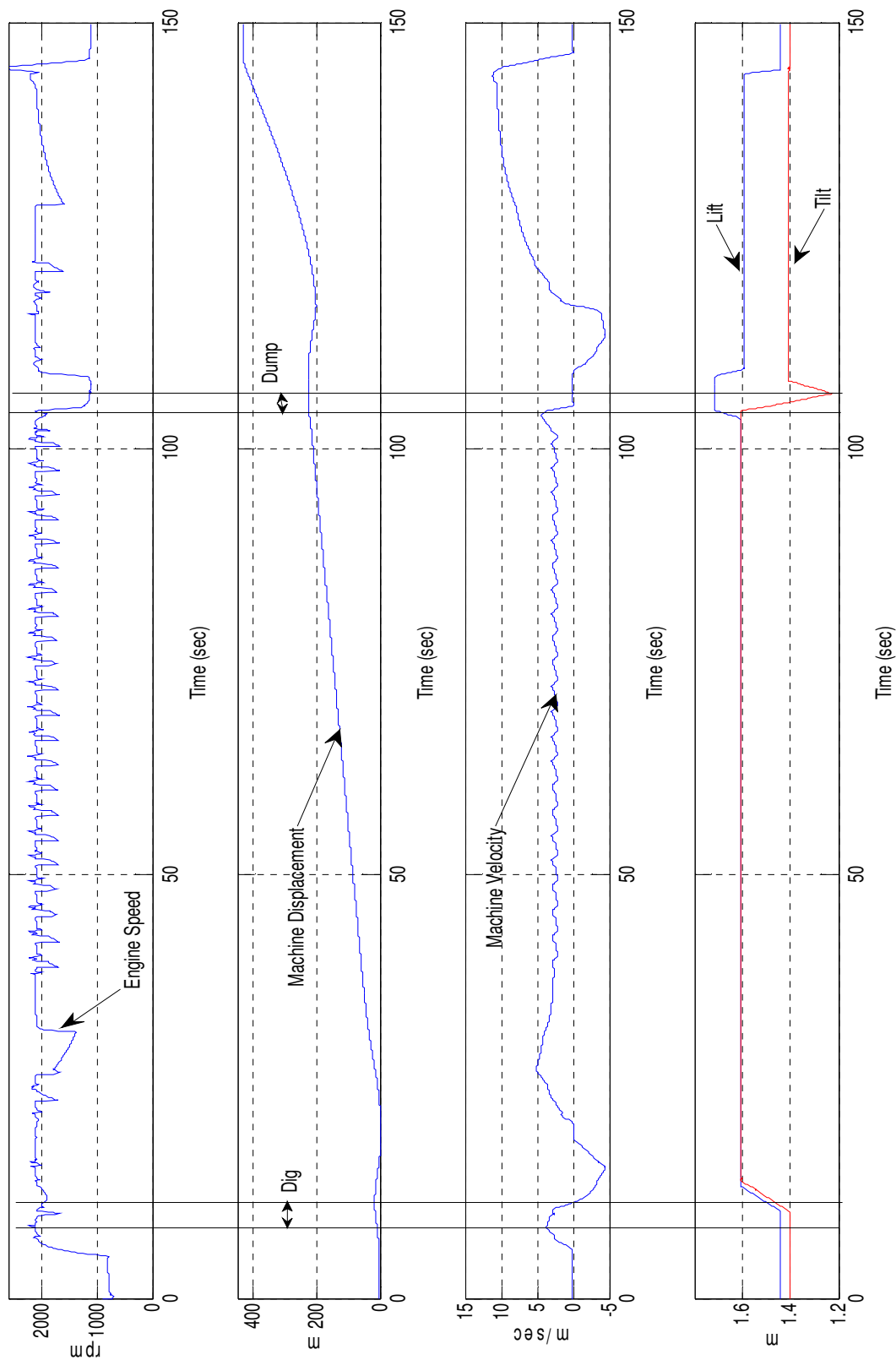


Figure 63: LLC hybrid versus baseline.

**TABLE XII LONG LOAD AND CARRY BASELINE AND HYBRID COMPARISON**

<b>Machine</b>	<b>Cycle Time (sec)</b>	<b>Fuel (grams)</b>	<b>Productivity (%)</b>	<b>Fuel consumption (%)</b>
Baseline	146	1874		
Hybrid	123.6	1262	16.03	-32. 6

**TABLE XIII LONG LOAD AND CARRY OPTIMIZED GAINS**

<b>Parameter</b>	<b>Value</b>
Timer	1
Assist Threshold	0.81
Charge Threshold	0.31
Low SOC Threshold	0.25
Idle Charge Torque	335.6
ISG Torque Required Threshold	133.83
Engine Speed Factor	1.4
Assist Charge Threshold Offset	0.28
Idle Charge SOC Threshold	0.96

#### **4.2.5. Usage of Single Set of Optimized Parameters in Any Cycle**

After the optimization of the control parameters for each independent cycle, the investigation of the effect of using these parameters in different cycles should be investigated. This investigation will determine if online cycle identification and GPS mapping of the worksite is needed. The optimized gain groups shown in table XIV display no common relation to one another that can help determine a single value for any specific gain. While two cycles may agree in one or two gains, the third cycle offers a value completely irrelevant the other two cycles. Hence, each gain group will be used in the other cycles to test how the machine will perform in those cycles with that gain group and compare the result to the cycle optimized gains results.

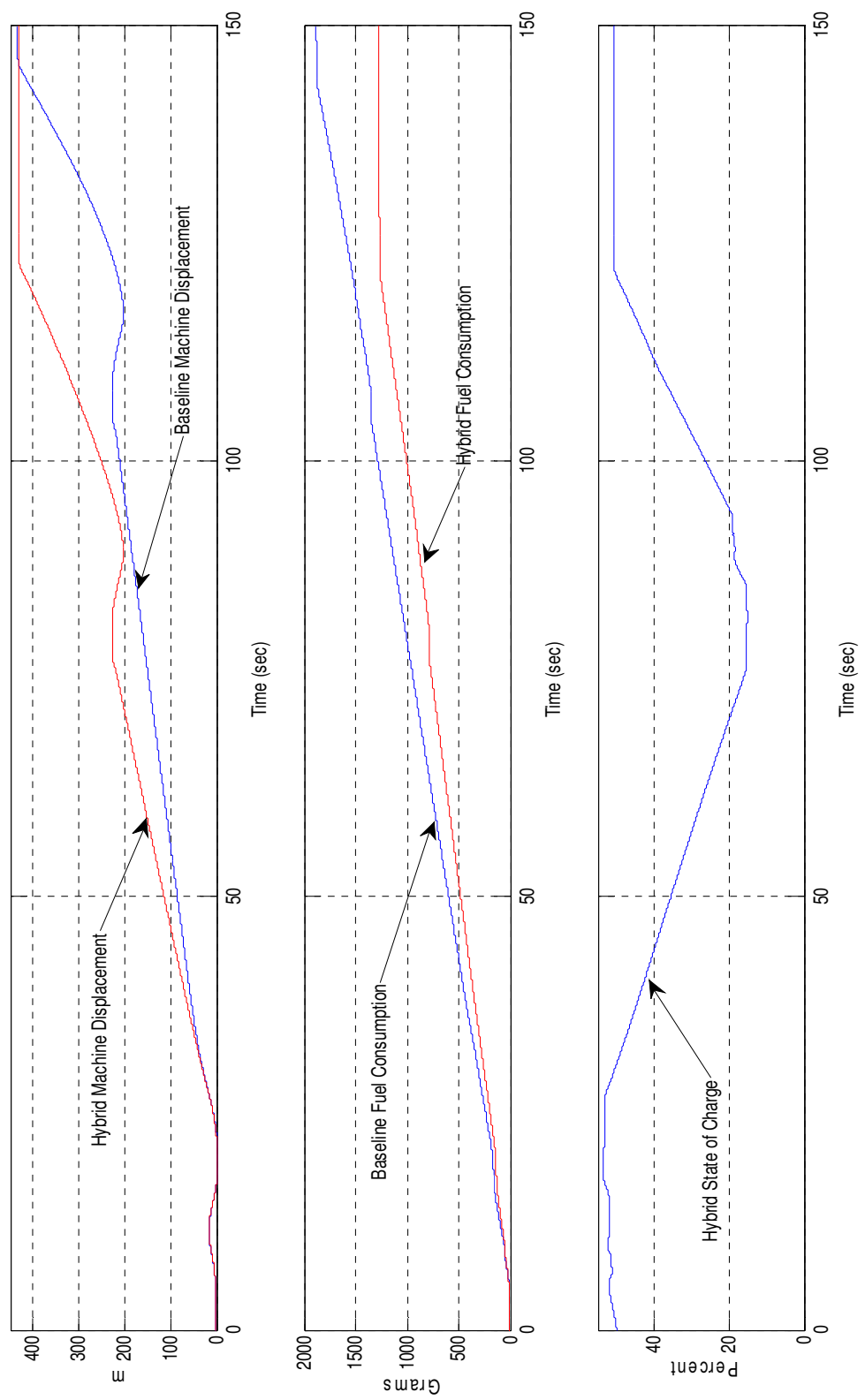


Figure 64: Long load and carry cycle.

In other words, the gain groups of the MTL, SLC and LLC will be tested in the ATL and compared to the results obtained by its optimized gains, the gain groups of the ATL, SLC and LLC will be tested in the MTL and compared to the results obtained by its optimized gains, and the gain groups of the ATL, MTL and LLC will be tested in the SLC and compared to the results obtained by its optimized gains.

**TABLE XIV OPTIMIZED GAINS**

<b>Parameter</b>	<b>ATL</b>	<b>MTL</b>	<b>SLC</b>	<b>LLC</b>
Timer	0	0	0.95	1
Assist Threshold	0.5	1.05	1	0.81
Charge Threshold	0	0.5	0.16	0.31
Low SOC Threshold	0	0.3	0.22	0.25
Idle Charge Torque	0	350	350	335.6
ISG Torque Required Threshold	145.82	42	65	133.83
Engine Speed Factor	1.4	1.35	1.37	1.4
Assist Charge Threshold Offset	0	0.25	0.32	0.28
Idle Charge SOC Threshold	1	0.5	1	0.96

Figures 65, 66, and 67 compare the results of these simulations. It is clear that the use of different gain groups in cycles they were not optimized have little effect on that cycle performance, and the SOC using any cycle gains return to the appropriate SOC range at cycle end. By examining the results closely (Fig 68, and 69), all the cycles exhibit a change of less than 2% in terms of productivity and less than 3% in terms of fuel reduction from that of the optimized cycle. From this it can be concluded that the knowledge of the running cycle is not needed as long as the machine is using any optimized set of parameters. Hence, online cycle identification and GPS mapping is not needed to be implemented on the machine but remains useful as an analysis tool for the worksite and operator performance [112, 113].

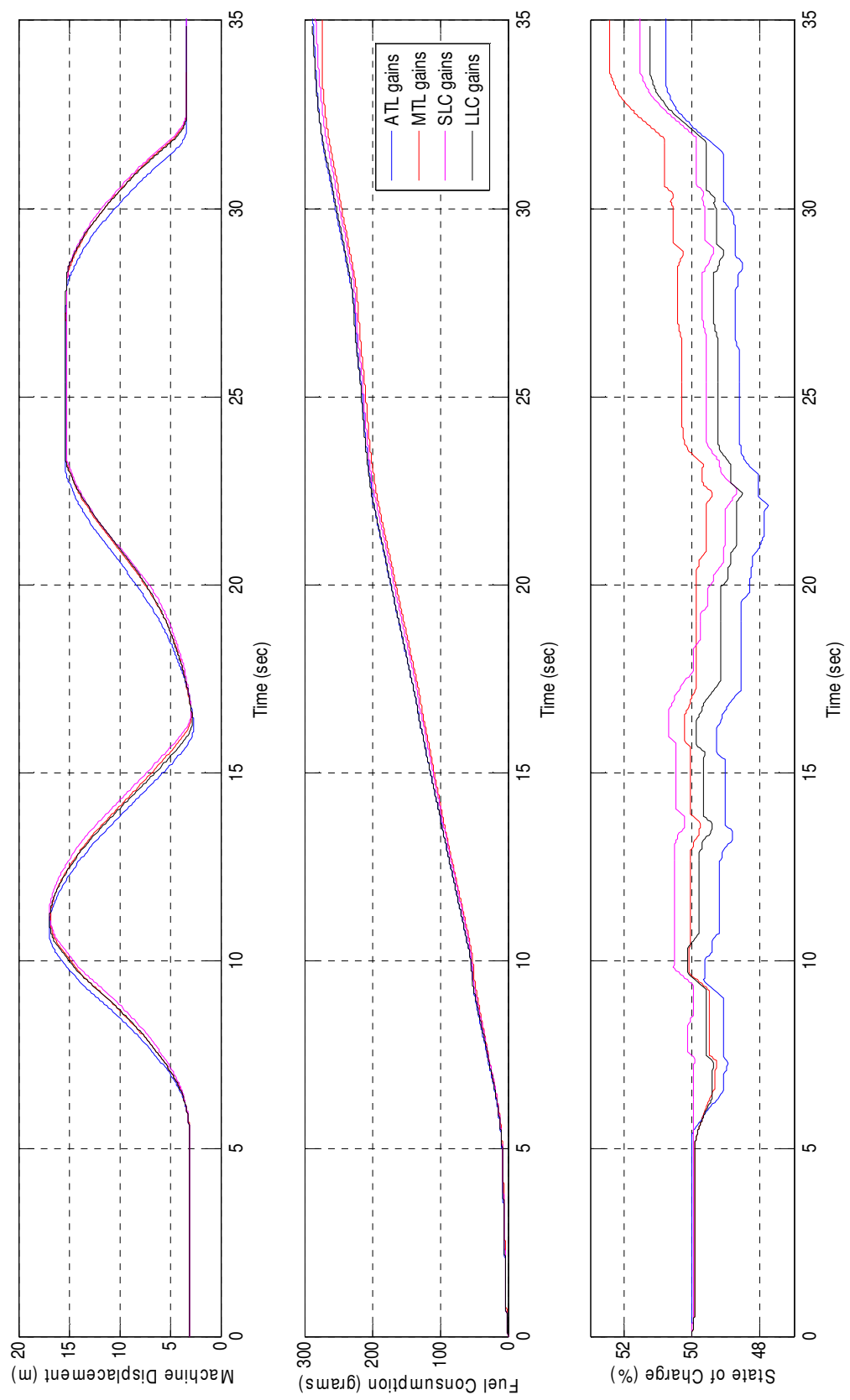


Figure 65: Effect of different gain groups on the ATL cycle.

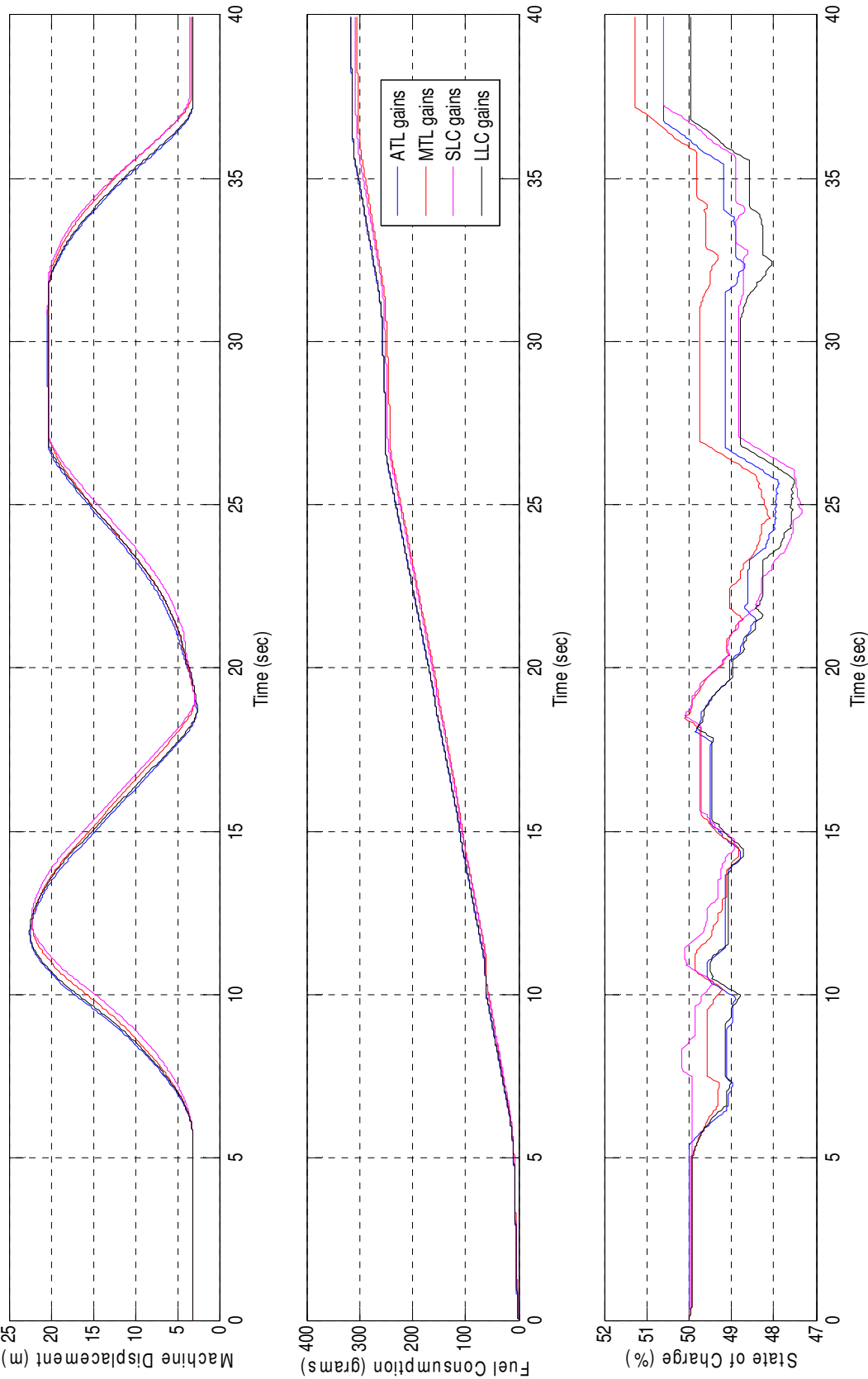


Figure 66: Effect of different gain groups on the MTL cycle.

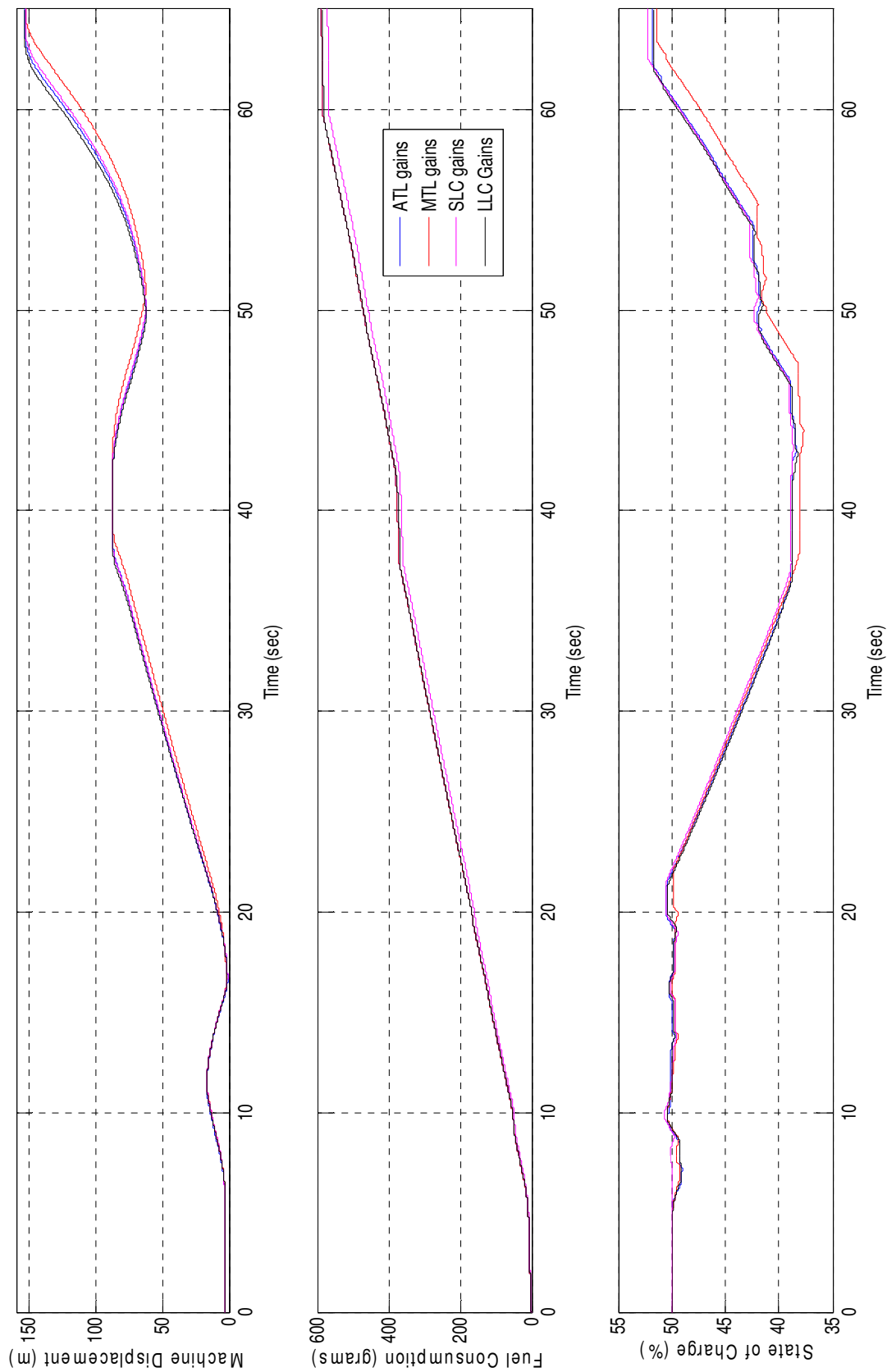


Figure 67: Effect of different gain groups on the SLC cycle.

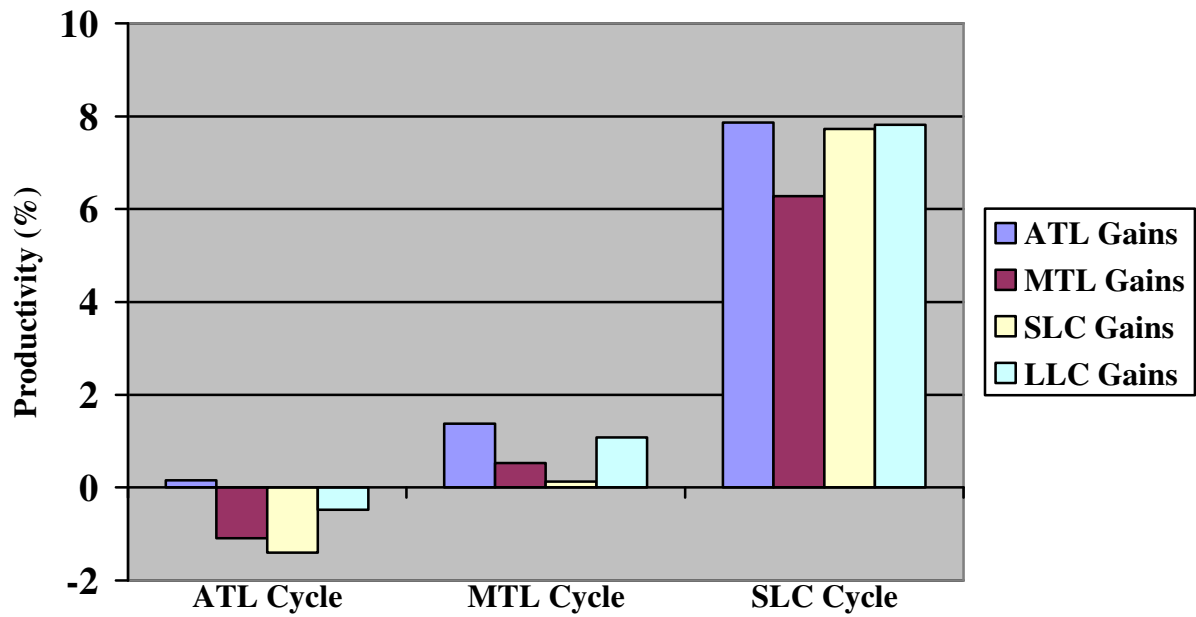


Figure 68: Effect of different gain groups on cycles' productivity.

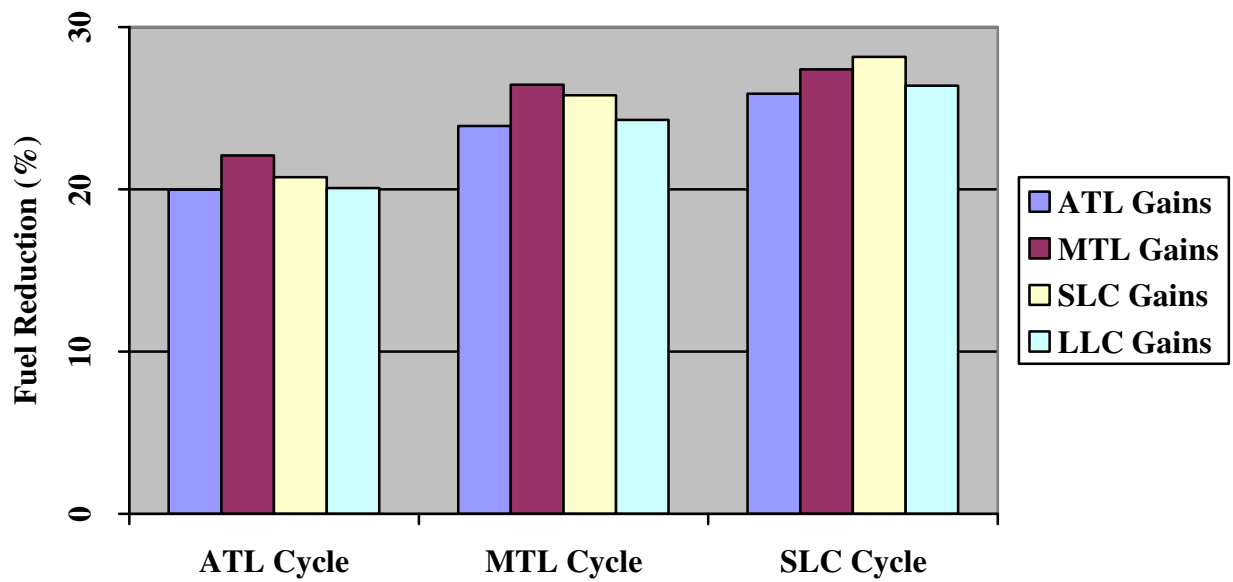


Figure 69: Effect of different gain groups on cycles' fuel reduction.



### 4.3. Results with the 9 Liters Engine

#### 4.3.1. Aggressive Truck Loading Cycle

Figure 70 and table VI compare between the baseline regular and the optimized hybrid wheel loader for the ATL cycle. The optimal values for the controller gains are shown in table VII. From the obtained results it is shown that maintaining productivity while decreasing the fuel consumption by 6.65% can be achieved by switching to the downsized hybrid machine. It is also shown that the ATL cycle does not require a lot of charge from the battery [114,115].

**TABLE XV AGGRESSIVE TRUCK LOADING BASELINE AND HYBRID COMPARISON**

<b>Machine</b>	<b>Cycle Time (sec)</b>	<b>Fuel (grams)</b>	<b>Productivity (%)</b>	<b>Fuel consumption (%)</b>
Baseline	32.15	344.6		
Hybrid	31.7	321.7	1.4	-6.65

**TABLE XVI AGGRESSIVE TRUCK LOADING OPTIMIZED GAINS**

<b>Parameter</b>	<b>Value</b>
Timer	0.5
Assist Threshold	0.8
Charge Threshold	0.1
Low SOC Threshold	0.3
Idle Charge Torque	175
ISG Torque Required Threshold	245
Engine Speed Factor	1.34
Assist Charge Threshold Offset	0.25
Idle Charge SOC Threshold	0.5

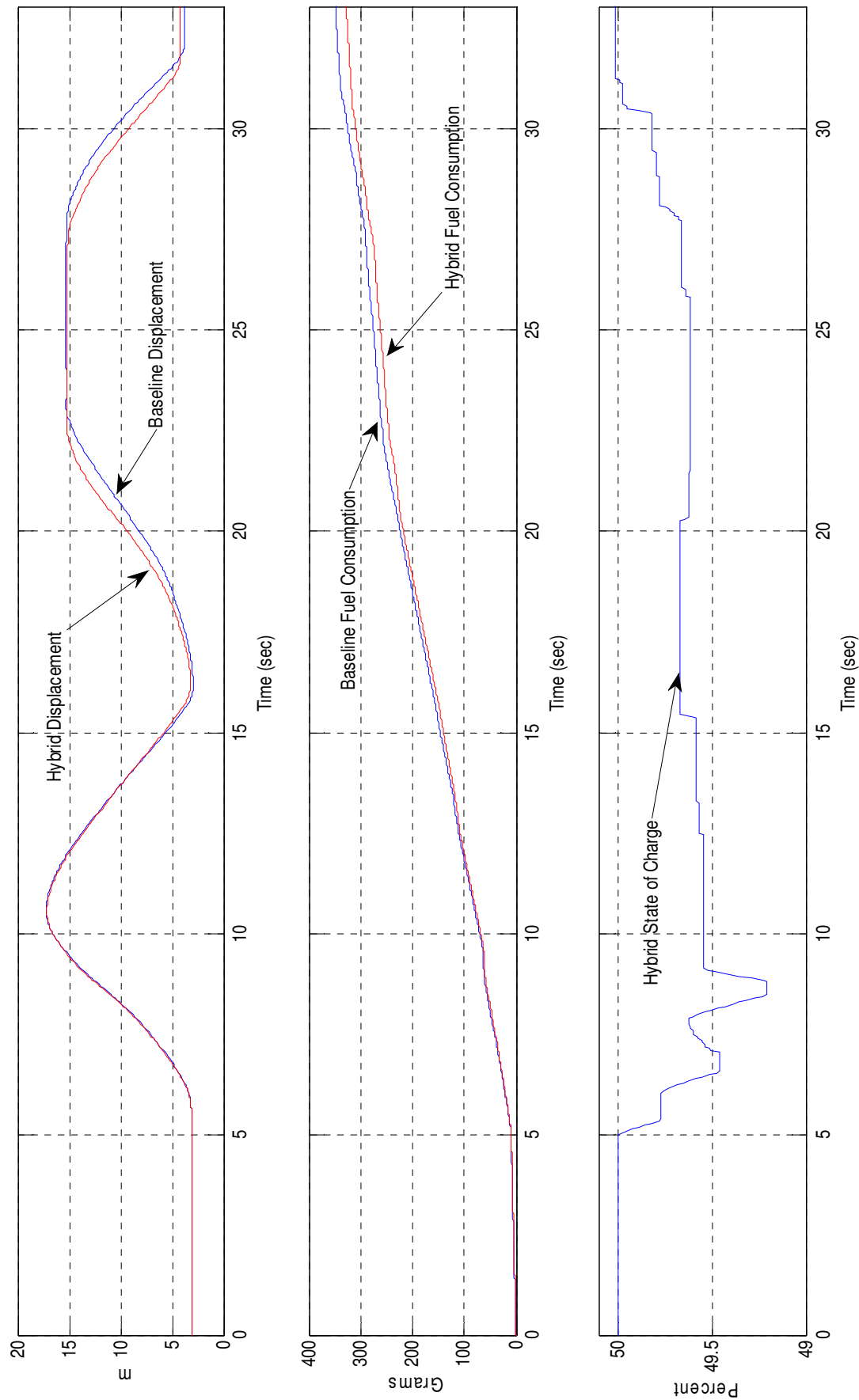


Figure 70: ATL 9 liters hybrid versus baseline.

#### 4.3.2. Moderate Truck Loading Cycle

Figure 71 and table XVII compare between the baseline regular and the optimized hybrid wheel loader for the MTL cycle. The optimal values for the controller gains are shown in table XVIII. From the obtained results it is shown that maintaining productivity while decreasing the fuel consumption by 26.5% can be achieved by switching to the downsized hybrid machine.

**TABLE XVII MODERATE TRUCK LOADING BASELINE AND HYBRID COMPARISON**

<b>Machine</b>	<b>Cycle Time (sec)</b>	<b>Fuel (grams)</b>	<b>Productivity (%)</b>	<b>Fuel consumption (%)</b>
Baseline	37.7	413.17		
Hybrid	38.8	387.8	-2.83	-6.14

**TABLE XVIII MODERATE TRUCK LOADING OPTIMIZED GAINS**

<b>Parameter</b>	<b>Value</b>
Timer	1
Assist Threshold	1.2
Charge Threshold	0.1
Low SOC Threshold	0.4
Idle Charge Torque	348.53
ISG Torque Required Threshold	240.78
Engine Speed Factor	1.35
Assist Charge Threshold Offset	0.29
Idle Charge SOC Threshold	0

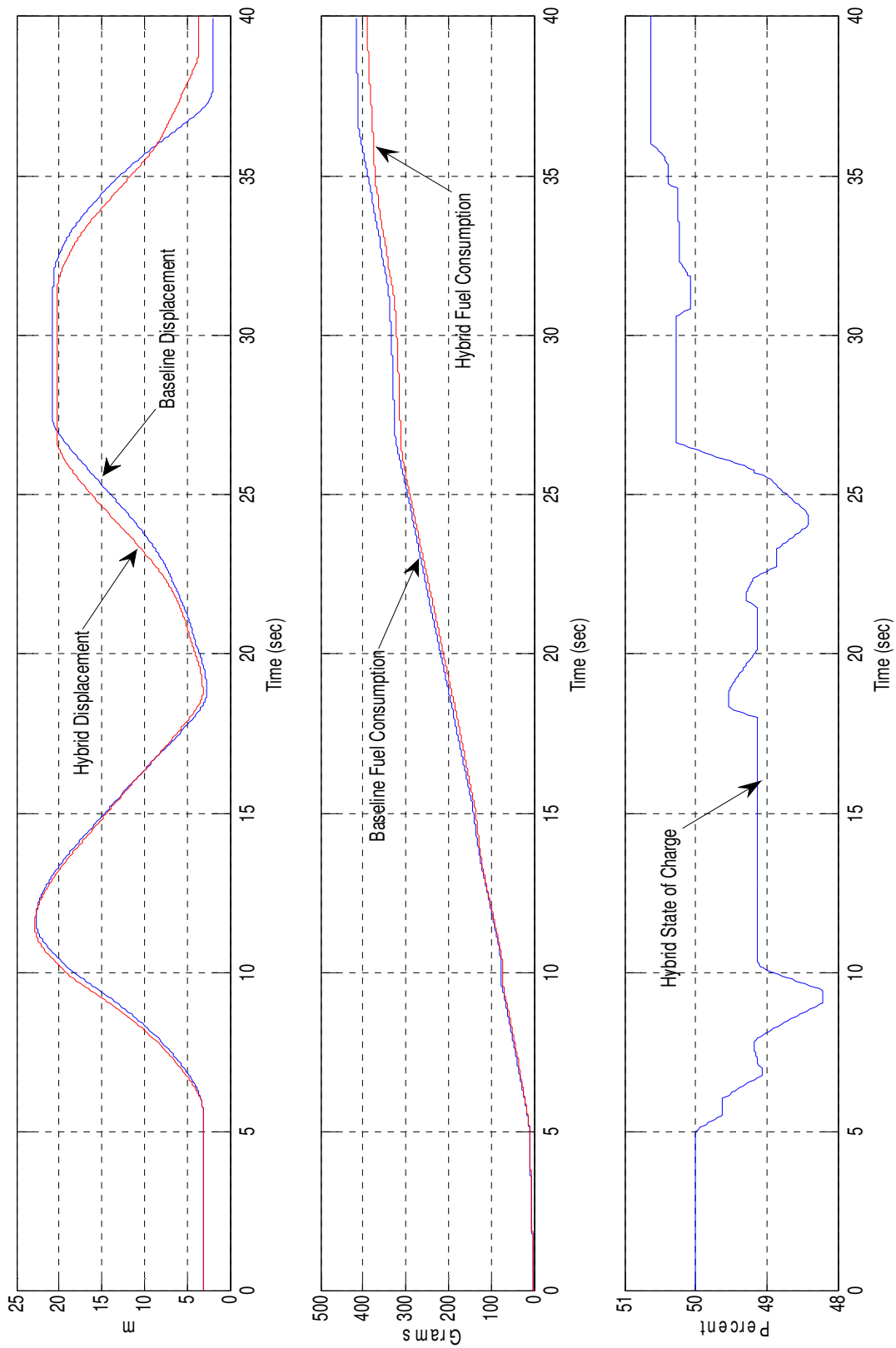


Figure 71: MTL 9 liters Hybrid versus Baseline.

#### **4.4. The Baseline, the Hybrid with 7 and 9 Liters Engines Comparison**

In order to determine the benefit behind the use of hybrid technology in MWL, a comparison between the baseline machine, the hybrid with the regular 9 liters engine, and the hybrid with the 7 liters engine is conducted. Figure 72 and table XIX show the comparison in case of ATL cycle. With the 9 liters engine, the hybrid system increases productivity by about 1.4% and decreases the fuel consumption by 6.65%. On the other hand, the hybrid system with the downsized seven liters engine maintains the productivity as it is but decreases the fuel consumption by about 20%. Figure 73 and table XX show the comparison in case of MTL cycle. With the 9 liters engine, the hybrid system decreases productivity by about 2.83% and decreases the fuel consumption by 6.14%. On the other hand, the hybrid system with the downsized seven liters engine maintains the productivity as it is but decreases the fuel consumption by about 26.5%. The disadvantage of using a downsized engine is that if the battery runs out of charge, the engine may not be able to support the machine functions. On the other hand, the hybrid with the original engine doesn't provide the desired fuel consumption reduction [114,115]. .

**TABLE XIX AGGRESSIVE TRUCK LOADING BASELINE AND HYBRID COMPARISON**

<b>Machine</b>	<b>Cycle Time (sec)</b>	<b>Fuel (grams)</b>	<b>Productivity (%)</b>	<b>Fuel consumption (%)</b>
Baseline	32.15	344.6		
9 Liters Hybrid	31.7	321.7	1.4	-6.65
7 Liters Hybrid	32.1	275.7	0.16	-20

**TABLE XX MODERATE TRUCK LOADING BASELINE AND HYBRID COMPARISON**

<b>Machine</b>	<b>Cycle Time (sec)</b>	<b>Fuel (grams)</b>	<b>Productivity (%)</b>	<b>Fuel consumption (%)</b>
Baseline	37.7	413.17		
9 Liters Hybrid	38.8	387.8	-2.83	-6.14
7 Liters Hybrid	37.5	303.9	0.53	-26.45

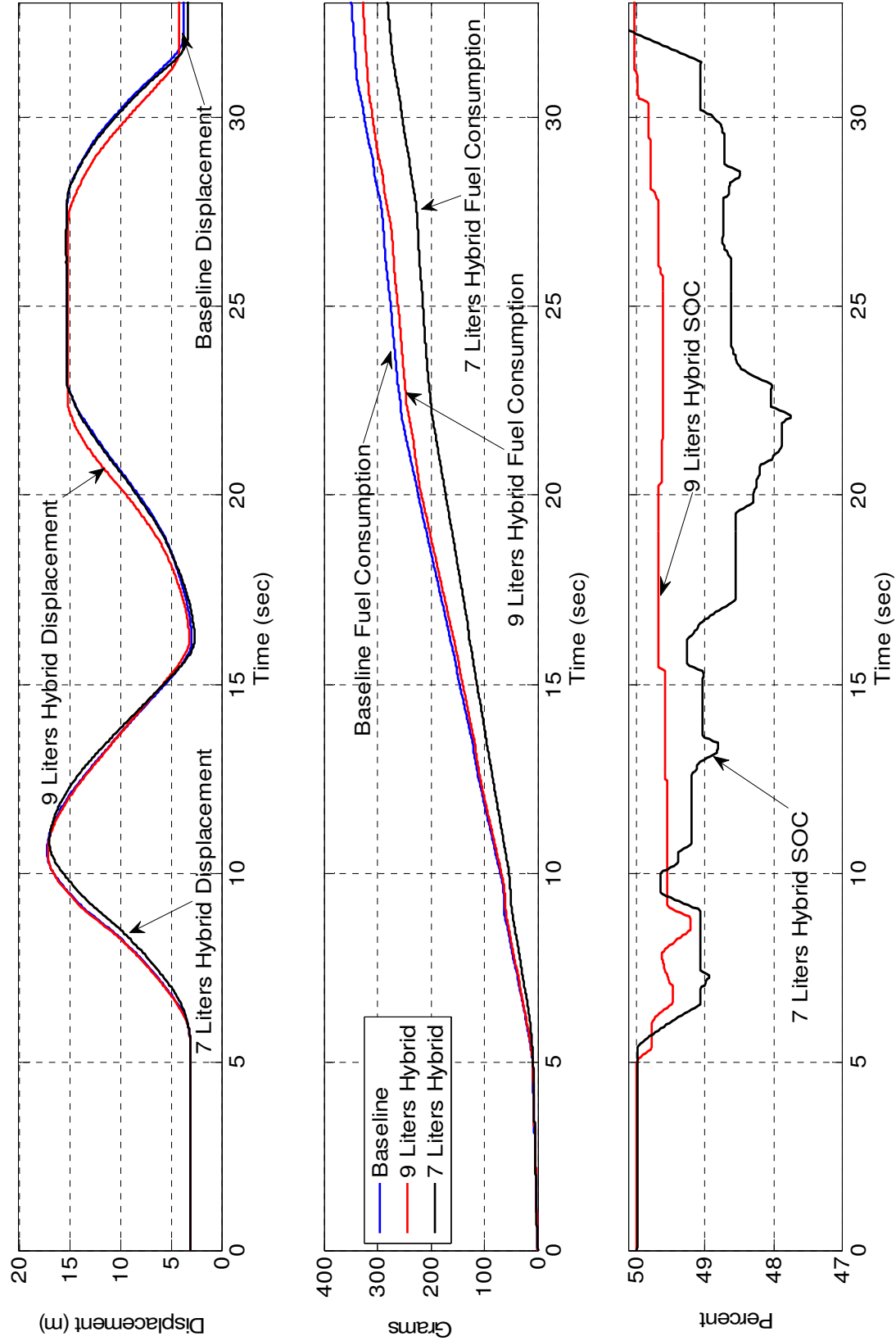


Figure 72: ATL Hybrid versus Baseline.

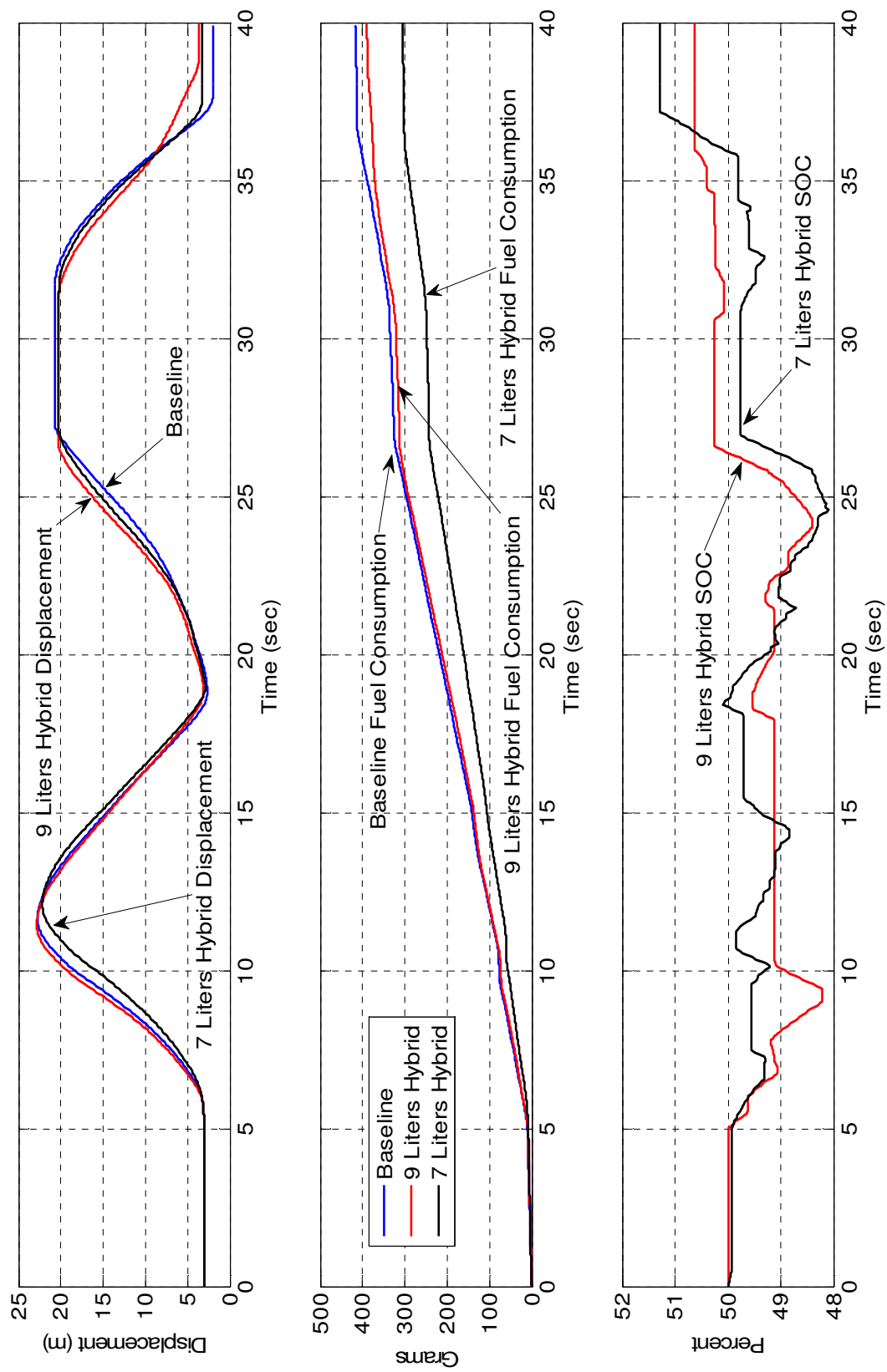


Figure 73: MTL Hybrid versus Baseline.

## **5. CONCLUSIONS AND FUTURE WORK**

### **5.1. Conclusions**

The implementation of the hybrid system on the medium wheel loader is expected to maintain the productivity of the machine within acceptable range. The usage of the hybrid system with a downsized engine is expected to reduce the fuel consumption on the machine by 20-30% at different cycles. The hybrid system supplies 14-17% of the torque required by the machine during its work cycle. By optimizing the hybrid controller gains for any work cycle, the controller can be used with any work cycle. Hence, the gains' values are cycle specific, the overall performance of the controller with these gains does not change significantly. This allows for the elimination of the necessity of implementing online cycle identification and GPS mapping of the machine, which would have been needed to identify the running cycle in order to perform gain scheduling. This elimination allows for the decrease in the software as well as the memory usage of the machine online control module. The hybrid with the original engine is expected to reduce the fuel consumption by about 6-7% and may lead to some loss in productivity equivalent to one shift per year.

### **5.2. Future Work**

The hybrid system performance is yet to be investigated with the original machine engine at more cycles to examine if better fuel consumption can be achieved. More work cycles will be investigated to check of the effect the hybrid system will have on their performance. Investigating the hydraulic and flywheel hybrid systems and optimizing their controllers is still to be completed. Designing other control algorithms and concepts and comparing them is also recommended.



### CITED LITERATURE

1. Rakopoulos, C.D., and Giakoumis, E.G.: “Diesel Engine Transient Operation: Principles of Operation and Simulation Analysis”, Springer, 2009.
2. Cetinkunt, S.: “Mechatronics”, John Wiley and Sons, 2007.
3. [http://www.toyota-global.com/innovation/environmental\\_technology/technology\\_file/](http://www.toyota-global.com/innovation/environmental_technology/technology_file/)  
(September 2011)
4. Gonder, J., and Simpson, A.: “Measuring and reporting the fuel economy of plug-in hybrid electric vehicles”, World Electric Vehicle Association Journal, May 2007.
5. Nermey, F., Leduc, G., and Babiano, A.M.: “Plug-in Hybrid and Battery-Electric Vehicles: State of the research and development and comparative analysis of energy and cost efficiency”, JRC 54699, 2009.
6. Axsen, J., Burke, A.F., and Kurani, K.S.: “Batteries for plug-in hybrid electric Vehicles (PHEVs): Goals and the state of technology circa 2008”, Institution of Transportation Studies University of California Davis, CA, May 2008.
7. Koebler, M., Goldstein, N.G., Brown, S.J., and Harper, J.H.: “Power Management Systems and Devices”, U.S. 7,925,426 B2, April 12, 2011.
8. Tamor, M.A.: “Control System and Control Method for a Hybrid Electric Vehicle Powertrain”, U.S. 6,746,366 B2, June 8, 2004.
9. Abe, S.: “Development of the Hybrid Vehicle and its Future Expectation”, Society of Automotive Engineers, 2000.
10. <http://www.insightcentral.net/encyclopedia/index.html> on (September 2011).

11. Teratani, T., Kuramochi, K., Nakao, H., Tachibana, T., Yagi, K., and Abou, S.: "Development of Toyota Mild Hybrid Vehicle (THS-M) with 42V Power Net", Electric Machines and Drives Conference, IEEE, Vol.1, pp. 3-10, 2003.
12. Yamaguchi, K., Obata, A., and Masuda, A.: "Hybrid Vehicle", U.S. 6,488,608 B2, December 3, 2002.
13. Boggs, D.L., Robichaux, J.D., Peters, M.W., and Kotre, S.J.: "Controlled Engine Shutdown for a Hybrid Electric Vehicle", U.S. 6,763,298 B2, July 13, 2004.
14. Koike, T., and Masuda, T.: "Control System for a Vehicle Mounted Battery", U.S. 5,965,991, October 12, 1999.
15. Sakai, S., and Kobayashi, T.: "Battery Control Method for Hybrid Vehicle", U.S. 6,608,482 B2, August 19, 2003.
16. Kimura, T., and Murakami, Y.: "Charging/Discharging Control Method for Secondary Battery", U.S. 6,573,687 B2, June 3, 2003.
17. Shen, S., and Veldpaus, F.E.: "Analysis and Control of a Flywheel Hybrid Vehicular Powertrain", IEEE Transaction on Control Systems Technology, Vol. 12, No. 5, pp. 645-660, 2004.
18. Schlurmann, J., and Schroder, D.: "Compensation of Dynamic Torques and Flywheel Start in a CVT Based Hybrid Powertrain", Proceedings of IEEE International conference on Control Applications, pp. 2456-2461, October 2006.
19. Diego-Ayala, U., Martinez-Gonzalez, P., and Pullen, K.R.: "A Simple Mechanical Transmission System for Hybrid Vehicles Incorporating a Flywheel", IET HEVC, pp.1-8, 2008.

20. Cross, D., and, Brockbank, C.: “Mechanical Hybrid System Comprising a Flywheel and CVT for Motorsport and Mainstream Automotive Applications”, SAE World Congress & Exhibition, 09PFL-0922, 2009.
21. Katrasnik, T., Trenc, F., and Opresnik, S.R.: “Analysis of Energy Conversion Efficiency in Parallel and Series Hybrid Powertrains”, IEEE Transactions on Vehicular Technology, Vol. 56, No.6, pp. 3649-3659, 2007.
22. Karden, E., Ploumen, S., Fricke, B, Miller, T., and Snyder, K.: “Energy Storage Devices for Future Hybrid Electric Vehicles”, Journal of Power Sources, Vol. 168, pp. 2-11, 2007.
23. He, X., and Hodgson, J.W.: “Modeling and Simulation for Hybrid Electric Vehicles – Part I: Modeling”, IEEE Transaction on Intelligent Transportation Systems, Vol. 3, No. 4, pp. 235-243, 2002.
24. He, X., and Hodgson, J.W.: “Modeling and Simulation for Hybrid Electric Vehicles – Part II: Simulation”, IEEE Transaction on Intelligent Transportation Systems, Vol. 3, No. 4, pp. 244-251, 2002.
25. Stecki, J., and Matheson, P.: “Advances in Automotive Hydraulic Hybrid Drives”, Proceedings of the 6<sup>th</sup> JFPS International Symposium on Fluid Power, pp. 664-669, November, 2005.
26. Donitz, C., Voser, C., Vasile, L., Onder, C., and Guzzella, L.: “Validation of the Fuel Saving Potential of Downsized and Supercharged Hybrid Pneumatic Engines using Vehicle Emulation Experiments” Journal of Engineering for Gas Turbines and Power, Vol.133, No.9, 2011.

27. Jang, S., Yeo, H., Kim, C., and Kim, H.: "A Study on Regenerative Braking for a parallel Hybrid Electric Vehicle", *KSME International Journal*, Vol. 15, No. 11, pp.1490-1498, 2001.
28. Cikanek, S.R., and Bailey, K.E.: "Regenerative Braking System for a Hybrid Electric Vehicle", *Proceedings of the American Control Conference*, pp.3129-3134, Anchorage, May, 2002.
29. Wen-yong, X., Feng, W., and Zhou, B.: "Regenerative Braking algorithm for an ISG HEV Based on Regenerative Torque Optimization", *Journal of Shanghai Jiaotong University Science*, Vol. 13, No. 2, pp. 193-200, 2008.
30. Yafu, Z., and Cheng, C.: "Study on the Powertrain for ISG Mild Hybrid Electric Vehicle", *IEEE Vehicle Power and Propulsion Conference*, Harbin, September, 2008.
31. Park, S., and Jung, D.: "Design of Vehicle cooling System Architecture for a heavy Duty Series-Hybrid Electric Vehicle Using Numerical System Simulations", *Journal of Engineering for Gas Turbines and Power*, Vol.132, No.9, 2010.
32. Tavares, F., Johri, R., and Filipi, Z.: "Simulation Study of Advanced Variable Displacement Engine Coupled to Power-Split Hydraulic Hybrid Powertrain", *Journal of Engineering for Gas Turbines and Power*, Vol.133, No.9, 2011.
33. Montazeri-Gh, M., and Soleymani, M.: "Investigation of the energy regeneration of Active Suspension System in Hybrid Electric Vehicles", *IEEE Transactions on industrial Electronics*, Vol. 57, no. 3, pp. 918-925, 2010.
34. Katrasnik, T.: "Analytical Method to Evaluate Fuel Consumption of Hybrid Electric Vehicles at Balanced Energy Content of the Electric Storage Devices" *Journal of Applied Energy*, Vol. 87, pp. 3330-3339, 2010.

35. Atkins, M.J., and Koch, C.R.: "A Well-to-Wheel Comparison of Several Powertrain Technologies", SAE Advanced Hybrid Vehicle Powertrains, pp. 1-9, 2003.
36. Ogawa, H., Matsuki, M., and Eguchi, T.: "Development of a Powertrain for the Hybrid Automobile – The Civic Hybrid", SAE Advanced Hybrid Vehicle Powertrains, pp. 11-22, 2003.
37. Flynn, M.M., Zierer, J., and Thompson, R.: "Performance Testing of a Vehicular Flywheel Energy System", SAE Advanced Hybrid Vehicle Powertrains, pp. 119-126, 2005.
38. Jackey, R.A., Smith, P., and, Bloxham, S.: "Performance Physical System Model of a Hydraulic Energy Storage Device for Hybrid Powertrain Applications", SAE Advanced Hybrid Vehicle Powertrains, pp. 127-138, 2005.
39. Su, G.J., McKeever, J.W., and Samons, K.S.: "Design of a PM Brushless Motor Drive for Hybrid Electrical Vehicle Application", PCIM 2000 Conference, Boston, October, 2000.
40. Destraz, B., Barrade, P., and Rufer, A.: "Supercapacitive Energy Storage for Diesel-Electric Locomotives", SPEEDAM, June, 2004.
41. Evans, D.G., Polom, M.E., Poulos, S.G., Van Maanen, K.D., and Zarger, T.H.: "Powertrain Architecture and Controls Integration for GM's Hybrid Full-Size Pickup Truck", SAE Advanced Hybrid Vehicle Powertrains, pp. 33-44, 2003.
42. Liang, C., Weihua, W., and Qingnian, W.: "Energy Management Strategy and Parametric Design for Hybrid Electric Military Vehicle", SAE Advanced Hybrid Vehicle Powertrains, pp. 45-50, 2003.
43. Steinmaurer, G., and Del Re, L.: "Optimal Energy Management for Mild Hybrid Operations of Vehicle with an Integrated Starter Generator", SAE Advanced Hybrid Vehicle Powertrains, pp. 73-80, 2005.

44. He, L., Wu, G., Meng, X., and Sun, X.: "A Novel Continuously Variable Transmission Flywheel Hybrid Electric Powertrain", IEEE Vehicle Power and Propulsion Conference, Harbin, September, 2008.
45. Setlur, P., Wagner, J.R., Dawson, D.M., and Samuels, B.: "Nonlinear Control of a Continuously Variable Transmission (CVT) for Hybrid Vehicle Powertrains", Proceedings of the American Control Conference, Arlington, June, 2001.
46. Kessels, J.T.B.A., Sijs, J., Hermans, R.M., Damen, A.A.H., and Van Den Bosch, P.P.J.: "On-line Identification of Vehicle Fuel Consumption for Energy and Emission Management: An LTP System Analysis", American Control Conference, Seattle, June, 2008.
47. Sciarretta, A., and Guzzella, L.: "Control of Hybrid Electric Vehicles", IEEE Control Systems Magazine, 2007.
48. Liu, J., and Peng, H.: "Modeling and Control of a Power-Split Hybrid Vehicle", IEEE Transactions on Control Systems Technology, Vol. 16, No. 6, pp. 1242-1251, 2008.
49. Paganelli, G., Guezennec, Y., and Rizzoni, G.: "Optimizing Control Strategy for Hybrid Fuel Cell Vehicle", SAE Warrendale, PA, Tech. Rep. 2002-01-0102, 2002.
50. Syed, F.U., Ying, H., Kuang, M., Okubo, S., and Smith, M.: "Rule-Based Fuzzy Gain-Scheduling PI Controller to Improve Engine Speed and Power Behavior in Power-split Hybrid Electric Vehicle", IEEE Transactions on Vehicle Technology, Vol. 58, No. 1, pp. 69-84, January 2009.
51. Canova, M., Guezennec, Y., and Yurkovich, S.: "On the Control of Engine Start/Stop Dynamics in a Hybrid Electric Vehicle", Journal of Dynamic Systems, Measurement, and Control, Vol. 131, 2009.

52. Lin, X., Banvait, H., Anwar, S., and Chen, Y.: "Optimal Energy Management for a Plug-in Hybrid Electric Vehicle: Real-time Controller", American Control Conference, Baltimore, July, 2010.
53. Hui, S., Lifu, Y., Junging, J., and Yanling, L.: "Control Strategy of Hydraulic/Electric Synergy System in Heavy Hybrid Vehicles", Energy Conversion and Management, Vol. 52, pp. 668-674, 2011
54. Saerens, B., Vandersteen, J., Persoons, T., Swevers, J. Diehl, M., and Van den Bulck, E.: "Minimization of the Fuel Consumption of a Gasoline Engine Using Dynamic Optimization", Applied Energy, Vol.86, pp. 1582-1588, 2009.
55. Feroldi, D., Serra, M., and Riera, J.: "Energy Management Strategies Based on Efficiency Map for Fuel Cell Hybrid Vehicles", Journal of Power Sources, Vol. 190, pp. 387-401, 2009.
56. Gokasan, M., Bogosyan, S., and Goering, D.J.: "Sliding Mode Based Powertrain Control for Efficiency Improvement in Series Hybrid-Electric Vehicles", IEEE Transactions on Power Electronics, Vol. 21, No.3, pp. 779-790, 2006.
57. Moura, S.J., Fathy, H.K., Callaway, D.S., and Stein, J.L.: "A Stochastic Optimal Control Approach for Power Management in Plug-In Hybrid Electric Vehicles", IEEE Transactions on Control Systems Technology, Vol. 19, No.3, pp. 545-555, 2011.
58. Johannessson, L., Asbogard, M., and Egardt, B.: "Assessing the Potential of Predictive Control for Hybrid Vehicle Powertrains Using Stochastic Dynamic Programming", IEEE Transactions on Intelligent Transportation Systems, Vol. 8, No. 1, pp. 71-83, 2007.

59. Fang, L., Qin, S., Xu, G., Li, T., and Zhu, K.: "Simultaneous Optimization for Hybrid Electric Vehicle Parameters Based on Multi-Objective Genetic Algorithms", *Energies*, Vol. 4, pp. 532-544, 2011.
60. Shupeng, Z., Shifang, Z., Pengyun, X., and Meng, L.: "Control Strategy and Simulation Analysis of Hybrid Electric Vehicle" IEEE 8<sup>th</sup> International Conference on Electronic Measurement and Instruments, Vol.1, pp.318-321, 2007.
61. Quigley, C.P.: "The Use of Vehicle Navigation Information and Prediction of Journey Characteristics for the Optimal Control of Hybrid and Electric Vehicles", SAE World Congress & Exhibition, 2011.
62. Ranjan, N., and Li, Y.: "Trip Based Stochastic Prediction of Battery State of Charge for Electric Vehicles", SAE World Congress & Exhibition, 2011.
63. Mathews, J.C., Walp, K.J., and Molen, M.: "Development and Implementation of a control System for Parallel Hybrid Powertrain", IEEE Vehicle Power and Propulsion Conference, pp.1-6, 2006.
64. Huang, Y.J., Yin, C. L., and Zhang, J.W.: "Design of an Energy Management Strategy for Parallel Hybrid Electric Vehicles Using a Logic Threshold and Instantaneous Optimization Method", *International Journal of Automotive Technology*, Vol.10, No. 4, pp. 513-521, 2009.
65. Hui, S., Ji-hai, J., and Xin, W.: "Torque Control Strategy for a Parallel Hydraulic Hybrid Vehicle", *Journal of Terramechanics*, Vol. 46, pp. 259-265, 2009.



66. Lei, Z., Yugong, L., Diange, Y., Keqiang, L., and Xiaomin, L.: "Development of Hybrid Powertrain Controller for a PSHEV", IEEE Vehicular Electronics and Safety, pp.222-227, Beijing, 2006.
67. Lee, S.H., Walters, S.D., and Howlett, R.J.: "Intelligent GPS-Based Vehicle Control for Improved Fuel Consumption and Reduced Emissions", Proceedings of the 12th international conference on Knowledge-Based Intelligent Information and Engineering Systems, pp. 701-708, 2008.
68. Wu, B., Lin, C., Filipi, Z., Peng, H., and Assanis, D.: "Optimization of Power Management Strategies for a Hydraulic Hybrid Medium Truck", Proceedings of the Advanced Vehicle Control Conference, Hiroshima, September, 2002.
69. Du, C., Yan, F., Hou, X., and Hu, J.: "Development Platform for the Control System of Hybrid Electric Vehicles Powertrain", Power and Energy Engineering Conference, pp. 1-4, 2010.
70. Kleimaier, A., and Schroder, D.: "An Approach for the Online Optimized Control of a Hybrid Powertrain", IEEE 7th International Workshop on Advanced Motion Control, pp. 215 – 220, Maribor, 2002.
71. Delprat, S., Lauber, J., Guerra, T.M., and Rimaux, J.: "Control of a Parallel Hybrid Powertrain: Optimal Control", IEEE Transactions on Vehicular Technology, Vol. 53, No. 3, pp. 872-881, 2004.
72. Fu, Z.X.: "Real-Time Predication of Torque Availability of an IPM Synchronous Machine Drive for Hybrid Electric Vehicles", IEEE Conference on Electric Machines and Drives, pp. 199-206, San Antonio, May, 2005.

73. Cacciatori, E., Vaughan N.D., and Marco J.: “Energy Management Strategies for a Parallel Hybrid Electric Powertrain: Fuel Economy Optimization with Driveability Requirements”, Proceedings of the PARD Hybrid Electric Vehicle Conference, pp.157-172, University of Warwick, December, 2006.
74. Sinoquet, D., Rousseau, G., and Milhau, Y.: “Design Optimization and Optimal Control for Hybrid Vehicles”, Optimization and Engineering, Vol. 12, No. 1-2, pp. 199-213, 2009.
75. Borhan, H.A., Vahidi, A., Phillips, A.M., Kuang, M.L., and Kolmanovsky, I.V.: “Predictive Energy Management of a Power-Split Hybrid Electric Vehicle”, American Control conference, pp. 3970-3976, June 2009.
76. Primbs, J.A., Nevistic, V., and Doyle, J.C.: “Nonlinear Optimal Control, a Control Lyapunov Function and Receding Horizon Perspective”, Asian Journal of Control Vol. 1, No.1, pp. 14-24, 1999.
77. Nevistic, V., and Primbs, J. A.: “Constrained Nonlinear Optimal Control, a Converse HJB Approach”, California Institute of Technology, Pasadena, CA 91125, Tech. Rep. CIT-CDS 96-021, 1996.
78. Kirk, D.E.: “Optimal Control Theory, an Introduction”, New York, Dover Publications Inc., 1998.
79. Elnagar, G.N., and Kazemi, M.A.: “Pseudospectral Chebyshev Optimal Control of Constrained Dynamical systems”, Computational Optimization and Applications, Vol. 11, pp. 195-217, 1998.
80. Kurzhanski, A.B., and Varaiya, P.: “The Hamilton-Jacobi Type Equations for Nonlinear Target Control and their Approximation”, Analysis and design of nonlinear control systems, Springer, pp.77-90, 2008.

81. Vlassenbroeck, J., and Van Dooren, R.: "A Chebyshev Technique for solving Nonlinear Optimal Control Problems", IEEE Transactions on Automatic Control, Vol. 33, No.4, pp. 333-340, 1988.
82. Beard, R., Saridis, G., Wen, J., and Wen Z, J.: "Galerkin Approximation of the Generalized Hamilton-Jacobi-Bellman Equation", IFAC Automatica, Vol.33, No.12, pp. 2159-2177, 1997.
83. Forsyth, P. A., and Labahn, G.: "Numerical methods for controlled Hamilton-Jacobi-Bellman PDEs in Finance", Journal of Computational Finance, Vol.11, pp.1-44, 2007.
84. Carma, Ph., and Schoukens, J.: "Hammerstein-Wiener System Estimator Initialization", Automatica, Vol. 40, No. 9, pp. 1543-1550, 2004.
85. Wei, H.L., and Billings, S.A.: "Identification of Time-Varying Systems using Multiresolution Wavelet Models", International Journal of Systems Science, Vol. 33, No.15, pp. 1217-1228, 2002.
86. Wei, H.L., and Billings, S.A.: "A New Class of Wavelet Networks for Nonlinear System Identification", IEEE Transactions on Neural Networks, Vol. 16, No. 4, pp. 862-874, 2005.
87. Camacho, E.F., and Bordons, C.: "Model Predictive Control", Springer-Verlag London Limited, 1999.
88. Clarke, D., Mohtadi, C., and Tuffs, P.: "Generalized predictive control: part I," Automatica, Vol. 23, No. 2, pp. 137-148, 1987.
89. Clarke, D., Mohtadi, C., and Tuffs, P.: "Generalized predictive control: part II. Extensions and Interpretations," Automatica, vol. 23, no. 2, pp. 149-160, 1987.

90. Salcedo, J.V.,Martines, M., Sanchis, J., and Blasco, X.: “Design of GPC’s in State Space”, *Automatika*, Vol.42, No. 3, pp.159-167, 2002.
91. Venkateswarlu, CH., and Gangiah, K.: “Constrained Generalized Predictive Control of unstable Nonlinear Processes”, *Transactions of Insitution of Chemical Engineers*, Vol. 75, pp. 371-376, 1997.
92. Saad, M.M., and Sanchez, G.: “Multivariable Generalized Predictive Adaptive Control with a Suitable Tracking Capability”, *Journal of Process Control*, Vol. 4, No. 1, pp. 45-52, 1994.
93. Dexian, H., Jingchun, W., and Yihui, J.: “Stable MIMO Constrained Predictive Control with Steady State Objective Optimization”, *Chinese Journal of Chemical Engineering*, Vol.8, No. 4, pp. 332-338, 2000.
94. Kerrigan, E.C., and Maciejowski, J.M.: “Feedback min-max Model Predictive Control using a Single Linear Program: Robust Stability and the Explicit Solution”, *International Journal of Robust and Nonlinear Control*, Vol. 14, pp. 395-413, 2004.
95. Sui, D., Feng, L., and Hovd, M.: “Robust Output Feedback Model Predictive Control for Linear Systems via Moving Horizon Estimation”, *American Control Conference*, Washington, pp. 453-458, June, 2008.
96. Lovaas, C., Seron, M.M., and Goodwin, G.C.: “Robust Output-Feedback MPC with Integral Action”, *IEEE Transactions on Automatic Control*, Vol. 55, No. 7, pp. 1531-1543, 2010.
97. Jain, A.K., Duin, R.P.W., and Mao, J.: “Statistical Pattern Recognition: A Review”, *IEEE Transactions on Pattern Analysis and Machine Intelligence*, Vol. 22, No. 1, pp. 4-37, 2000.

98. Giannotti, F., Nanni, M., Pedreschi, D., and Pinelli, F.: "Trajectory Pattern Mining", Proceedings of ACM SIGKDD Conference on Knowledge Discovery and Data Mining, 2007.
99. Chen, C., Ibanez-Guzman, J., and Le-Marchand, O.: "Pattern Recognition for Loosely-coupled GPS/Odometer Fusion", IEEE International Conference on Intelligent Robots and Systems, pp. 3853-3858, Nice, September, 2008.
100. Abed, M.A., Ismail, A.N., and Hazi, Z.M.: "Pattern Recognition Using Genetic Algorithm", International Journal of Computer and Electrical Engineering, Vol. 2, No. 3, pp. 583-588, 2010.
101. Grammatico, S., Balluchi, a., and Cosoli, E.: "A Series-Parallel Hybrid Electric Powertrain for Industrial Vehicles", IEEE, Vehicle Power and Propulsion Conference, pp. 1-6, 2010.
102. Caterpillar Inc.: "966K Wheel Loader Brochure", Technical Brochure, Caterpillar Inc., 2011.
103. Caterpillar Inc.: "Getting Started with Dynamic", Technical Training Manual, Caterpillar Inc., 2010.
104. Caterpillar Inc.: "Dynamic Basic Hydraulics", Technical Training Manual, Caterpillar Inc., 2010.
105. Caterpillar Inc.: "Dynamic Basic Linkages Training", Technical Training Manual, Caterpillar Inc., 2010.
106. Caterpillar Inc.: "C9.3 ACERT<sup>TM</sup> Industrial Engine", Technical Brochure, Caterpillar Inc., 2011.
107. Caterpillar Inc.: "C7.1 ACERT<sup>TM</sup> Industrial Engine", Technical Brochure, Caterpillar Inc., 2011.

- 108.Croce, F.: “Optimal Design of Powertrain and Hydraulic Implement Systems for Construction Equipment Applications”, Ph.D. thesis, University of Illinois at Chicago, 2010.
- 109.Ehsani, M, Gao, Y., and Emadi, A.: “Modern Electric, Hybrid Electric, and Fuel Cell Vehicles: Fundamentals, Theory, and Design Second Edition”, CRC Press, Taylor and Francis Group, 2010.
- 110.Fowlkes, Y.W., and Creveling, C.M.: “Engineering Methods for Robust Product Design Using Taguchi Methods in Technology and Product Development”, Prentice Hall, 1995.
- 111.Ramkumar, C.: “MWL Machine Performance Monitor Onboard Segmentation Version”, Technical Report, Caterpillar Inc., 2011.
- 112.Zaher, M.H., Cetinkunt, S., Real Time Energy Management Control for Hybrid Electric Powertrains, Journal of Control Science and Engineering, Hindawi, 2012, Submitted .
- 113.Zaher, M.H., Cetinkunt, S., Real Time Energy Management Strategy for Hybrid Electric Powertrains, SAE 2013 Commercial Vehicle Engineering Congress, 13CV-0074, Rosemont, Illinois, USA, October 1-3, 2013, Submitted.
- 114.Zaher, M.H., Cetinkunt, S., Fuel Saving and Control for Hybrid Electric Powertrains, Control Engineering Practice, Elsevier, 2013 Submitted.
- 115.Zaher, M.H., Cetinkunt, S., Fuel Saving and Control Strategy for Hybrid Electric Powertrains, SAE 2013 Commercial Vehicle Engineering Congress, 13CV-0066, Rosemont, Illinois, USA, October 1-3, 2013, Submitted.

## **VITA**

### **PERSONAL INFORMATION**

Full name: Mohamed Zaher

E-mail address: [mhzaher@asme.org](mailto:mhzaher@asme.org)

### **ACADEMIC BACKGROUND**

Doctor of Philosophy: University of Illinois at Chicago, 2013

Master of Science: Cairo University, 2009

Bachelors of Engineering: Cairo University, 2005

### **PROFESSIONAL BACKGROUND**

Teaching and Research Assistant: University of Illinois at Chicago, 2009-2013

Teaching and Research Assistant: Cairo University, 2005-2009

### **PUBLICATIONS**

Zaher, M.H., Cetinkunt, S., Fuel Saving and Control for Hybrid Electric Powertrains, Control Engineering Practice, Elsevier, 2013.

Zaher, M.H., Cetinkunt, S., Real Time Energy Management Control for Hybrid Electric Powertrains, Journal of Control Science and Engineering, Hindawi, 2012.

Zaher, M.H., Cetinkunt, S., Fuel Saving and Control Strategy for Hybrid Electric Powertrains, SAE 2013 Commercial Vehicle Engineering Congress, 13CV-0066, Rosemont, Illinois, USA, October 1-3, 2013.

Zaher, M.H., Cetinkunt, S., Real Time Energy Management Strategy for Hybrid Electric Powertrains, SAE 2013 Commercial Vehicle Engineering Congress, 13CV-0074, Rosemont, Illinois, USA, October 1-3, 2013.

### **LANGUAGES**

English, Arabic, French